Answers to the Interactive comment on “Ice injected into the tropopause by deep convection – Part 2: Over the Maritime Continent” by Iris-Amata Dion et al.

Dear Dr Michelle Santee and Anonymous Referee #2, thank you very much for your very detailled comments that were very helpful for the improvement of our study. We tried as much as possible to answer all of your comments. Please consider in this document your comments in black, our answers in dark blue and the change on the text in clear blue. Pages 1 to 27 present the answers to Dr Michelle Santee’s review, and pages 28 to the end present the answers to Anonymous Referee #2 ‘s review.

Referee #1 Michelle Santee
(Referee) michelle.l.santee@jpl.nasa.gov
Received and published: 11 November 2019

This manuscript is a follow-on study from Dion et al. [ACP, 2019], which reported a novel method of correlating the twice-daily measurements of cloud ice water content (IWC) from the Aura Microwave Limb Sounder (MLS) with higher temporal resolution measurements of precipitation (Prec) from the Tropical Rainfall Measurement Mission (TRMM) to reconstruct the diurnal variation of ice in the upper troposphere (UT, 146 hPa) and tropopause level (TL, 100 hPa), thereby estimating the amount of ice injected at those levels by deep convection (ΔIWC). Since the previous study found the largest convective injection of IWC over the Maritime Continent (MariCont), here that region is divided into separate island, sea, and coastal zones. The approach to deriving ΔIWC in the UT and TL from MLS IWC and TRMM Prec data is also applied to TRMM lightning (Flash) data. Results using both TRMM data sets are compared to those based on IWC from ERA5. Java island is found to be the area with the highest ΔIWC. The roles of small-scale processes in controlling the ΔIWC over the different areas are assessed. In general, I think that this is a very interesting and valuable paper that demonstrates the great potential of the authors’ innovative technique to “fill in” the climatological diurnal cycle of IWC and the estimates of ΔIWC in the UT and TL at 2◦×2◦ horizontal resolution that have been derived from it. Thus I would very much like to see this paper in print. Unfortunately, however, the manuscript is riddled with inaccurate, erroneous, or inconsistent statements, many instances of unclear wording, and numerous typos. In my opinion, it requires a substantial amount of “cleaning up” before it can be published. A (fairly long) list of specific issues is detailed below. In most cases these concerns can be allayed simply by correcting and clarifying the discussion, with few if any requiring additional analysis. But, although each point is perhaps minor when considered in isolation, in aggregate they add up to major revisions. Moreover, even after the large number of minor corrections listed below, the manuscript will need copy-editing to improve the English.

Specific substantive comments and questions (in sequential order through the manuscript):

L9, L45-46, L105-106: I believe that the representation of the temporal resolution of the

TRMM Prec measurements in the Abstract (L9) and Introduction (L45-46) is somewhat misleading. In both places it is stated that Prec data are available at 1-hr resolution. My understanding, however, is that the TRMM-3B42 data are provided as 3-hr averages. Only by taking advantage of the precessing orbit of TRMM and the long study period (13 years) are the authors able to average the data in 1-hr bins. This binning is obliquely alluded to in L105-106 in the TRMM description subsection, but it should be explained more clearly.

Thank you, we decided to change the TRMM description in L105-106 by :

> ~~As the TRMM orbit precesses, the diurnal cycle of Prec averaged over the study period is105calculated with a 1-h temporal resolution.~~ The granule temporal coverage of TRMM-3B42 data is 3 hours, but the temporal resolution of individual measurements is 1 minute. Thus, it is statistically possible to degrade the resolution to 1 hour. TRMM-3B42 are provided in Universal Time that we converted into local time (LT). Details of the binning methodology of TRMM-3B42 is provided by Huffman and Bolvin (2018).

The reference is : G. J. Huffman, D. T. Bolvin, E. J. Nelkin, D. B. Wolff, R. F. Adler, G. Gu, Y. Hong, K. P. Bowman, and E. F. Stocker. The TRMM multisatellite precipitation analysis (TMPA): quasi-global, multiyear, combined-sensor precipitation estimates at fine scales. Journal of hydrometeorology, 8(1):38–55, 2007.

L72: Liu & Zipser [2009] is missing from the reference list, but actually it is not the correct citation here anyway. The 2009 JGR paper did not use TRMM LIS data. Abetter reference here is Liu & Zipser [JGR, 2005].

Thank you, it is a mistake. We wanted to wrote Liu and Zipser (2008) with the following reference:

Liu, C., and Zipser, E. J. (2008), Diurnal cycles of precipitation, clouds, and lightning in the tropics from 9 years of TRMM observations, *Geophys. Res. Lett.*, 35, L04819, doi:10.1029/2007GL032437.

Section 2.1:
Several aspects of the MLS description require revision. The most significant issue is the implication that the MLS team should have but failed to provide averaging kernels for the IWC measurements (L90-92). This statement and related discussion in Section 2.4 (L130) and Section 7.2 (L383-385) suggest that the authors have misconstrued how the MLS IWC product is derived. In fact, although optimal estimation is used to retrieve almost all other MLS products, that is not the case for IWC, for which a cloud-induced radiance technique is used. Consequently, no averaging kernels are calculated for IWC. It would be appropriate to reference two of the first papers describing and validating the MLS IWC retrievals: Wu et al. [JGR, 2008] and Wu et al. [JGR, 2009]. According to Wu et al. [2008], the IWC measurements represent spatially averaged quantities whose volume can be approximated by a box with dimensions of~4 km high by~300 km long; a simple box like this could have been used to degrade the vertical resolution of the ERA5 IWC rather than the unitary triangular function the authors devised, likely leading to slightly different results.

In agreement with the reviewers' comments, we have used an unitary box function instead of a unitary triangular function to degraded the vertical resolution of ERA5 data.
L383-385, the incriminated sentence has been changed into:

> Consistently with the MLS observations, we have degraded the ERA5 vertical resolution to assess the impact of the vertical resolution on ΔIWC^{ERA5}. According to Wu et al. (2008), IWC^{MLS} estimation derived from MLS represent spatially-averaged quantities within a volume that can be approximated by a box of ~ 300 x 7 x 4 km³ near the pointing tangent height.
> In order to compare IWC^{MLS} and IWC^{ERA5}, we degraded: 1) the horizontal resolution of ERA5 from 0.25°x0.25° to 2°x2° and 2) ERA5 data by connecting the vertical profiles of IWC^{ERA5} with a unitary box function whose width is 5 and 4 km at 100 and 146 hPa, respectively.

L. 168 has been changed as follow:

> IWC^{ERA5} have been degraded along the vertical at 100 and 150 hPa ($<IWC^{ERA5}>$) consistently with the MLS vertical resolution of IWC^{MLS} (5 and 4 km at 100 and 146 hPa, respectively) using an unitary box function (see section 7.2).

Other issues are: (1) Information on the quality of the IWC measurements and the screening steps taken to filter out poor-quality data points should be given.
(1) L94, we added the following sentence:

> The IWC measurements were filtered following the recommendations of the MLS team described in Livesey et al. (2018).

(2) MLS provides IWC measurements at 6 levels in the UTLS, not just at 146 and 100 hPa.
(2) L88, the following sentence has been added:

> The Microwave Limb Sounder (MLS, Version 4.2) instrument on board the NASA's Earth Observing System (EOS) Aura platform (Livesey et al., 2017) launched in 2004 provides ice water content (IWC^{MLS}, mg m-3) measurements ~~at 146 hPa (in85the UT) and at 100 hPa (in the TL)~~. MLS provides IWC^{MLS} are given at 6 levels in the UTLS (82, 100, 121, 146, 177 and 215 hPa). However, we have chosen to study only two levels: an upper and a lower level of the TTL. Because the level at 82 hPa does not provide enough significant measurements of IWC to have a good signal-to-noise, we have selected 2 levels: 1) at 100 hPa as the uppermost level of the TTL (named TL for tropopause level). Then, the level at 146 hPa has been chosen as the lowermost level of the TTL (named UT for upper troposphere). MLS follows a sun-synchronous near-polar orbit, ...

(3) Although it is essential to specify the version of the MLS data being used in this study, as written the sentence in L84 makes it sound like it is Version 4.2 of the instrument itself

and not the data processing algorithms.
(3) L84 the sentence has been changed into:

> The Microwave Limb Sounder (MLS, data processing algorithm version 4.2) instrument …

(4) It would be appropriate to cite the original paper describing the Aura MLS instrument, Waters et al. [2006], in addition to the MLS Data Quality Document.
(4) L85 the following reference has been added:

> … on board the NASA's Earth Observing System (EOS) Aura platform (Waters et al., 2006; Livesey et al., 2018) launched in 2004

Waters, J. W., Froidevaux, L., Harwood, R. S., Jarnot, R. F., Pickett, H. M., Read, W. G., ... & Holden, J. R. (2006). The earth observing system microwave limb sounder (EOS MLS) on the Aura satellite. IEEE Transactions on Geoscience and Remote Sensing, 44(5), 1075-1092.

(5) The most up-to-date version of the latter document is Livesey et al. [2018], not 2017.
(5) Thank you, it has been changed.

(6) It might be better to say "horizontal" rather than "spatial" in L92.
(6) L92, Thank you, we changed the incriminated word as follow:

> In our study, high horizontal resolution study is now possible because…

Section 2.2:
It is stated that TRMM provided observations until 2015 and that the Prec product has been extended through 2019, but the source of the data for the most recent years is not explained (GPM?). No mention is made of Prec data quality (e.g., biases,random errors).

Yes, this is a GPM. L99, we added the following sentences to clarify this point:

> The Tropical Rainfall Measurement Mission (TRMM) has been launched in 1997 and has been able to provide measurements of Prec until 2015. TRMM is composed by five instruments, three of them are complementary sensor rainfall suite (PR, TMI,VIRS). TRMM had an almost circular orbit at 350 km altitude height performing a complete revolution in one and a half hour. Since, the TRMM satellites re-entered the Earth's atmosphere on 2015, the 3B42 algorithm product (TRMM-3B42) (version V7) has been created to estimate the precipitation and extend the precipitation product through 2019. TRMM-3B42 is a multi-satellite precipitation analysis composing a Global Precipitation Measurement (GPM) Mission. TRMM-3B42 is computed from the various precipitation-relevant satellite passive Microwave (PMW) sensors using GPROF2017 computed at the Precipitation Processing System (PPS) (e.g., GMI, DPR, Ku, Ka, Special Sensor Microwave Imager/Sounder [SSMIS], etc.) and including TRMM measurements from 1997 to 2015 (Huffman et al., 2007, 2010; and Huffman and Bolvin, 2018). Work is currently underway with NASA funding to develop more appropriate estimators for random error, and to introduce estimates of bias error (Huffman and Bolvin, 2018). ~~Thus, the TRMM-3B42, a Prec dataset is based on TRMM observations from 1997 to 2015 and provides~~ Prec data are provided ~~from 1997 to 2019~~ at a 0.25°×0.25°

(∼29.2 km) horizontal resolution, extending from 50°S to 50°N (https://pmm.nasa.gov/data-access/downloads/trmm, last access: April 2019).

Section 2.3:
Not a single reference for the LIS instrument is cited, nor is there any discussion of data quality, detection limits, etc. I do not understand what is meant by "allowing to observe a point within 90 seconds with a temporal resolution of 2 milliseconds" (L110-111). Within 90 seconds of what?

L110-111, we changed the paragraph by the following one:

> The Lightning Imaging Sensor (LIS) aboard of the TRMM satellite measures several parameters relative to lightning. According to Christian et al. (2000), LIS used a Real-Time Event Processor (RTEP) that discriminates lightning event from Earth albedo light. ~~in itself was composed by a grid of 128×128 detectors allowing to observe a point within 90 seconds with a temporal resolution of 2 milliseconds~~. A lightning event corresponds to the detection of a light anomaly on a pixel representing the most fundamental detection of the sensor. After a spatial and temporal processing, the sensor was able to characterize a flash from several detected events. The instrument detects lightning with storm-scale resolution of 3-6 km (3 km at nadir, 6 km at limb) over a large region (550-550 km) of the Earth's surface. A significant amount of software filtering has gone into the production of science data to maximize the detection efficiency and confidence level. Thus, each datum is a lightning signal and not noise. Furthermore, the weak lightning signals that occur during the day are hard to detect because of background illumination. A real-tile event processor removes the background signal to enable the system and detect weak lightning and achieve a 90% detection efficiency during the day. LIS horizontal resolution is provided at 0.25◦×0.10◦. LIS is thus able to provide the number of flashes (Flash) measured. The TRMM LIS detection efficiency ranges from 69% near noon to 88% at night. The LIS instrument performed measurements between 1 January 1998 and 8 April 2015. To be as consistent as possible to the MLS and TRMM-3B42 period of study, we are using LIS measurements during DJF from 2004 to 2015. ~~LIS spatial resolution varies between 3 km at nadir and 6 km off-nadir.~~ The observation range of the sensor is between 38◦N and 38◦S. As LIS is on the TRMM platform, with an orbit that precesses, Flash from LIS can be averaged to obtain the full 24-h diurnal cycle of Flash over the study period with a 1-h temporal resolution. In our study, Flash measured by LIS is studied at 0.25◦×0.25◦ horizontal resolution to be compared to Prec from TRMM-3B42.

Reference added: *Christian, H. J., Blakeslee, R. J., Goodman, S. J., & Mach, D. M. (2000). Algorithm Theoretical Basis Document (ATBD) for the Lightning Imaging Sensor (LIS), 53 pp. NASA/Marshall Space Flight Cent., Alabama.*

Section 2.4:
As noted by Duncan & Eriksson [ACP, 2018], ERA5 differs from other reanalyses in that it differentiates between precipitating ice, classified as snow water, and non-precipitating ice,

classified as cloud ice water. In their study, Duncan & Eriksson typically combined the two products. Presumably only cloud ice water was used here, so it would be good for the authors to comment on whether that approach has any impact on their results. In addition, it might be useful to discuss the conclusions of Duncan & Eriksson regarding the ability of ERA5 to capture both seasonal and diurnal variability in cloud ice.

L121-132, we changed sentences in the section 2.4 as follow:

> …. ERA5 provides hourly estimates for a large number atmospheric, ocean and land surface quantities and covers the Earth on a 30 km grid with 137 levels from the surface up to a height of 80 km. Reanalyses such as ERA5 provide a physically constrained, continuous, global, and homogeneous representation of the atmosphere through a large number of observations (space-borne, air-borne, and ground-based) with short-range forecasts. Although there is no direct observation of atmospheric ice content in ERA5, the specific cloud ice water content (mass of condensate / mass of moist air) (IWC^{ERA5}) corresponds to the changes in the analysed temperature (and at low levels, humidity) which is mostly driven by the assimilation of temperature-sensitive radiances from satellite instruments (https://cds.climate.copernicus.eu/cdsapp!/dataset/reanalysis-era5-pressure-levels-monthly-means?tab=form, last access: July 2019). IWC^{ERA5} used in our analysis is representative of non-precipitating ice, classified as cloud ice water. Precipitating ice, ~~refered to as~~ classified as snow water, is also provided by ERA5 but not used in this study in order to focus only on the injected and non-precipitating ice into the TTL. Furthermore, results from Duncan and Eriksson (2018) have highlighted that ERA5 is able to capture both seasonal and diurnal variability in cloud ice water but the reanalyses exhibit noisier and higher amplitude diurnal variability than borne out by the satellite estimates. The present study uses the IWC^{ERA5} at 100 and 150 hPa averaged over DJF from 2005 to 2016 with one-hour temporal resolution. ….

L134: The statement that ERA5 does not provide winds at 100 and 150 hPa is incorrect.

This was a mistake. As explained below (P18 of the present document), we decided to suppress the paragraph 2.5 as well as the Fig. 12.

Section 3: The algebra is backwards here: either the correlation should be flipped in Eq n. (1) or Prec(t) should be multiplied by 1/C in Eqn. (2).

Section 3, thank you. This is a mistake, we changed the equation 1 into:

$$C = IWC_x^{MLS} / Prec_x$$

Section 4.2:

I am confused about exactly what message Fig. 3 is conveying. As I understand it, a pixel is represented in the maps for 1:30 and 13:30 LT only if it is experiencing the growing phase of convection at that time. Thus all pixels in the map for 1:30 LT are undergoing increasing deep convection then, and likewise for the map at 13:30 LT. The description is

ambiguous, but when I read it I assumed that the mean was calculated for each individual pixel, as was done in Fig. 2c and 2e, and not over the MariCont as a whole.

Thank you to highlight that it is not clear about which « mean » we are talking about. This is the average of the whole IWC or Prec at 01:30 LT or 13:30 LT over the whole MariCont. Thus, the anomaly (deviation from the mean) shows the areas where Prec of IWC at 01:30 LT or 13:30 LT (per pixel) deviate from the MariCont mean of Prec of IWC at these hours.

In order to detail the explanations about these figures, we propose to describe the Figure 3a only. In Fig. 3a, the Prec values at 01:30 LT are presented as an anomaly (i. e. deviation from the average of the Prec values at 01:30 LT for the entire MariCont area). However, in this figure, it is shown only the pixels where the values from Prec to 01:30 LT are during the increasing phase of convection. Since we know the diurnal cycle of Prec for some pixels, the value of Prec at 01:30 LT is during the decreasing phase of convection. However, we decided to highlight the pixels when 01:30 LT is during the decreasing phase of the convection in grey. Furthermore, pixels with a reddish tending color indicates regions where precipitation (Prec) is greater than the average at 01:30 LT (when observations at 01:30 LT is during the increasing phase of convection). Conversely, pixels with a bluish color indicate regions where there is little precipitation compared to the Prec average at 01:30 LT.
Finally, Figures 3b, c and d are similar to Figure 3a but for Prec at 13:30 LT, IWC at 01:30 LT and IWC at 13:30 LT, respectively

We modified the incriminated sentences (L181) into:

> Figures 3a and b present the anomaly (deviation from the mean) of Prec measured by TRMM–3B42 over the MariCont at 01:30 LT and 13:30 LT, respectively, only over pixels when the convection is in the growing phase. The anomaly of IWC measured by MLS over the MariCont is shown in Figs. 3c and d, over pixels when the convection is in the growing phase at 01:30 LT and 13:30 LT, respectively. ~~Thus, e~~ Each pixel of Prec at 01:30 LT or 13:30 LT during the growing phase of the convection deviates from the average of the all Prec at 01:30 LT or 13:30 LT during the growing phase of the convection over the whole MariCont. The gray color denotes pixels for which convection is not ongoing. Some pixels can be presented on both sets of Prec and IWC panels in Figs. 3 when: 1) the onset of the convection is before 01:30 LT and the end is after 13:30 LT or 2) the onset of the convection is before 13:30 LT and the end is after 01:30 LT. Note that, whithin each 2°x2° pixel, at least 60 measurements of Prec or IWC at 13:30 LT or 01:30 LT over the period 2004-2017 have been selected for the average.

The caption of the Fig. 3 has been modified as follow:

> Anomaly (deviation from the mean) of Prec (a-b) and Ice Water Content (IWC M LS) at 146 hPa (c-d), at 01:30 LT (left) and at 13:30 LT (right) over pixels where 01:30 LT and 13:30 LT are during the growing phase of the convection,

respectively, averaged over the period of DJF 2004-2017. The gray color denotes pixels for which convection is not ongoing.

If so, then the sign of the deviations from the mean value in a particular pixel indicates whether deep convection is in the early stages (negative) or late stages (positive) of the increasing phase at that time, and the magnitude merely identifies whether the convection is just getting started or is just about to reach its peak (large) versus whether it is near the middle of the increasing phase (small). If that is the case, then I do not see how the inferences being drawn from this plot are supported.

We realize that our first explanation of the Fig.3 has not been easy to understand. For that reason, we have better explained the Fig. 3 in the previous answer.

It is stated (L188-189) that the growing phase of convection is mainly over land at 13:30 LT, but colored (i.e., non-grey, if indeed grey is meant to denote pixels for which convection is not ongoing, which is not at all clear) pixels seem to be present over nearly the entire domain in Fig. 3b and 3d, and IWC and, especially, Prec show fairly large anomalies over most of the sea areas.

We clarified this point in the previous answer Section 4.2. Furthermore, the sentence (L188-189) has been changed into:

~~At 13:30 LT, t~~ The growing phase of the convection over land is mainly at 13:30 LT ~~while, at 01:30 LT, the growing phase of the convection is mainly over seas and coastlines.~~

The strongest Prec anomaly at 13:30 LT is stated (L190) to be over Java Island, but (a) that may only mean that convection is not in the middle of the growing phase there,

See answer above (P7-8), explaining that the colors do not refer to the timing of the growing phase but to the anomalies of Prec.

and (b) the one pixel with the largest deviation from the mean over the island of Java does not stand out above the similarly large anomalies in the surrounding seas. It is stated (L190-191) that the strongest Prec anomaly at 1:30 LT occurs over coastlines and coastal seas, but equally large anomalies are seen in several pixels over Borneo and New Guinea.

Our analyses are describing the land and the sea separately. To be clearer, the sentence L190-191 has been changed as follow:

At 13:30 LT, over land, the strongest Prec and IWC anomalies (+0.15 mm h^{-1} and 2.50 mg m^{-3}, respectively) are found over the Java island, (and north of Australia for IWC). At 01:30 LT, the growing phase of the convection is found mainly over sea (while the pixels of the land are mostly gray), with maxima of Prec and IWC anomalies over coastlines and seas close to the coasts such as the Java Sea and the Bismark Sea.

It is stated (L192) that the strongest IWC anomaly at 13:30 LT is located over Java, but again comparably large values are located over North Australia and the North Australian Sea.

The previous answer presents the changes we performed to clarify L192:

Furthermore, L192, we canceled the following sentence :

> ~~The strongest value of IWC anomaly at 13:30 LT is found over Java, while the strongestvalues of IWC anomaly at 01:30 LT is found over coastlines and seas close to the coasts, such as the North Australia Sea, JavaSea, China Sea and coast around the New Guinea.~~

Finally, the region over the North Australian Sea is identified as having a negative Prec anomaly and a positive IWC anomaly, but that is really only true at 1:30 LT – at 13:30 LT, both anomalies are largely positive in that area.

We changed the sentence L197 into:

> … iii) area where Prec anomaly is negative and IWC anomaly is positive (e.g. over the North Australia Sea at 01:30 LT).

Section 4.3:
The discussion is muddled in places. (1) It is not true that the anomalies of Prec and IWC during the growing phase are positive over the West Sumatran Sea (L207-208); in fact, this area was identified in Section 4.2 to fall into category #2, with positive Prec anomalies but negative IWC anomalies, and this discrepancy is why it is discussed in detail in Section 8.2.

It is a mistake. It should be North Australia Sea instead of West Sumatra Sea. We changed the incriminated sentence L207 as follow:

> We can note that the anomalies of Prec and IWC during the growing phase of the convection over North Australia Sea at 13:30 LT are positive (> 0.2 ~~0.15~~ mg m^{-3}, Fig. 3a and b and > 2.5~~0~~ mg m^{-3}, Fig. 3c and d, respectively).

(2) In L207, "< 0.15 mg m^{-3}" should be "> 0.15 mm h^{-1}".

This has been corrected.

(3) The sentence in L208-209 doesn't make sense: the quoted TL ΔIWC max and min values overlap (3 and 2-3 mg m^{-3}, respectively), the min value in the TL is clearly much lower than 2 mg m^{-3} in Fig. 4, and the difference between the values in the TL and the UT is larger than a factor of 3-4 – indeed, it is stated to be a factor of 6 over land on L210.

We change the min value into 0.2-0.3 mg m^{-3} and the factor values as follow :

In the TL, the maxima (up to 3.0 mg m^{-3}) and minima (down to 0.2 – 0.3 mg m^{-3}) of ΔIWC are located within the same pixels as in the UT, although 3 to 6 times lower than in the UT.

(4) The TL is mentioned in L213, but Fig. 5 shows only the UT.

The sentence L213 has been changed into:

In order to better understand the impact of deep convection on the strongest ΔIWC injected per pixel up to the TTL, ~~into the UT~~ isolated pixels selected in Fig. 4a are presented separately in Figure 5a and f.

(5) In L215, it should be "large enough to observe the diurnal cycle of IWC between 2 and 5 mg m^{-3}", not Prec.

The sentence has been changed.

(But large enough to observe the diurnal cycles of IWC between 2.0 and 5.0 mg m^{-3}, Fig. 5g, h, i, j).

(6) It is stated (L225) that pixels with large ΔIWC have IWC values between 4.5 and 5.7 mg m^{-3}, but that is not true for New Guinea point #2, for which the IWC is much lower.

We changed the sentence L225:

For pixels with large values of ΔIWC, IWC observed by MLS is between 4.5 and 5.7 mg m^{-3} over North Australia Sea, South Sumatra and New Guinea.

Moreover, the range of IWC values (1.9 to 4.7 mg m^{-3}) for low-ΔIWC points overlaps that of high-ΔIWC points. Thus, large ΔIWC values are not always associated with large IWC values at 13:30 LT over land, as asserted in L227-228. Nor is it possible on the basis of Fig. 5 to make a similar assertion for 1:30 LT over the seas, since no such cases were actually examined in that figure.

We changed the sentence L227-228:

To summarize, large values of ΔIWC are observed over land in combination to i) longer growing phase of deep convection (> 9 hours), ~~ii) high value of IWC (>~4.5mg m-3, excepted) at 13:30 LT over land and 01:30 LT over seas,~~ and/or ~~i~~ ii) large diurnal amplitude of Prec (> 0.5 mm h^{-1}).

(7) L228-229 states "This shows that ΔIWC is strongly correlated with the shape of the diurnal cycle of Prec". But isn't that true by definition, since ΔIWC is simply scaled from the min and max in the diurnal cycle of Prec (Eqn. 3)?

We suppressed the incrimitated sentence:

~~This shows that ΔIWC is strongly correlated with the shape of the diurnal cycle of Prec.~~

Section 5.2:
A number of points need clarification. (1) The discussion throughout this section is inconsistent with Fig. 7, which shows the coastlines of the MariCont in the middle panel, not the bottom one. The figure caption is also incorrect.

We changed the Fig. 7 caption as follow:

> Figure 7. Diurnal cycle of Prec (solid line) and diurnal cycle of Flash (dashed line) over MariCont_L (top), MariCont_C (middle) and Mari-Cont_O (bottom).

We changed the L251-253 as follow:

> Diurnal cycles of Prec and Flash over the MariCont land, coastlines and offshore (MariCont_L, MariCont_C, MariCont_O, respectively) are shown in Figs. 7a–c, respectively. Within each 0.25°×0.25° bin, land/coast/ocean filters were applied from the Solar Radiation Data (SoDa, \url{http://www.soda-pro.com/web-services/altitude/srtm-in-a-tile}). MariCont_C is the average of all coastlines defined as 5 pixels extending into the sea from the land limit.

And we changed the organisation of the paragraph L264-275 in order to describe results over coastline before results over ocean as follow:

> Over coastlines (Fig. 7c), the Prec diurnal cycle is delayed by about + 2 to 7 h with respect to the Flash diurnal cycle. Prec minimum is around 18:00 LT while Flash minimum is around 11:30 LT. Maxima of Prec and Flash are found around 04:00 LT and 02:00 LT, respectively. This means that the increasing phase of Flash is 2-3 h longer than that of Prec. These results are consistent with Mori et al. (2004) showing a diurnal maximum of precipitation in the early morning between 02:00 LT and 03:00 LT and a diurnal minimum of precipitation around 11:00 LT, over coastal zones of Sumatra. According to Petersen and Rutledge (2001) and Mori et al. (2004), coastal zones are areas where precipitation results more from convective activity than from stratiform activity and the amplitude of diurnal maximum of Prec decreases with the distance from the coastline.
> Over offshore areas (Fig. 7b), minima of diurnal cycle of Prec and diurnal cycle of Flash are in the late afternoon, between 16:00 LT and 17:00 LT (Flash) and 17:00 LT and 18:00 LT (Prec), whilst maxima of diurnal cycle of Prec and Flash are reached in the early morning, between 06:00 LT and 07:00 LT (Flash) and around 08:00 LT – 09:00 LT (Prec). Results over offshore areas are consistent with diurnal cycle of Flash and Prec calculated by Liu and Zipser (2008) over the whole tropical ocean,showing the increasing phase of the diurnal cycle of Flash starting 1–2 hours before the increasing phase of the diurnal cycle of Prec.

Finally we changed the sentence (L280-285) as follow:

> To summarize, diurnal cycles of Prec and Flash show that:
> i) over land, Flash increases proportionally with Prec during the growing phase of the convection,

ii) over coastlines, Flash increasing phase is advanced by more than 6–7 hours compared to Prec increasing phase,
iii) over offshore areas, Flash increasing phase is advanced by about 1–2 hours compared to Prec increasing phase.

(2) I think the description of how coastlines are defined is unclear; it would help to say "extending into" rather than "over" the sea in L255.

We changed the sentence L254-255 as follow:

MariCont-C is the average of all coastlines defined as 5 pixels ~~over~~ extending into the sea from the lands limits.

It is clear from previous figures that a number of pixels straddle coastlines – are they categorized into the land or the coastal bins?

The calculation of the pixel value is not well described. We added the following sentences to make it clearer:

Within each 0.25°×0.25° bin, land/ocean/coast filters were applied from the Solar Radiation Data (SoDa,http://www.soda-pro.com/web-services/altitude/srtm-in-a-tile). MariCont-C is the average of all coastlines defined as 5 pixels ~~over~~ extending into the sea from the lands limits. The MariCont_O is the average of all offshore pixels defined as sea pixels excluding 10 pixels over the sea from the land coasts, thus coastline pixels are excluded, as well as all the coastal influences. MariCont_L is the area of all land pixels. A given 0.25°x0.25° pixel can contain information from different origins : land/coastlines or sea/coastlines. In that case, we can easily discriminate between land and coastlines or sea and coastlines by applying the land/ocean/coastlines filter. Consequently, this particular pixel will be flagged both as land and coastlines or sea and coastlines.

(3) Liu and Zipser [2008] is not included in the reference list, but it is unlikely to be the correct citation in any case. Perhaps the authors meant Liu et al. [JAMC, 2008], but I am not sure that that paper made the specific points about the diurnal cycles of Prec and Flash being made in L259 and L267.

Liu and Zipser [2008] has been forgotten in the reference list. In this paper, authors made similar comparison between diurnal cycle of Prec and Flash showing consistent results. We included them in the reference list:
*Liu, C., and Zipser, E. J. (2008), Diurnal cycles of precipitation, clouds, and lightning in the tropics from 9 years of TRMM observations, Geophys. Res. Lett., 35, L04819, doi:*10.1029/2007GL032437*.*

(4) The max in the diurnal cycle of Flash over MariCont_O is stated (L266) to be reached between 4 and 9 LT, but the peak is more like 6-7 LT and values are fairly low by 9 LT.

We changed the sentence L266 :

Over offshore areas (Fig. 7b), minima of diurnal cycle of Prec and diurnal cycle of Flash are in the late afternoon, between 16:00 LT and 17:00 LT (Flash) and 17:00 LT and 18:00 LT (Prec), whilst maxima of diurnal cycle of Prec and Flash are reached in the early morning, between 06:00 LT and 07:00 LT (Flash) and around 08:00 LT – 09:00 LT (Prec).

(5) Petersen & Rutledge [2001] is also missing from the reference list.

We inserted them in the reference list:

Petersen, W. A., & Rutledge, S. A. (2001). Regional variability in tropical convection: Observations from TRMM. *Journal of Climate*, *14*(17), 3566-3586.

(6) I think that another sentence or two of discussion to put the results of the Love et al. [2011] paper into the context of this study would be helpful.

We updated the incriminated paragraph:

The time of transition from maximum to minimum of Prec is always longer than that of Flash. The period after the maximum of Prec is likely more representative of stratiform rainfall than deep convective rainfall. Consistently, ~~over the MariCont ocean,~~ model results from Love et al. (2011) have shown the suppression of the deep convection over offshore area in West of Sumatra from the early afternoon due to downwelling wavefront highlighted by deep warm anomalies around noon. According to the authors, later in the afternoon, gravity waves are forced by the stratiform heating profile and propagate slowly offshore. They also highlighted that the diurnal cycle of the offshore convection responds strongly to the gravity wave forcing at the horizontal scale of 4 km.

Section 5.3:
(1) Sulawesi is singled out (L301-302) for exhibiting the same onset of the growing phase of convection as Java, but it seems to me that all of the islands in Fig. 8 show fairly similar timing for the increase in Prec and Flash as Java; rather, it is the declining phase when Sulawesi more closely resembles the steeper decrease over Java than the other islands do.

We changed the incriminated sentence L301-302 into:

~~Sulawesi is also a small islandand presents the same onset of growing phase for the convection than Java, consistently with results presented in Nesbittand Zipser (2003) and Qian (2008).~~
Sulawesi is also a small island with high topography as Java. However, the amplitude of the diurnal cycle of Prec and Flash over Sulawesi is not as strong as over Java.

(2) It is stated (L287) that Prec and Flash are studied at 0.25°×0.25° resolution in this subsection. Therefore, couldn't the fact that the diurnal max in Prec over the 5 small islands in Fig. 8 is much higher than that reported by Dion et al. [2019] over the broad

tropical regions of South America, SouthAfrica, and MariCont_L – based on 2° bins – merely be a consequence of the much greater horizontal resolution used here?

You are right, thank you. We modified the following sentence L295-297 into:

> The particularity of Java is related to the increasing phase of the diurnal cycle of Prec (6 h), that is faster than over all the other land areas considered in our study (7 – 8 h). ~~and is very consistent with the diurnal cycle of Prec over South America and South Africa (Dion et al., 2019).~~

(3) In L323-324, it is stated that Flash reaches a max of only 0.1 flashes h^{-1} over the North Australian and Bismark Seas, but (a) the value should be 0.1 x 10^{-3} and (b) it is not true for NAuSea, for which the max is about 0.6 x 10^{-3} flashes h^{-1}.

We corrected L323-324 as follow:

> Over China Sea and Bismark Sea, the diurnal cycle of Flash shows a ~~very~~ weak amplitude with maxima reaching only 0.1-0.2 x10^{-3} flashes h^{-1}.

(4) While the diurnal min in Prec is around 18:00 LT over the Bismark Sea, there are several local min in Flash (8, 14, 18 LT).

We changed the sentence L324-325 by the following one:

> ~~However, the diurnal minima of Prec and Flash over Bismark Sea are found to be at the same time (~17:00 LT).~~
> Furthermore, over the Bismark Sea, while the diurnal minimum in Prec is around 18:00 LT, there are several local minima in Flash (08:00, 14:00 and 18:00 LT).

Section 6:

(1) The duration of the increasing phase of the diurnal cycles of Prec, Flash, and ERA5 IWC is stated (L349) to be 4-5 h over islands, but in L296 this interval for Prec was given as 8-10 h over all land areas besides Java (6 h).

We firstly corrected L296 as follow:

> The particularity of Java is related to the increasing phase of the diurnal cycle of Prec (6 h) that is faster than over all the other land areas considered in our study (7 – 8 h).

Then, we changed L349 as follow:

> The duration of the increasing phase of the diurnal cycles of Prec, Flash and IWCERA5 are all consistent to each other (6 – 8 h).

(2) Over sea areas, the max of the diurnal cycle of ERA5 IWC is stated (L350) to occur mainly between 7 and 10 LT, but this is not true for the Bismark Sea (~3 LT), WSumSea (there is another essentially equal peak at 17 UT, as noted in L354-355), or China Sea (16

UT), nor is it true in those cases that the timing is consistent with the max in Prec. The statement that the max in the diurnal cycle comes 2-3 h after that in Flash is in consistent with what was said in L330-331 (4-7 h).

We changed L349-351 as follow:

> Over sea (Fig. 9), the maximum of the diurnal cycle of IWC^{ERA5} is mainly found between 07:00 LT and 10:00 LT over Java Sea and North Australia Sea, consistently with the diurnal cycle of Prec and a second peak is found around 16:00 LT. ~~(which is 2 – 3 hours after the diurnal maxima for Flash).~~ Thus, the duration of the increasing phase of the diurnal cycles of IWC^{ERA5} is consistent with the one of Prec over these two sea study zones (~10 hours), but not with the one of Flash. Over Bismark Sea, the diurnal maxima of IWC^{ERA5} are found at 04:00 LT with a second peak later at noon. Over West Sumatra Sea, two diurnal maxima are found at 08:00 LT and 17:00 LT. Over China Sea, the diurnal maxima of IWC^{ERA5} are found at 16:00 LT with a second peak at 08:00 LT.

(3) The sentence in L353-355 appears to contradict itself ("consistent with the one of Prec...but not with the one of Prec") – perhaps "Flash" was meant in the latter case.

Yes, it should be 'Flash' instead of 'Prec'. The incriminated sentence has been corrected.

(4) Although the comparisons with ERA5 IWC are interesting, I am wondering what the main goal in including them is. Is the intention to use ERA5IWC, and the ΔIWC estimated from it, to confirm the observationally derived values? Or, conversely, is the idea to use the Prec and Flash to "validate" the new ERA5 values?

A sentence has been added L335 to clarify the motivations to use IWC from ERA5:

> The ERA5 reanalyses provide hourly IWC at 150 and 100 hPa (IWC^{ERA5}). The diurnal cycle of IWC over the MariCont from ERA5 will be used to calculate ΔIWC from ERA5 in order to assess the horizontal distribution and the amount of ice injected in the UT and the TL deduced from our model combining MLS ice and TRMM Prec or MLS ice and LIS flash. Figures 10a, b, c and d present …

Section 7.1:

(1) It is very difficult for the reader to judge any of the ΔIWC values stated here in the absence of any y-axis minor tick marks in Fig. 11.

The Fig. 11 has been changed as follow:

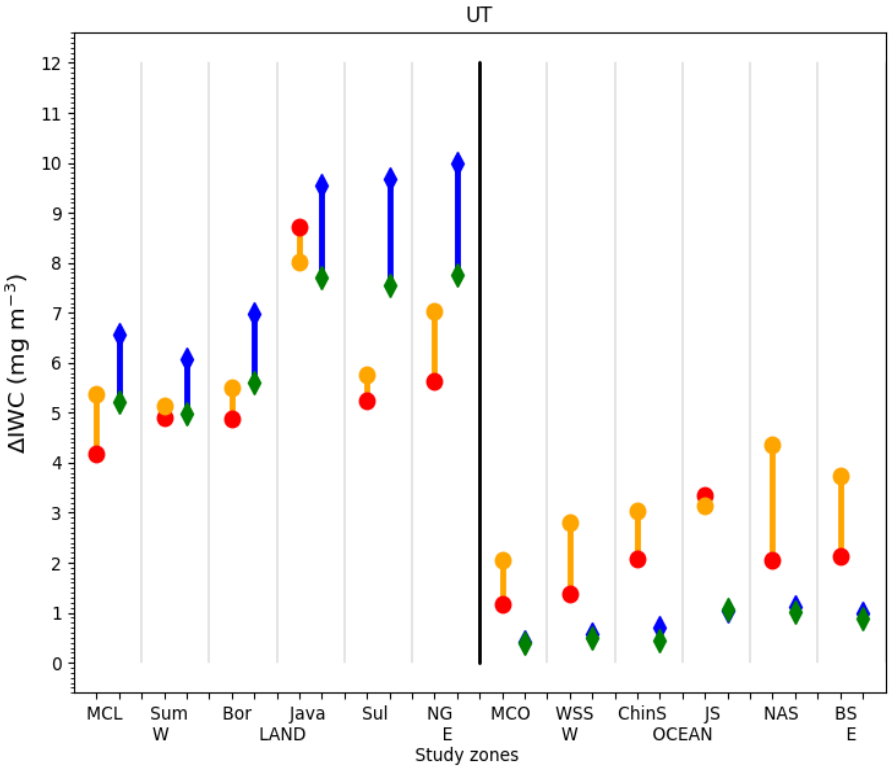

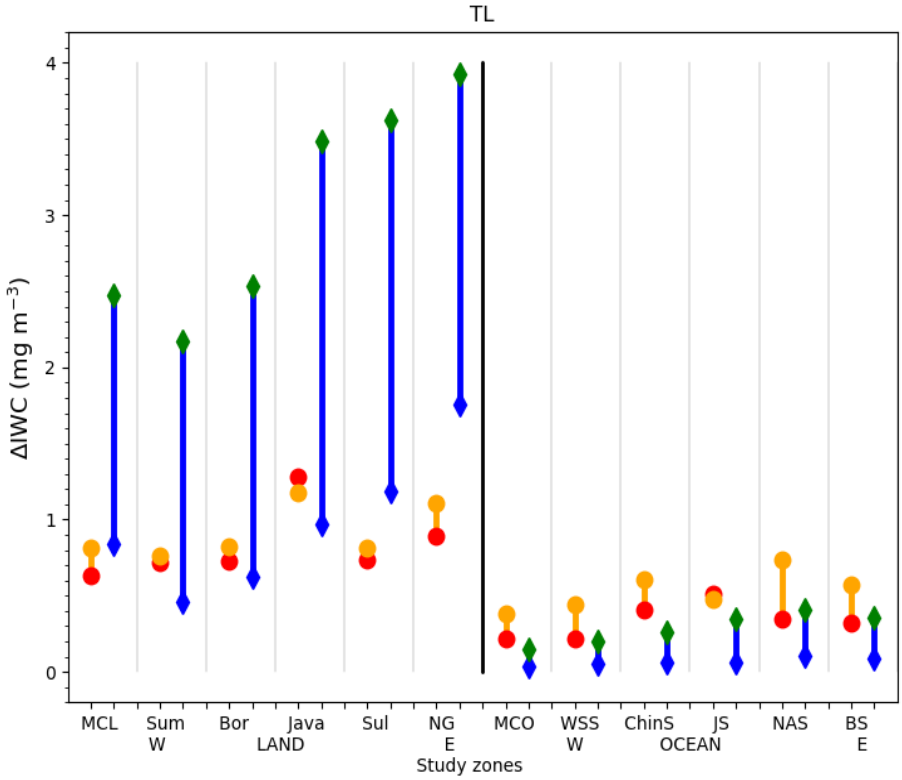

(2) It is not clear how the quoted percentages are being calculated (i.e., relative to what). For example, a range of values of 4.87–6.86 mg m^{-3} is given for ΔIWC over a subset of islands in the UT. It is then stated (L368) that ΔIWC from Flash is greater than that from Prec by "less than 1.0 mg m^{-3} (41%)". I have no idea how a value of 41% could possibly have been calculated.

The percentage has been recalculated as follow: for each land study zone, the percentage is calculated as the difference between the Flash value minus the Prec value divided by the Flash value. For each study zone, results are detailled as follow:
MCL=22%, Sum = 4%, Bor = 11%, Java=-8%, Sul = 9% and NG =19% over island and MCO=43 %, WSS=50 %, ChinS=31 %, JS =-7 %, NAS=53 % and BS = 43 % over sea).
As a consequence, the previous sentences L367-372 have been changed as follow:

> ΔIWC^{Flash} is generally greater than ΔIWC^{Prec} by less than 1.0 mg m^{-3} (((ΔIWC^{Flash}-ΔIWC^{Prec})/ΔIWC^{Flash})x100 ranges from 4 to 22%) ~~(41\%)~~ for all the islands, except ~~for New Guinea where the difference reaches 1.40 mg m^{-3} (20%)~~. for Java where ΔIWC^{Prec} is larger than ΔIWC^{Flash} by 0.7 mg m-3 (-8%). ~~Conversely, over Java,ΔIWCPrec is larger than ΔIWCFlash by 0.71 mg m^{-3} (8%).~~ Over sea, ΔIWC varies from 1.~~17~~2 to 4.~~37~~4 mg m^{-3}. ΔIWC^{Flash} is greater than ΔIWC^{Prec} from 0.6 to 2.1 mg m^{-3} (31-53%), except for Java Sea, where ΔIWC^{Prec} is greater than ΔIWC^{Flash} by 0.2~~1~~ mg m^{-3} (-7%). Over North Australia Sea, ~~probably because of the 7-hours lagged diurnal cycle of Flash compared to Prec (Fig. 9),~~ ΔIWC^{Flash} is almost twice as large as than ΔIWC^{Prec} ~~values~~ (53%).

(3) I am not convinced that the methodology and measurements employed in this study truly allow ΔIWC to be estimated to three significant digits.

We changed all results to two significant digits.

(4) The fact that ΔIWC from Flash is almost twice as large as that from Prec over the North Australia Sea is attributed to the lagged diurnal cycle of Flash compared to Prec (L371-372), but (a) this is backward: it is Prec that is lagged compared to Flash, as noted in L325-326, and (b) I did not follow why a lag in the diurnal cycle would cause larger ΔIWC values.

You are right, there is no specific reason why a lag in the diurnal cycle would cause larger ΔIWC values. We deleted the part of the sentence L371-372:

~~probably because of the 7-hours lagged diurnal cycle of Flash compared to Prec (Fig. 9), …~~

(5) The third paragraph is confusing. It starts with a sentence about Java, but then the rest of the paragraph is about the differences between Prec and Flash ΔIWC estimates in general, making the Java sentence seem out of place. The final sentence is badly written and difficult to parse, but it appears to say that Flash (unlike Prec) is not contaminated by stratiform precipitation and thus should serve as a better proxy than Prec over the sea, but because it is negligible there it cannot be used to calculate ΔIWC in those regions – but of course Flash has been used to do exactly that, with the results shown in Fig. 11. And the statement that Flash is a better proxy for deep convection than Prec because it is not contaminated by stratiform rainfall is repeated in Section 8.2 for the West Sumatra Sea specifically. So the discussion here needs to be clarified.

We clarified the last paragraph (L376-379) as below and replaced the last sentence which was confusing by a new one concluding that both proxies can be used in our model, with more confidence over land:

> ~~At both altitudes,~~ To summarize, independently of the proxies used for the calculation of ΔIWC, and at both altitudes, Java shows the largest injection of ice over the MariCont. ~~ΔIWC^{Prec} and ΔIWC^{Flash} are consistent to within 4-20 \% over islands and 6-50 \% over seas in the UT and the TL.~~ Furthermore, it has been shown that both proxies can be used in our model, with more confidence over land: IWC^{Prec} and ΔIWC^{Flash} are consistent to each other to within 4-22% over island and 7-53% over sea in the UT and the TL. The largest difference over sea is probably due to the larger contamination of stratiform precipitation included in Prec over sea. ~~Although Flash, is not contaminated by stratiform clouds, it could be a better proxy than Prec over sea but it is unfortunately negligible: less than 10-2 flashes per day (Fig. 6).~~

Section 7.2:
(1) the definitions of the UT and TL in L381 are switched.

The definitions have been corrected:

> ΔIWC from ERA5 (ΔIWC^{ERA5}) is calculated in the UT and the TL (z_0= 150 and 100 hPa, respectively) as the max–min difference in the amplitude of the diurnal cycle.

(2) The reference on L384, which was likely supposed to be Rodgers [2000], is missing, but as discussed above it is not relevant here anyway, as optimal estimation is not used to retrieve MLSIWC data. Thus the discussion related to that point needs to be rewritten.

Correction has been done and answers has been detailed previously page 3 of this document.

(3) There is no Livesey et al. [2019] document – the latest version of the MLS Data Quality Document is Livesey et al. [2018].

The reference has been changed.

(4) It is not clear what is meant by the statement “xx% of variability per study zones”, which appears in numerous places throughout this subsection and also in Sections 7.3 and 8.3, nor how those values are calculated. Please clarify.

Similarly as the percentage previously calculated in section 7.1 (comparing ΔIWC^{Prec} and ΔIWC^{Flash}), the percentage calculated here is an average of all percentages of difference between ΔIWC^{ERA5} and $<\Delta IWC^{ERA5}>$ calculated for each study zone as follow: $((\Delta IWC^{ERA5}-<\Delta IWC^{ERA5}>/\Delta IWC^{ERA5})x100)$. For each study zone, results over land are :
MCL=21%, Sum=21%, Bor=27%, Java=22%, Sul=23%, NG=23%.

To clarify, this we changed the paragraph as follow:

> Figure 11 shows ΔIWC^{ERA5} and ~~($\langle\Delta IWC^{ERA5}z_0\rangle$)~~ at z_0 = 150 and 100 hPa, over the island and the sea study zones. In the UT (Fig. 11a), over island, ΔIWC^{ERA5}_{150} and $\langle\Delta IWC^{ERA5}_{150}\rangle$ calculated over Sumatra and Borneo vary from ~~4.75~~ 4.9 to ~~6.97~~ 7.0 mg m^{-3} (the relative variation calculated as $((\Delta IWC^{ERA5}-<\Delta IWC^{ERA5}>)/\Delta IWC^{ERA5})x100$ is 18-19%) ~~($\sim$22% of variability per study zones)~~ whilst ΔIWC^{ERA5}_{150} and $\langle\Delta IWC^{ERA5}_{150}\rangle$ over Java, Sulawesi and New Guinea reach ~~7.41–9.97~~ 7.4-10.0 mg m^{-3} (~19-22% of variability per study zone).

(5) The convolved ERA5ΔIWC values are greater than the unconvolved values in the TL, not lower as stated in L398.

The sentence has been corrected. :

> In the TL, over land, ΔIWC^{ERA5}_{100} and $\langle\Delta IWC^{ERA5}_{100}\rangle$ vary from ~~0.46~~ 0.5 to ~~3.65~~ 3.7 mg m^{-3} (~68% of variability per study zone) with $\langle\Delta IWC^{ERA5}_{100}\rangle$ being larger than ΔIWC^{ERA5}_{100} by less than 2.1~~2~~ mg m^{-3}.

Section 7.3:
(1) I assume that the statement “observation and reanalysis ΔIWC ranges agree to within 0–0.64 mg m^{-3}” (L404-405) is meant to indicate that the ranges generally overlap, not that the estimates precisely agree. I think it might be clearer to say “observation and reanalysis ΔIWC ranges overlap, except over New Guinea and Sulawesi, where the differences between the extrema of the two ranges are 0.64 mg m^{-3} and 1.63 mg m^{-3}, respectively”.

The sentence L403-405 has been changed as follow :

> The comparison between the observational ΔIWC range and the reanalysis ΔIWC range is presented in Fig. 11. In the UT, over land, observation and reanalysis ΔIWC ranges overlap (agree to within 0.1 to 1.0 mg m^{-3}), which

highlights the robustness of our model over land, except over Sulawesi and New Guinea, where the observational ΔIWC range and the reanalysis ΔIWC range differ by 1.7 and 0.7 mg m^{-3}, respectively).

(2) Does the fact that the observational ΔIWC range is more or less consistent with the reanalysis range over most islands but is systematically greater than the reanalysis range over all sea regions imply anything about either the validity of the methodology used here or the reliability of the ERA5 IWC values over offshore areas?

As noted in the sentence L403-405, these results highlighted the robustness of our model over land, but over sea, a systematic positive bias and a too large variability range were depicted in our model compared to ERA5.

To clarify, the sentence L405 has been completed as follow:

Over sea, the observational ΔIWC range is systematically greater than the reanalysis ΔIWC range to within ~1.0~~0~~ – 2.1~~9~~2 mg m^{-3} (75 %), showing a systematic positive bias and a too large variability range in our model over sea compared to ERA5.

(3) The combined ΔIWC range over land in the TL is stated (L408) to be 0.63–3.65 mg m^{-3}, but the lowest value (which occurs over Sumatra) looks smaller than that (below 0.5) to me. Again I question whether the degree of precision in all of the ΔIWC values quoted throughout the manuscript is really supportable.

Thank you. We checked all the values quoted in the manuscript. We changed the value of 0.6 (which is the minimum for the MCL study zones) to 0.5 which is the minimum among all the study zones. Here are the changes:

Combining observational and reanalysis ranges, the total ΔIWC variation range is estimated in the UT between ~~4.17 and 9.97~~ 4.2 and 10.0 mg m^{-3} (~20% of variability per study zone) over land and between 0.~~35~~4 and 4.~~37~~4 mg m^{-3} (~30% of variability per study zone) over sea and, in the TL, between 0.5 and 3.~~65~~7 mg m^{-3} (~70% of variability per study zone) over land, and between 0.1 and 0.7 mg m^{-3} (~80 % of variability per study zone) over sea.

(4) The consistency between ΔIWC estimates is discussed in L410-412. It is not clear to me why Sumatra was left off the list of specific land areas where agreement is good. On the other hand, although MariCont_O is identified as showing large differences, it seems to me that it should be noted that agreement is poor for all individual offshore areas.

Sumatra has been forgotten in the sentence L140-412. The sentence L410-412 has been modified into:

The amounts of ice injected in the UT deduced from observations and reanalyses are consistent to each other over MariCont_L, Sumatra, Borneo and Java, with significant differences ~~between observations and reanalyses~~ over Sulawesi, New Guinea (within 1.7 to 0.7 mg m^{-3}, respectively) and all individual offshore study zones (within 0.7 to 2.1 mg m^{-3}).

Section 8.2: It is stated (L449-450) that Flash is a better proxy for deep convection over the West Sumatra Sea than Prec. I note that Flash shows higher ΔIWC than Prec over the WWS (as in almost all offshore areas) in Fig. 11. But I am puzzled about how the discussion of ΔIWC estimates in this section relates to the negative IWC anomaly in this region in Fig. 3, which is based directly on MLS IWC data, not estimates of ΔIWC derived from either Prec or Flash. More discussion tying the IWC / Prec anomalies of Fig. 3 (and how they differ over the WSS from other regions) to the ΔIWC estimates in Fig. 11 would be helpful here.

The whole paragraph has been changed for a better clarification:

> In section 4.3, it has been shown that the West Sumatra Sea is an area with positive anomaly of Prec during the growing phase of the convection but negative anomaly of IWC, which differs from other places. ~~The diurnal cycle of Prec over West Sumatra440Sea has been studied by Mori et al. (2004) using 3 years of TRMM precipitation radar (PR) datasets, following the 2A23Algorithm Awaka (1998) separating stratiform to convective rainfall type.~~ These results suggest that Prec is representative not only of convective precipitation but also of stratiform precipitation. The diurnal cycle of stratiform and convective precipitations over West Sumatra Sea has been studied by Mori et al. (2004) using 3 years of TRMM precipitation radar (PR) datasets, following the 2A23Algorithm (Awaka, 1998). The authors have shown that rainfall over Sumatra is characterized by convective activity with a diurnal maximum between 15:00 and 22:00 LT while, over the West Sumatra Sea, the rainfall type is convective and stratiform, with a diurnal maximum during the early morning (as observed in Fig. 9). Furthermore, their analyses have shown a strong diurnal cycle of 200-hPa wind, humidity and stability, consistent with the diurnal cycle of precipitation measured by TRMM Precipitation Radar (PR) over Sumatra West Sea and Sumatra island. Stratiform and convective clouds are both at the origin of heavy rainfall in the tropics (Houze and Betts, 1981; Nesbitt and Zipser, 2003) and in the West Sumatra Sea, but stratiform clouds are mid-altitude clouds in the troposphere and do not transport ice up to the tropopause. Thus, over the West Sumatra Sea, the calculation of ΔIWC estimated from Prec is possibly overestimated because Prec include a non-negligible amount of stratiform precipitation over this area.
>
> ~~Flash measured over the West Sumatra Sea would thus be a better proxy of deep convectionin order to estimate ΔIWC than Prec because Prec is contaminated by stratiform rainfall.~~

Section 8.3: I'm not sure that I follow the discussion in this section. The authors note that daily mean Flash rates are higher than daily mean Prec values over the North Australian Sea, and that difference is why ΔIWC estimates from the two sources differ most strongly in that region. They then go on to suggest that IWC injected during the day over North Australia land areas is transported to the coastlines and sea areas over night. But the bottom-line point of this argument is not clear – what observations presented in this paper is it intended to explain? Are the authors contending that this transport of IWC some how affects their ΔIWC estimates? That appears to be the case based on the final sentence

(L517-519) of the Conclusions section. If so, then I find that very confusing, because the underlying basis for their approach in estimating ΔIWC is the assumption that deep convection is the dominant process driving the diurnal increase in IWC in the TTL and that other processes, such as horizontal advection, can be neglected. If indeed horizontal advection of IWC is a factor here, then wouldn't that mechanism operate in other regions as well? (Even just in the North Australia Sea, it seems that similar contributions from New Guinea might also play a role.). Fundamentally, it seems to me that this has potentially serious implications for the validity of their technique for deriving ΔIWC over any offshore areas that should be discussed in more detail here and stated more explicitly in the Conclusions.

We deleted Fig. 12 and paragraph 2.5. We decided not to discuss about the assumptions of the impact of processes than the vertical deep convective processes on the ice injected over offshore because we do not have enough information to assess their implications and make hypothese. Thus, we changed and simplified the whole paragraph as follow:

8.3 North Australia Sea and seas with nearby islands

The comparisons between Figs. 2c and 6a have shown strong daily mean of Flash (10^{-2} –10^{-1} flashes day^{-1}) but low daily mean of Prec (2.0 – 8.0 mm day^{-1}) over the North Australia Sea. Additionally, Fig. 11 shows that the strongest differences between ΔIWC^{Prec} and ΔIWC^{Flash} are found over the North Australia Sea, with ΔIWC^{Flash} greater than ΔIWC^{Prec} by 2.3 mg m^{-3} in the UT and by 0.4 mg m^{-3} in the TL (53% of variability between ΔIWC^{Flash} and ΔIWC^{Prec}). These results imply that the variability range in our model is too large and highlight the difficulty to estimate ΔIWC over this study zone.
Furthermore, as for Java Sea or Bismarck Sea, North Australia Sea has the particularity to be surrounding by several islands. According to the study from Pope et al. (2009), the cloud size is the largest during the afternoon over the North Australia land, during the night over North Australia coastline and during the early morning over the North Australia sea. These results suggest that deep convective activity moves from the land to the sea during the night. Over the North Australia Sea, it seems that the deep convective clouds are mainly composed by storms with lightnings but precipitations are weak or do not reach the surface and evaporating before.

Furthermore, the sentence L517 has been deleted.

References:

(1) There is a pervasive lack of proper capitalization throughout the references listed, as well as several instances of bizarre (and unnecessary) hyphenation. Done

(2) The correct reference for the MLS Data Quality Document is: Livesey, N.J., Read,W.G., Wagner, P.A., Froidevaux, L., Lambert, A., Manney, G.L., Millan, L.F., Pumphrey,H.C., Santee, M.L., Schwartz, M.J., Wang, S., Fuller, R.A., Jarnot, R.F., Knosp, B.W.,Martinez, E., and Lay, R.R., Version 4.2x Level 2 data quality and description document, Tech. Rep.

JPL D-33509 Rev. D, Jet Propulsion Laboratory, available at:http://mls.jpl.nasa.gov (last access: dd MMM yyyy), 2018. Done

Minor points of clarification, wording suggestions, and grammar / typo corrections:

L11: lightnings –> lightning events OK

L14 (also L38, 166, 167,169, 189, 205, 210, 211, 216, 219, 241, 252, 255, 289, 309,311, 407, 421): lands –> land OK

L16: I think it would be clearer to add “they agree” in front of “to within 4-20%” OK

L28: dimentional –> dimensional OK

L29 and L31: add “e.g.” at the beginning of the lists of references on these lines OK

L35: add a comma after “respectively”L38: add a comma after “areas” OK

L41: The first sentence of this paragraph seems out of place, as it has nothing to dowith the rest of the paragraph. It would be better to move it somewhere else or delete it.

OK we deleted it.

L53: center –> centers OK

L56: Is the statement “a comprehensive work has been done around the study of the diurnal cycle of precipitations and convection over the MariCont” referring to previous studies other than Yang & Slingo (cited in the previous sentence)? If so, references are needed. In any case, the sentence needs to be clarified. OK we added the missing reference as follow:

> Yang and Slingo (2001) have shown that over the Indonesian area, the phase of the convective activity diurnal cycle drifts from land to coastlines and to offshore areas. Even though authors have done a comprehensive work around the study of the diurnal cycle of precipitation and convection over the MariCont, the diurnal cycle of ice injected by deep convection up to the TL over this region is still not well understood.

L56 (also L104, 430): precipitations –> precipitations OK

L65: It is not clear what is meant by “the authors were expected”

We clarified this point as follow:

> Consequently, the amount of ice injected in the UT and the TL is greater over MariCont_L than over MariCont_O. ~~Considering a higher horizontal resolution over small islands and seas of the MariCont and investigating other proxies of deep convection, the authors were expected a better characterisation of the amount of ice injected up to the TTL .~~
>
> Building upon the results of Dion et al. (2019), ~~the present study is~~

~~addressing the evaluation of ΔIWC at a resolution of~~ the present study aims to improve the methodology of Dion et al. (2019) by i) studying smaller study zones than in Dion et al. (2019) and by distinguishing island and sea of the MariCont, ii) assessing the sensibility of model to different proxies of deep convection and iii) assessing the amount of ice injected in the UT and the TL inferred by our model by comparinf with that of ERA5 reanalyses. Based on space-borne observations and meteorological reanalyses, ΔIWC is provided at a horizontal resolution of 2°×2° over 5 islands (Sumatra, Borneo, Java, Sulawesi and New Guinea) and 5 seas (West Sumatra Sea, Java Sea, China Sea,North Australia Sea, and Bismark Sea) of the MariCont during convective season (December, January and February, here after DJF) from 2004 to 2017. ΔIWC will be first estimated from Prec measured by TRMM-3B42. A sensitivity study of ΔIWC based on the number of flashes (Flash) detected by the TRMM Lightning Imaging Sensor (TRMM-LIS), an alternative proxy for deep convection as shown by Liu and Zipser (2009), is secondly proposed. Finally, we will use IWC calculated by the ERA5 reanalyses from 2005 to 2016 to estimate ΔIWC in the UT and the TL over each study zone and compare it to ΔIWC estimated from Prec and Flash.

L73: that will be compared –> and compare OK
L84: the NASA's –> NASA's OK
L91: add a comma after "respectively" OK
L92-93: delete "study" after "resolution"; datasets –> data OK

L96: has been launched in 1997 and has been able to provide –> was launched in 1997 and provided OK
L97: composed by –> composed of OK
L102-103: depend –> depends; add "and does" in front of "not differentiate" OK
L108: lightnings –> lightning OK
L109: was using –> used OK
L123: number –> number of OK
L129 (also L292, 304, 337, 348, 350, 435): consistently –> consistent OK
L136: Est –> East OK
L167 (also L194, 241, 245, 337, 339, 416, 431, 464, 516): the New Guinea –> NewGuinea OK
L175: Fig. 2c –> Fig. 2^{e} OK
L176 (P7): it would be helpful if the Timor Sea and the Arafura Sea were also indicated on the map in Fig. 2a

These two seas compose what we named the North Australia Sea. However, the map on Fig. 2a is too small to show these two seas separately.

P8, Fig. 2 caption: It would be helpful if the information about the horizontal resolution of the TRMM and MLS data were added to the caption in addition to being stated in the main text

The caption has been changed as follow:

Main islands and seas of the MariCont (S is for Sumatra) (a), elevation from Solar Radiation Data (SoDa) (b); daily mean of Prec measured by TRMM over

the Maritime Continent, averaged over the period of DJF 2004-2017 (c), hour (local solar time (LST)) of the diurnal maxima of Prec over the MariCont (d); daily mean (01:30 LT + 13:30 LT)/2 of IWC^{MLS} at 146 hPa from MLS over the MariCont averaged over the period of DJF 2004-2017 (e). Observations are presented with a horizontal resolution is 0.25°x0.25° for (b, c and d) and 2°x2° for (e).

L179: that –> as OK
L180-181: each duration –> the duration; can be defined –> can then be defined OK
L185: present both in Figs. 3a and b (Figs. 3c and d, OK

L187: this doesn't make sense – I think 13:30 LT –> 1:30 LT OK

L193: is –> are OK
P10, Fig. 3 caption: It would be good to state in the caption that the IWC plots are for 146 hPa. Also, add a comma after "respectively"

OK :

Anomaly (deviation from the mean) of Prec (a-b) and Ice Water Content (IWC^{MLS}) at 146 hPa (c-d), at 01:30 LT (left) and at 13:30 LT (right) over pixels where 01:30 LT and 13:30 LT are during the growing phase of the convection, respectively, averaged over the period of DJF 2004-2017.

L210: more important –> larger OK
L232: lightnings are created into –> lightning is created in OK
L233: lightnings –> lightning OK

L244: the pervasive lack of superscripts in units (e.g., "month -1", "mg m-3", "m s-1","mm h-1") is puzzling, given that superscripts are used for other purposes, but it is only a trivial annoyance in most places in the manuscript. In the case of Flash, however, it is a bigger issue, since it is hard to read "10-2- 10-3" in this line. Sometimes the units on Flash are given as per day and sometimes as day-1. Also, I don't think it is true that Flash values are lower than 10-2 per day over New Guinea, at least not in the interior of the island.

We changed the superscripts in units.

P12, Fig. 5: It would be more convenient if the y-axis for Prec had 4 (not 3) minor tickmarks, as is the case for the IWC y-axis. The solid and dashed lines should also be described in the caption. OK

L246: Fig. 2c –> Fig. 2d OK
L252 (also L264, 269, 314): as noted above, the panels in Fig. 7 are mislabeled Corrected, see below.

P14, Figure 7: It would be very helpful to have more minor tick marks on the x-axis. In the caption: full line –> solid line; dash –> dashed OK

L289: delete “areas” OK
L289-290: add commas after “(2008)” and “1 mm h^{-1}” OK
L294: add commas after ”6h” and “Flash” OK
L299: it might be good to remind readers that the elevation is shown in Fig. 2b OK
L302: than Java –> as Java OK
L304: maintaining –> maintain OK
L305: rainfalls –> rainfall OK
L306: convections –> convection OK
P16-17, Figs. 8 and 9: again, it would be very helpful to have more minor tick marks on the x-axis. Also for Fig. 9, the label for the North Australia Sea is given in panel (b) and the figure caption as “NAusSea”, but in the main text it is “NAuSea”. The labels should be consistent. OK

L312-313: it would be clearer to say “either coastline or offshore areas depending onthe area” OK

L320: most of –> most OK

L332: In the next section –> In Section 7 OK

P19, Fig. 10: It would aid the comparisons with Fig. 2e discussed in the text if the same color bar were used, particularly since the ERA5 IWC values reach higher values than those of MLS, yet the color bar in Fig. 2e extends to larger values. This might also alleviate the issue that the highest values of ERA5 IWC over New Guinea and North Australia appear to saturate the color bar in Fig. 10 (that is, white colors appear in the map in those regions).

Fig. 10 is presented at 0.25°x0.25° while Fig. 2 is presented at 2°x2°. According to us, it is not needed to use the same color bar, because the horizontal degradation from 0.25°x0.25° to 2°x2° tends to decrease the averaged values per pixel. Thus it is not pertinent to compare the scale value between the Fig. 10 and Fig. 2. However, it is interesting to compare the areas of maxima and minima over these two maps.

Also, since panels (c) and (d) have been labeled “TL”, it would be good to add “UT” to panels (a) and (b).

OK

L340 (also L342, 347, 366, 373, 377, 391): island –> islands OK
L344: is –> are OK
L353: cycles –> cycle; zone –> zonesOK
L363: calculated –> calculateOK
L366: Fig. 10a –> Fig. 11aOK
L368: excepted –> except OK
L370: from –> byOK
L372: twice greater than –> twice as large as; also delete “values”OK
L373: Fig. 10b –> Fig. 11bOK
P21, Fig. 11 caption: West Sumatra Coast (WSS) –> West Sumatra Sea (WSS)OK
L390: why are there parentheses around the convolved ERA5ΔIWC term in this line?OK
L406: to within –> by OK

L410: observational –> observations OK
L412: negligeable –> negligible OK
L414: are –> is; twice larger than –> twice as large as OK
L433: merged –> merging OK
L433 (also L516): tiny –> small (not only does “tiny” not sound very scientific, but also it could come across as dismissive) OK
L436: transport –> transports OK
L437: Fig. 10 shows IWC, not ΔIWC, so it should not be listed with Fig. 4 here; perhaps Fig. 11 was meant instead OK
L439: section 4.3 –> section 4.2 OK
L442: Awaka (1998) –> (Awaka, 1998); to –> fromOK
L446: “PR” has already been defined in L441OK
L453: Fig. 10 –> Fig. 11OK
L462: would be –> isOK
L479: from by –> from OK
L481: to impact –> injecting OK
L482: into –> in OK
L495: amount –> amounts OK
L500 (also L504, 517): combination between –> combination of OK
L510: delete commas after “that” and “Flash” OK
L513: delete commas after “Guinea” and “Sulawesi”; range –> ranges OK
L514: as Java –> than Java OK
L516: cumulus merged –> merged cumulus OK

Anonymous Referee #2
Received and published: 19 November 2019

The paper by Dion et al. is the second part of a work aiming at quantifying the diurnal cycle of ice particles in the tropical tropopause layer (TTL), and more precisely, the amount of ice injected by deep convection up the tropospheric part of the TTL, and up to the tropopause. It is mostly based on the analysis of 13 years of ice water content (IWC) data from MLS onboard the AURA satellite, as well as precipitations data from TRMM, and lightning flashes from the LIS instrument onboard TRMM. While the first part of the study, already published in ACP, is dedicated to the study of all tropical regions over the globe, this companion paper only focuses on the Maritime Continent (MariCont) during the austral convective season of December January and February, because the MariCont has been shown to be one of the most efficient tropical regions to transport ice up to the TTL in Dion et al. (2019). Here the study focuses on each sub-region of the Maritime Continent, that is the different islands and seas composingit. The main contribution from this study is to present the Maritime Continent not as awhole continent but as the sum of very different contributions. It was already shownin the first paper that the land parts had a different impact and cycle than the oceanicpart. Here the authors are going further in estimating the climatological contributionof each main islands and seas of the MariCont. For example, Java and New Guinea are shown to be the main contributors in the transport of ice up to the TTL. In thatsense, this innovative work and point of view deserve a publication. Before it can be done, I have major comments and minor comments that should be addressed

before the paper can be accepted in ACP. Some of them can be easily addressed by adding explanations and references, some others may require additional calculations.

Major comments:

Instrumental part:
Information is missing in the description of the satellite products that are used. Most of all, I would expect information on the accuracy, precision, or biases for MLS IWC, TRMM prec, and TRMM LIS (detection limit, false detection of fashes, etc). See “minor comments” for details.

We added more information for MLS IWC, TRMM prec and TRMM Flash.
Firstly, we added to the 2.1 MLS IWC paragraph, L94:

> … In our study, high spatial resolution study is now possible because we consider 13 years of MLS datasets, allowing to average the IWC^{MLS} measurements within the bins of horizontal resolution of 2°×2°(~230 km). We select IWC^{MLS} during all austral convective seasons DJF between 2004 and 2017. The IWC measurements were filtered following the recommendation of the MLS team described in Liversey et al. (2018). The resolutions of IWC^{MLS} (horizontal along the path, horizontal perpendicular to the path, vertical) measured at 146 and 100 hPa are 300x7x4 km and 250x7x5 km, respectively. The precision of the measurement is 0.10 mg m^{-3} at 146 hPa and 0.25 to 0.35 mg m^{-3} at 100 hPa. The accuracy is 100 % for values less than 10 mg m^{-3} at both levels and the valid range is 0.02-50.0 mg.m^{-3} at 146 hPa and 0.1-50.0 mg m^{-3} at 100 hPa (Wu et al., 2008).

We added the following sentence into the paragraph 2.3 TRMM-LIS, previously modified P.4-5 of the present document:

> LIS is thus able to provide the number of flashes (Flash) measured. The TRMM LIS detection efficiency ranges from 69% near noon to 88% at night.

More details about the accuracy, precision, or biases of each instrument has been described P4-5 and 6 of the present document.

The use of ERA 5 to estimate ΔIWC. I have a significant problem with this part. ERA5 is a relatively new reanalysis from ECMWF. The Authors are using ERA5 ice products to compare ΔIWC from satellite observations and from ERA5. But here, no reference is made on any estimation of the quality of ice from ERA5, nor how the ice is provided or calculated in ERA5. Is ice assimilated in the ECMWF model? If yes, from which instrument?

IWC is not assimilated but modeled in ECMWF. See explanations below (P30) providing more information and references about the use of ERA5.

If not, how it is calculated, is there a correlation between the ice product and any reported bias in ECMWF model ? As a consequence, is ΔIWC^{ERA5} used to validate ΔIWC^{Prec}, and ΔIWC^{Flash}, or should it be understood the other way round? To make a meaningful comparison between both types of estimation, all of this question should be addressed in

the manuscript.

We do not use ΔIWC^{ERA5} in order to 'validate' ΔIWC^{Prec}, and ΔIWC^{Flash}, but in order to assess the amounts estimated by our model.

We added more detail on ERA5 in the paragraph 2.4 ERA5, L127:

> … The present study uses the IWC^{ERA5} at 100 and 150 hPa averaged over DJF from 2005 to 2016 with one-hour temporal resolution. IWC^{ERA5} is governed by the model microphysics which allows ice supersaturation with respect to ice (100-150% RH) but not with respect to liquid water. Although microwave radiances at 183 GHz (sensitive to atmospheric scattering induced by ice particles) (Geer et al., 2017) are assimilated, cloud and precipitations are used as control variable in the 4D-Var assimilation system and cannot be adjusted independently in the analysis (Geer et al., 2017). The microwave data have sensitivity to the frozen phase hydrometeors but mainly to larger particles, such as those in the cores of deep convection (Geer et al., 2017), but the sensitivity to cirrus clouds in ERA5 is strongly dependent on microphysical assumptions on the shape and size of the cirrus particles. Indirect feedbacks are also acting on cirrus representation in the model – e.g. changing the intensity of the convection will change the amount of outflow cirrus generated. This is why observations that affects the troposphere by changing for example the stability, the humidity, or the synoptic situation can affect the upper level ice cloud indirectly (Geer et al., 2017). IWC^{ERA5} is used to assess the amount of ice injected in the UT and the TL as estimated by the model developed in Dion et al., (2019) and in the present study.

Geer, A. J., Baordo, F., Bormann, N., Chambon, P., English, S. J., Kazumori, M., ... & Lupu, C. (2017). The growing impact of satellite observations sensitive to humidity, cloud and precipitation. *Quarterly Journal of the Royal Meteorological Society*, *143*(709), 3189-3206.

Lopez, P. (2011). Direct 4D-Var assimilation of NCEP stage IV radar and gauge precipitation data at ECMWF. *Monthly Weather Review*, *139*(7), 2098-2116.

A sentence, described P.15 of the present document, has also been added L335 to remind the motivation to use IWC from ERA5.

Furthermore, to my knowledge, the ice in ERA5 is composed of 2 different variables. Are you using the total ice, or only one parameter (which should be non-precipitating ice)? The authors should be more explicit on this point and justify the choice of the variable they have used.

This point has been already developped in the replies to the reviewer « 1 's comments L121-132. We have changed sentences in the section 2.4.

More details about the accuracy, precision, or biases of each instrument has been described P4-5 and 6 in the replies to the reviewer #1.

Winds from NCEP. In Section 8, winds from NCEP are used instead of winds of ERA5. It is stated that ERA5 winds are not available. For sure they are. What would be the results shown in Fig 12 if ERA5 winds were used? Does it impact the duration of transport of ice from North Australia land to seas westward?

We have choosen to delete the Fig. 12 as well as the discussion about this figure in section 8. Thus, the paragraph describing NCEP has also been deleted. See more justification P.6 and 20-21 in the replies to the reviewer # 1.

Minor comments:

- Abstract: one of the key highlights of the study is to present the MariCont as a jigsaw puzzle of different contributions with respect to the effect of deep convection on ice in the TTL. For example, Java and New Guinea are presented as very efficient locations for the injection of ice into the TTL. Thus to me, some key findings on the effect of subregions of the MariCont should appear in the abstract.

We added some information on the abstract as follow L22-23:

> Finally, from IWC^{ERA5}, Prec and Flash, this study highlights 1) ΔIWC over land has been found larger than ΔIWC over sea with a limit at 4.0 mg m^{-3} in the UT between minimum of ΔIWC estimated over land and maximum of ΔIWC estimated over sea, and 2) small islands with high topography present the strongest amounts of ΔIWC such as the Java Island, the area of the largest ΔIWC in the UT (7.9 – 8.7 mg m^{-3} daily mean).

- L11 Lightning is always singular. See also p4 and p11. OK

- Introduction L31. Jensen et al. (2007) are providing important inputs on the effect of deep convection on the hydration or dehydration in the TTL. It seems appropriate to cite this study here.

We added Jensen et al., 2007 L.31 and in the reference list.

Jensen, E. J., Ackerman, A. S., & Smith, J. A. (2007). Can overshooting convection dehydrate the tropical tropopause layer?. *Journal of Geophysical Research: Atmospheres*, *112*(D11).

- Section 2.1: though the reference for the MLS ice product is given, no information is given on the accuracy and the uncertainties on the IWC. Please add it.

We added information in the Section 2.1 MLS IWC. See the replies to the reviewer #1 (P.26).

- Section 2.1 L90. This sentence is not clear to me. Please rephrase. At least it should be explained why you need the averaging Kernel at 100 hPa and 146 hPa.

We decided to delete the sentence. Since IWC from MLS is retrieved using optimal estimate theory, averaging kernels do not exist for IWC. We changed the previous sentence L90 by the following one:

> ~~Since the averaging kernels ofIWCMLSare not provided by MLS, we will use an unitary triangular function centered at 14690and 100 hPa, having a width at half-maximum of 4 and 5 km, respectively to represent the averaging Kernels of MLS IWC at146 and 100 hPa (see section 7.2).~~ Although optimal estimation is used to retrieve almost all other MLS products, a cloud-induced radiance technique is used to estimate the MLS IWC (Wu et al., 2008; Wu et al., 2009).

See replies to the reviewer #1 to have more information about the ERA5 vertical degradation as a function the IWC MLS box function.

- **Section 4.1** L170: there is a very strong contrast in the maximum time of Prec between land and coastal region. If convection and Prec maxima are due to a sea breeze effect and orography over land, as stated before, why coastal region maximum of Prec is clearly not influenced by the sea breeze (otherwise the time of maximum of Prec should not be so different)? On the other hand, the coastal behavior seams relatively independent from the oceanic behavior since the oceanic behavior is very dependent on the sea considered, whereas the Prec maximum for coastal region is relatively well identified. A longer comment or hypothesis should be presented here to explain this behaviour.

Sea breeze impacts the land convection at the end of the day, when land temperature surface is higher than oceanic temperature surface: maximum of Prec is observed at the end of the day (15-24h). Over coasts, because the sea-breeze transports air masses from the sea to the land at the end of the day, the conditions are not favorable for the development of the convection. This is only once the sea breeze is stopped/reduced that the convection can be strong over coast: time of the observed maximum of Prec is during night-morning (0-6h) over coasts. Then, during the night-morning, the sea surface temperature become larger than the land surface temperature (water releases its heat much slower than land causing the air over the water to be warmer than the air over the land) and the land-breeze favours the convection development over coasts and sea (time of the maximum of Prec over sea is observed mainly in the morning-noon: 09-12h and 15-24h depending of the sea considered).

We have inserted the following sentence L.200:

> Areas where the daily mean of Prec is maximum are usually surrounding the highest elevation over lands (e.g. over the New Guinea) and near coastal areas (North West of Borneo in the China Sea and South of Sumatra in the Java Sea) (Fig. 2b and c). ~~Qian (2008) explained that high precipitation is mainly concentrated over lands in the MariCont because of the strong sea-breeze convergence, combinedwith the mountain–valley winds and cumulus merging processes. The diurnal maximum of Prec over land is observed between 18:00 LT and 00:00 LT (Fig. 2d) whereas, over coastal parts, it is in the early morning before 05:00 LT.~~ ~~Over seas, the time of the diurnal maximum varies as a function of the region. Java Sea and North of Australia Sea present maxima around 13:30LT while the west Sumatra Sea and the Bismark Sea show maxima around 01:30 LT.~~ The times of the maxima of Prec are over land, during

the evening (18:00-00:00 LT), over coast during the night-morning (00:00-06:00 TL) and over sea during the morning-noon and even evening depending of the sea considered (09:00-12:00 LT and 15:00-00:00 LT). These differences could illustrate the impact of the land/sea breeze within the 24 hours. The sea breeze during the day favours the land convection at the end of the day when land temperature surface is higher than oceanic temperature surface. During the night, the coastline sea surface temperature becomes larger than the land surface temperature and the land-breeze favours systematically the convection development over coast. These observations are consistent with results presents in Qian (2008), explaining that high precipitation is mainly concentrated over land in the MariCont because of the strong sea-breeze convergence, but also because of the combination with the mountain–valley winds and cumulus merging processes. Amplitudes of the diurnal cycles of Prec over the MariCont will be detailed as a function of islands and sea in section 5.

- Section 4.2 about Fig. 3. From what I understand, the number of occurrences (=cases per pixel that are during the growing phase at 13:30 or 01:30) on which the average/the anomaly is calculated depends on the pixel. What is the amplitude of the number of occurrences to get this figure?

We selected at least 60 measurements of Prec or IWC at 13:30 LT or 01:30 LT per pixel of 2°x2° over the period 2004-2017. We already provided more information about this question into the replies to the rewiever #1.

- Section 4 Fig. 4. This is one of the key finding of the publication. However, I am surprised that qualitatively, the same patterns are found at 146 hPa and at 100 hPa, the only difference being the scale. I would expect a slightly different behavior at 100hPa because the ice amount might be also driven by other processes than just deep convection (e.g. in situ formation of cirrus or ice particles close to the tropopause). Does the result mean that other processes than deep convection are negligible, or cannot be detected by this method or the instrument? A discussion should be given at the end of the comment of Fig. 4.

ΔIWC is the amount of ice injected by deep convection (during the growing phase of the convection). Thus other processes are not considered into the calculation of ΔIWC. Dion et al. (2019) have suggested that the main process controlling ΔIWC is the deep convective process. Authors also suggest that other processes such as the in situ formation of ice, the sublimation, precipitation, horizontal advection, … are minor during the growing phase of the deep convection and could become major after the growing phase of the deep convection (namely during the decreasing phase). However, ot is out of the scope of the present paper to estimate the impact of each process on the diurnal cycle of IWC during the decreasing phase. Thus, authors have suggested that the growing phase of the diurnal cycle of Prec, representative of the growing phase of the deep convection, is correlated with the growing phase of ice into the UT and the TL. Thus, the only difference between ΔIWC into the UT and the TL is the amount of ice measured by MLS at 01:30 or 13:30 LT. The following discussion has been added L211:

… altitude is larger over land (by a factor 6) than over sea (by a factor 3). We can note that the similar pattern between the two layers come from the diurnal

cycle of Prec in the calculation of ΔIWC at 146 and 100 hPa. Only the measured value of IWC^{MLS} at 146 and 100 hPa can explain the observed differences in ΔIWC values at these two levels. Thus, similar ΔIWC patterns are expected between the two levels because, according to the model developed in Dion et al. (2019), the deep convection is the main process transporting ice into the UT and the TL during the growing phase of the convection. Convective processes associated to ~~these~~ land and sea are further discussed in Sect. 6.

- Section 4.3 : 228 “this shows that...” Ok but what can we learn about the diurnal cycle or the intensity of deep convection from this correlation?

We deleted the following sentence :

> ~~This shows that ΔIWC is strongly correlated with the shape of the diurnal cycle of Prec.~~

- Section 5 l231: potential energy –> electric potential energy OK

- Section 5.2, l254. The choice of 5 pixels over the sea from the land limits: why this choice? Was a sentivity test made on the number of pixel to infer the behavior of coastal regions?

We did a sensitivity test in order to select the exact number of pixels that were the most representative of the coastal areas. We observed that considering less than 5 pixels is too low and decrease the signal-to-noise ratio, while considering more than 5 pixels presents no differences with the offshore sea signal. The following sentence has been changed:

> MariCont-C is the average of all coastlines defined as 5 pixels extending into the sea from the land limit. This choice of 5 pixels has been taken applying some sentitivity tests in order to have the best compromise between a high signal-to-noise ratio and a good representation of the coastal region.

- L255: 10 pixels offshore for oceanic behavior. Please justify.

We justified it in the following sentence :

> The MariCont_O is the average of all offshore pixels defined as sea pixels excluding 10 pixels (~2000 km off the land) over the sea from the land coasts, thus coastline pixels are excluded as well as all the coastal influences. MariCont_L is the area of all land pixels.

- P14 fig 7 and results from it. There is a mismatch between the titles of the middle and bottom panels and the corresponding figure captions.

We already answered to this mismatch into the replies to the reviewer #1.

Middle panel is entitled Mari-Con_C and It is captioned MariCont_O. The other way round

for the bottom panel. In a general manner, the results for the coasts are relatively close to the one offshore. At least the time shift is weaker between MariCont_O Vs MariCont_C than for MariCont_C Vs. MariCont_L. Is the choice of 5 pixels from the land to define the MariCon_C has something to do with it? What if you had chosen 3 or 2 pixels only? Would the coastal diurnal cycle of Prec and FLash be closer to the Land cycle?

Diurnal cycles of Prec or Flash considering 2 or 3 pixels presented a too low signal-to-noise ratio to be interpreted. A number of pixels greater than 5 in the definition of the coastal region produced diurnal cycles of Prec or Flash to be the same than that over the offshore region.

- P15: References Liu and Zipser (2008) and (2009) appear in the text but not in the reference list.

P3, L71 has been changed has follow :

> ...an alternative proxy for deep convection as shown by Liu and Zipser (2009~~8~~)

P15 : Liu and Zipser (2008) is now in the reference list.

- Fig 8 and 9. The ERA5 IWC is also presented in the figures and is not commented in section 5. This does not make any problem since it is commented later on in section 6 but at least, a sentence should inform that the ERA5 results would be commented later.

A sentence L.291 has been added as follow:

> Diurnal cycles of Prec and Flash are presented over land for a) Java, b) Borneo, c) New Guinea, d) Sulawesi and e) Sumatra as shown in Figure 8 and over sea for the a) Java Sea, b) North Australia Sea (NAuSea), c) Bismark Sea, d) West Sumatra Sea (WSumSea) and e) China Sea as shown in Figure 9. Diurnal cycles of IWC from ERA5 (IWC^{ERA5}) are also presented in Fig. 8 and 9 and will be discussed in Section 6.

About the same figs in **section 6**, L346: it would be interesting to over plot an equivalent value of the MLS IWC and comment it. As written in my major comment, there no real estimation of the ice product in ERA5. Adding the MLS IWC here could give an idea of a potential bias in the reanalysis.

Thank you, it is good idea. However, we have chosen not to add the diurnal cycle of IWC estimated from IWC^{MLS} and Prec, nor the one estimated from IWC^{MLS} and Flash because the figure becomes unreadable due to many curves on each figure. Furthermore, the model developed on Dion et al. (2019) although producing a full diurnal cycle of IWC, is only valid during the increasing phase. Thus, the Fig. 11 is relevant to show the differences between the estimated IWC and the one of IWC^{ERA5} during the increasing phase of the diurnal cycle. Finally, by definition of eq (1), the shape of the diurnal cycle of the estimated IWC from IWC^{MLS} and Prec and from IWC^{MLS} and Flash would be exactly the same as the shape of the diurnal cycle of Prec and Flash, respectively.

In **section 6** the authors comment on the consistency or the inconsistency of the ERA5 IWC diurnal cycle with the Prec one. But no reason or hypothesis are given to explain this disagreement. I wish a discussion appeared at the end of section 6 on that point.

We are not able to explain or hypothesize the differences observed over sea. However we can clarify the sentence L.359 as follow (the deleted sentence was deleted and changed following a comment by Michelle Santee explained on P13-14 of the present document):

> Over Bismark Sea, the diurnal maxima of IWC^{ERA5} is found at 04:00 LT with a second peak later at noon. Over West Sumatra Sea, two diurnal maxima are found at 08:00 LT and 17:00 LT. Over China Sea, the diurnal maximum of IWC^{ERA5} is found at 16:00 LT and a second peak is found at 08:00 LT. ~~Over West Sumatra Sea and China Sea, the two maxima in the diurnal cycle of IWC^{ERA5} are not observed in the diurnal cycle of Prec and Flash, consequently the increasing phase of IWC^{ERA5} is not consistent with the one of Prec nor the one of Flash.~~ These differences in the timing of the maximum of the diurnal cycle of Prec, Flash and IWC^{ERA5} observed at small-scale over sea of the MariCont are not well understood. However, these differences do not impact on the calculation of the ΔIWC^{Prec}, ΔIWC^{Flash} or ΔIWC^{ERA5}. Results are presented Section 7.

- Section 7. Before reading the whole paper, I did not understand why results from ΔIWC offshore could be given for flash since it was shown previously that IWC^{Flash} are not synchronous over seas. Thus, one could deduce that the method to estimate IWC (and ΔIWC) cannot be applied offshore. We understand later that some regions are better described by the IWC^{Flash} approach than by the IWC^{Prec}, due for example, to the higher contribution of stratiform Prec. So in section 7.1, the part where Fig11 is presented and commented, it should be justified more clearly why ΔIWC^{Prec} and ΔIWC^{Flash} can be presented as a range of observational ΔIWC.

We clarified the use of the two proxies L363:

> Figure 11 synthesizes ΔIWC in the UT and the TL over the 5 islands and 5 seas of the MariCont studied in the previous section. Eqs. (1-3) are used to calculate ΔIWC from Prec (ΔIWC^{Prec}) and from Flash (ΔIWC^{Flash}). As presented in the previous section, Prec and Flash can be used as two proxies of deep convection, with differences more or less accentuated in their diurnal cycles as a function of the region considered. Thus, the observational ΔIWC range calculated between ΔIWC^{Prec} and ΔIWC^{Flash} provides an upper and lower bound of ΔIWC calculated from observational datasets.

In **section 7.2** p20 and 22. It would be interesting to recall here the number of model levels from 150 to 100 hPa to have an idea of the vertical resolution of the undegraded ERA5 data.

The previous paragraph has been changed as follow according to the review of Michelle Santee. We added the last sentence in clear blue in order to recall the number of model level used in the calculation:

> In order to compare IWC^{MLS} and IWC^{ERA5}, we firstly degraded the horizontal resolution of ERA5 from 0.25°x0.25° to 2°x2° (~200 kmx200 km) and secondly, we degraded the vertical distribution of IWC^{ERA5} ($IWC^{ERA5}(z_0)$) following a unitary box function whose width is 5 and 4 km at 100 and 146 hPa, respectively.

Thus, the available IWC^{ERA5} at 175 hPa and the one at 70 hPa have been used in the calculation of the convolved IWC^{ERA5}.

- **7.3** Obviously, a comparison section is needed here, but without describing how ERA5 ice is produced/calculated, the results presented here are meaningless. I do not say it is out of interest to do so. There is probably something to learn in this comparison (for example from the fact that over seas, ERA5 ΔIWC is systematically lower than the observational ΔIWC), but here one must be aware the meaning of the product used.

We detailed how IWC^{ERA5} is calculated in section 2.4 ERA5 Ice. At present, no more interpretation can be done regarding the differences highlighted.

- L418. Considering the large range of ERA5 to <ERA5>, the numbers given may not be representative.

The sentence L417-418 has been deleted:

> ~~Whatever the datasets used, the vertical distribution ofΔIWC in the TTL has shown a gradient of - 6 mg m-3 between the UTand the TL over land compared to a gradient of - 2 mg m-3 between the UT and the TL over ocean.~~

- **Section 8.3** L459. I would have added Corti et al. (2008) for the references concerning Hector.

This part of the paragraph has been deleted. See answer P.20-21 of the present document.

- Section 8.3 from L465. See my major comment about the NCEP winds.

This part of the paragraph has been deleted. See answer P.20-21 of the present document.

- L471 and 472. Ice in the UT and at the tropopause is not a passive tracer. So, to state that, an estimation of the lifetime of ice particles for both altitudes should be given.

This part of the paragraph has been delated. See answer P.20-21 of the present document.

- L503 “consistent to within 75 % over seas”. This corresponds to a relatively fair agreement, and the use of “consistent” seams exaggerated.

The percentage has been corrected as follow :

... consistent to within 30-50 % over seas in the UT ...

- L517. “ΔIWC is a combination...” Again, you can write this statement only if you show that the lifetime of ice particle is long enough for such a transport.

This sentence L517 has been deleted.

~~Over sea areas,ΔIWC is a combination between the vertical transport of air masses by deep convectionduring night and early morning over offshore sea and by the westward horizontal transport of air masses near the tropopause,coming from land through coastline areas, during the end of the afternoon and at night (such as in North of Australia seas).~~

Suggested references:

- Jensen, E.J., A.S. Ackerman, and J.A. Smith, 2007: Can overshooting convection dehydrate the tropical tropopause layer? J. Geophys. Res.,112, D11209, doi:10.1029/2006JD007943.

- Corti, T., et al. (2008), Unprecedentedevidence for deep convection hydrating the tropical stratosphere, Geophys. Res. Lett.,35, L10810, doi:10.1029/2008GL033641.

Ice injected into the tropopause by deep convection – Part 2: Over the Maritime Continent

Dion Iris-Amata[1], Dallet Cyrille[1], Ricaud Philippe[1], Carminati Fabien[2], Haynes Peter[3], and Dauhut Thibaut[4]

[1]CRNM, Meteo-France - CNRS, Toulouse, 31057, France
[2]Met Office, Exeter, Devon, EX1 3PB, UK
[3]DAMTP, University of Cambridge, Cambridge, CB3 0WA, UK
[4]Max Planck Institute for Meteorology, Hamburg, Germany

Correspondence: Iris-Amata Dion (iris.dion@meteo.fr)

Abstract. The amount of ice injected up to the tropical tropopause layer has a strong radiative impact on climate. In the tropics, the Maritime Continent (MariCont) region presents the largest injection of ice by deep convection into the upper troposphere (UT) and tropopause level (TL) (from results presented in the companion paper Part 1). This study focuses on the MariCont region and aims to assess the processes, the areas and the diurnal amount and duration of ice injected by deep convection over islands and over seas using a 2° × 2° horizontal resolution during the austral convective season of December, January and February. The model presented in the companion paper is used to estimate the amount of ice injected (ΔIWC) up to the TL by combining ice water content (IWC) measured twice a day in tropical UT and TL by the Microwave Limb Sounder (MLS; Version 4.2), from 2004 to 2017, and precipitation (Prec) measurement from the Tropical Rainfall Measurement Mission (TRMM; Version 007) at high temporal resolution (1 hour). The horizontal distribution of ΔIWC estimated from Prec (ΔIWC^{Prec}) is presented at 2° × 2° horizontal resolution over the MariCont. ΔIWC is also evaluated by using the number of lightning events (Flash) from the TRMM-LIS instrument (Lightning Imaging Sensor, from 2004 to 2015 at 1-h and 0.25°×0.25°resolutions). ΔIWC^{Prec} and ΔIWC estimated from Flash (ΔIWC^{Flash}) are compared to ΔIWC estimated from the ERA5 reanalyses (ΔIWC^{ERA5}) degrading the vertical resolution to that of MLS observations ($\langle \Delta IWC^{ERA5} \rangle$). Our study shows that, while the diurnal cycles of Prec and Flash are consistent to each other in timing and phase over lands and different over offshore and coastal areas of the MariCont, the observational ΔIWC range between ΔIWC^{Prec} and ΔIWC^{Flash} is small (they agree to within 4 – ~~20~~22% over land and to within ~~6~~ 7 – ~~50~~53% over ocean) in the UT and TL. The reanalysis ΔIWC range between ΔIWC^{ERA5} and $\langle \Delta IWC^{ERA5} \rangle$ has been also found to be small in the UT (~~22~~ 4 – ~~32~~ 29 %) but large in the TL (~~68~~ 55 – ~~71~~ 78 %), highlighting the stronger impact of the vertical resolution on the TL than in the UT. Combining observational and reanalysis ΔIWC ranges, the total ΔIWC range is estimated in the UT between ~~4.17 and 9.97 mg m~~4.2 and 10.0 mg m^{-3} (20 % of variability per study zone) over land and between ~~0.35 and 4.37 mg m~~0.3 and 4.4 mg m^{-3} (30% of variability per study zone) over sea, and, in the TL, between ~~0.63 and 3.65 mg m~~0.6 and 3.9 mg m^{-3} (70% of variability per study zone) over land and between ~~0.04 and 0.74 mg m~~0.1 and 0.7 mg m^{-3} (80% of variability per study zone) over sea. Finally, from IWC^{ERA5}, Prec and Flash, this study highlights 1) ΔIWC over land has been found larger than ΔIWC over sea with a limit at 4.0 mg m^{-3} in the UT between minimum of ΔIWC estimated over land and maximum of ΔIWC estimated over

sea, and 2) small islands with high topography present the strongest amounts of ΔIWC such as the Java Island, the ~~Java Island is the~~ area of the largest ΔIWC in the UT (~~7.89~~ 7.7 – ~~8.72 mg m~~9.5 mg m^{-3} daily mean).

1 Introduction

In the tropics, water vapour (WV) and ice cirrus clouds near the cold point tropopause (CPT) have a strong radiative effect on climate (**?**) and an indirect impact on stratospheric ozone (**?**). WV and water ice crystals are transported up to the tropopause layer by two main processes: a three-dimensional large-scale slow process (3-m month $^{-1}$), and a small scale fast convective process (diurnal timescale) (e.g. **??**). Many studies have already shown the impact of convective processes on the hydration of the atmospheric layers from the upper troposphere (UT) to the lower stratosphere (LS) ~~(e.g. **???**)~~(e.g. **????**). However, the amount of total water (WV and ice) transported by deep convection up to the tropical UT and LS is still not well understood. The vertical distribution of total water in those layers is constrained by thermal conditions of the CPT (**?**). During deep convective events, **?** have shown that air masses transported up to 146 hPa in the UT and up to 100 hPa in the tropopause layer (TL) have ice to total water ratios of more than 50% and 70%, respectively, and that ice in the UT is strongly spatially correlated with the diurnal increases of deep convection, while WV is not. **?** hence focused on the ice phase of total water to estimate the diurnal amount of ice injected into the UT and the TL over convective tropical areas, showing that it is larger over land than over ocean, with maxima over land of the Maritime Continent (MariCont), the region including Indonesian islands. For these reasons, the present study is focusing on the MariCont region in order to better understand small-scale processes impacting the diurnal injection of ice up to the TL.

A method to estimate the amount of ice injected into the UT and up to the TL over convective areas and during convective seasons has been proposed by **?**. This method provides an estimation of the amplitude of the diurnal cycle of ice in those layers using the twice daily Ice Water Content (IWC) measurements from the Microwave Limb Sounder (MLS) instrument and the full diurnal cycle of precipitation (Prec) measured by the Tropical Rainfall Measurement Mission (TRMM) instrument, at one hour resolution. The method first focuses on the increasing phase of the diurnal cycle of Prec (peak to peak from the diurnal Prec minimum to the diurnal Prec maximum) and shows that the increasing phase of Prec is consistent in time and in amplitude with the increasing phase of the diurnal cycle of deep convection, over tropical convective zones and during convective season. The amount of ice (ΔIWC) injected into the UT and the TL is estimated by relating IWC measured by MLS during the growing phase of the deep convection to the increasing phase of the diurnal cycle of Prec. **?** conclude that deep convection over the MariCont region is the main process impacting the increasing phase of the diurnal cycle of ice in those layers.

The MariCont region is one of the main convective ~~centers~~ center in the tropics with the wettest troposphere and the coldest and driest tropopause (**???**). **?** have shown that over the Indonesian area, the phase of the convective activity diurnal cycle drifts from land to coastlines and to offshore areas. Even though authors have done a comprehensive work around the study

of the diurnal cycle of precipitation and convection over the MariCont, the diurnal cycle of ice injected by deep convection up to the TL over this region is still not well understood. **?** have tentatively evaluated the upper tropospheric diurnal cycle of ice from Superconducting Submillimeter-Wave Limb-Emission Sounder (SMILES) measurements over the period 2009-2010 but without differentiating land and sea over the MariCont, which caused their analysis to show little diurnal variation over that region. **?** have 1) highlighted that the MariCont must be considered as two separate areas: the MariCont land (MariCont_L) and the MariCont ocean (MariCont_O), with two distinct diurnal cycles of the Prec and 2) estimated the amount of ice injected in the UT and the TL. Over these two domains, it has also been shown that convective processes are stronger over MariCont_L than over MariCont_O. Consequently, the amount of ice injected in the UT and the TL is greater over MariCont_L than over MariCont_O. ~~Considering a higher horizontal resolution over small islands and seas~~

Building upon the results of **?**, the present study aims to improve the methodology of Dion et al. (2019) by i) studying smaller study zones than in Dion et al. (2019) and by distinguishing island and sea of the MariCont~~and investigating other~~ , ii) assessing the sensitivity of model to different proxies of deep convection ~~, the authors were expected a better characterisation of the~~ and iii) assessing the amount of ice injected ~~up to the TTL. Building upon the results of **?**, the present study is addressing the evaluation of~~ in the UT and the TL inferred by our model to that of ERA5 reanalyses. Based on space-borne observations and meteorological reanalyses, ΔIWC ~~at a~~ is assessed at a horizontal resolution of $2° \times 2°$ over 5 islands (Sumatra, Borneo, Java, Sulawesi and New Guinea) and 5 seas (West Sumatra Sea, Java Sea, China Sea, North Australia Sea, and Bismark Sea) of the MariCont during convective season (December, January and February, hereafter DJF) from 2004 to 2017. ΔIWC will be first estimated from Prec measured by TRMM-3B42. A sensitivity study of ΔIWC based on the number of flashes (Flash) detected by the TRMM Lightning Imaging Sensor (TRMM-LIS), an alternative proxy for deep convection as shown by Liu and Zipser (~~2009~~2008), is also proposed. Finally, we will use IWC calculated by the ERA5 reanalyses from 2005 to 2016 to estimate ΔIWC in the UT and the TL over each study zone and compare it to ΔIWC estimated from Prec and Flash.

The observational datasets used in our study are presented in Sect. 2. Method is recalled in Sect. 3. The amount of ice (ΔIWC) injected up to the TL estimated from Prec is evaluated in Sect. 4. Diurnal cycles of Prec and Flash are compared to each other over different areas of the MariCont in Sect. 5. Results of the estimated ΔIWC injected up to the UT and the TL over five islands and five seas of the MariCont are presented and compared with the ERA5 reanalyses in Sect. 6. Results are discussed in Sect. 7, and conclusions are drawn in Sect. 8. This paper contains many abbreviations and acronyms. To facilitate reading, they are compiled in the Acronyms list.

2 Datasets

This section presents the instruments and the reanalyses used for this study.

2.1 MLS Ice Water Content

The Microwave Limb Sounder (MLS, ~~Version~~ data processing algorithm version 4.2) instrument on board NASA's Earth Observing System (EOS) Aura platform ~~(?)~~ (??) launched in 2004 provides ice water content (IWC^{MLS}, mg m~~) measurementsat~~

$^{-3}$) measurements. MLS provides IWC^{MLS} are given at 6 levels in the UTLS (82, 100, 121, 146hPa (in the UT), 177 and at 215). However, we have chosen to study only two levels: an upper and a lower level of the TTL. Because the level at 82 hPa does not provide enough significant measurements of IWC to have a good signal-to-noise, we have selected 2 levels: 1) at 100 hPa (in the TL)as the upper level of the TTL (named TL for tropopause level), and 2) at 146 hPa as the lower level of the TTL (named UT for upper tropopshere). MLS follows a sun-synchronous near-polar orbit, completing 233 revolution cycles every 16 days, with daily global coverage every 14 orbits. The instrument is crossing twice a day the equator at fixed time, measuring IWC^{MLS} at 01:30 local time (LT) and 13:30 LT. The horizontal resolution of IWC^{MLS} measurements is $\sim$ 300 and 7 km along and across the track, respectively. The vertical resolution of IWC^{MLS} is 4 and 5 km at 146 and 100 hPa, respectively. Since the averaging kernels of IWC^{MLS} are not provided by MLS , we will use an unitary triangular function centered at 146 and 100 hPa, having a width at half-maximum of 4 and 5 km, respectively, to represent the averaging Kernels of MLS IWC at 146 and 100 hPa (see section **??**Although optimal estimation is used to retrieve almost all other MLS products, a cloud-induced radiance technique is used to validate the MLS IWC (Wu et al., 2008; Wu et al., 2009). In our study, high spatial horizontal resolution is now possible because we consider 13 years of MLS data, allowing to average the IWC^{MLS} measurements within the bins of horizontal resolution of 2° ×2° ($\sim$ 230 km). We select IWC^{MLS} during all austral convective seasons DJF between 2004 and 2017. The IWC measurements were filtered following the recommendations of the MLS team described in **?**. The resolutions of IWC^{MLS} (horizontal along the path, horizontal perpendicular to the path, vertical) measured at 146 and 100 hPa are 300×7×4 km and 250×7×5 km, respectively. The precision of the measurement is 0.10 mg m^{-3} at 146 hPa and 0.25 to 0.35 mg m^{-3} at 100 hPa. The accuracy is 100% for values less than 10 mg m^{-3} at both levels and the valid range is 0.02-50.0 mg m^{-3} at 146 hPa and 0.1-50.0 mg m^{-3} at 100 hPa (Wu et al., 2008).

2.2 TRMM-3B42 Precipitation

The Tropical Rainfall Measurement Mission (TRMM) was launched in 1997 and provided measurements of Prec until 2015. TRMM is composed of five instruments, three of them are complementary sensor rainfall suite (PR, TMI, VIRS). TRMM had an almost circular orbit at 350 km altitude height performing a complete revolution in one and a half hour. The 3B42 algorithm product (TRMM-3B42) (version V7) has been created to estimate the precipitation and extend the precipitation product through 2019. Thus, the TRMM-3B42 , a Prec dataset is based on TRMM observations is a multi-satellite precipitation analysis composing a Global Precipitation Measurement (GPM) Mission. TRMM-3B42 is computed from the various precipitation-relevant satellite passive Microwave (PMW) sensors using GPROF2017 computed at the Precipitation Processing System (PPS) (e.g., GMI, DPR, Ku, Ka, Special Sensor Microwave Imager/Sounder [SSMIS], etc.) and including TRMM measurements from 1997 to 2015 and provides Prec data from 1997 to 2019 (Huffman et al., 2007, 2010; and Huffman and Bolvin, 2018). Work is currently underway with NASA funding to develop more appropriate estimators for random error, and to introduce estimates of bias error (Huffman and Bolvin, 2018). Prec data are provided at a 0.25° × 0.25° ($\sim$ 29.2 km) horizontal resolution, extending from 50° S to 50° N (https://pmm.nasa.gov/data-access/downloads/trmm, last access: April 2019). Prec from TRMM-3B42 products depends on input from microwave and IR sensors (**?**) and does not differentiate between stratiform and convective precipitation. In our study, Prec from TRMM-3B42 is selected over the austral convective seasons (DJF) from 2004 to 2017

and averaged to a horizontal grid of 2° ×2° to be compared to IWC^{MLS}. ~~As the TRMM orbit precesses,~~ The granule temporal coverage of TRMM-3B42 data is 3 hours, but the temporal resolution of individual measurements is 1 minute. Thus, it is statistically possible to degrade the resolution to 1 hour. TRMM-3B42 are provided in Universal Time that we converted into local time (LT). Details of the ~~diurnal cycle of Prec averaged over the study period is calculated with a 1-h temporal resolution~~binning methodology of TRMM-3B42 is provided by Huffman and Bolvin (2018).

2.3 TRMM-LIS number of Flashes

The Lightning Imaging Sensor (LIS) aboard of the TRMM satellite measures several parameters relative to lightning. According to Christian et al. (2000), LIS used a Real-Time Event Processor (RTEP) that discriminates lightning event from Earth albedo light. ~~The instrument in itself was composed of a grid of 128 × 128 detectors allowing to observe a point within 90 seconds with a temporal resolution of 2 milliseconds.~~ A lightning event corresponds to the detection of a light anomaly on a pixel representing the most fundamental detection of the sensor. After a spatial and temporal processing, the sensor was able to characterize a flash from several detected events. The instrument detects lightning with storm-scale resolution of 3-6 km (3 km at nadir, 6 km at limb) over a large region (550-550 km) of the Earth's surface. LIS horizontal resolution is provided at 0.25°×0.10°. A significant amount of software filtering has gone into the production of science data to maximize the detection efficiency and confidence level. Thus, each datum is a lightning signal and not noise. Furthermore, the weak lightning signals that occur during the day are hard to detect because of background illumination. A real-tile event processor removes the background signal to enable the system and detect weak lightning and achieve a 90% detection efficiency during the day. LIS is thus able to provide the number of flashes (Flash) measured. The ~~LIS~~ TRMM LIS detection efficiency ranges from 69% near noon to 88% at night. The LIS instrument performed measurements between 1 January 1998 and 8 April 2015. To be as consistent as possible to the MLS and TRMM-3B42 period of study, we are using LIS measurements during DJF from 2004 to 2015. ~~LIS spatial resolution varies between 3 km at nadir and 6 km off-nadir.~~ The observation range of the sensor is between 38° N and 38° S. As LIS is on the TRMM platform, with an orbit that precesses, Flash from LIS can be averaged to obtain the full 24-h diurnal cycle of Flash over the study period with a 1-h temporal resolution. In our study, Flash measured by LIS is studied at 0.25° × 0.25° horizontal resolution to be compared to Prec from TRMM-3B42.

2.4 ERA5 Ice Water Content

The European Centre for Medium-range Weather Forecasts (ECMWF) Reanalysis 5, known as ERA5, replaces the ERA-Interim reanalyses as the fifth generation of the ECMWF reanalysis providing global climate and weather for the past decades (from 1979) (**?**). ERA5 provides hourly estimates for a large number of atmospheric, ocean and land surface quantities and covers the Earth on a 30 km grid with 137 levels from the surface up to a height of 80 km. ~~Cloud ice water content from~~ Reanalyses such as ERA5 ~~reanalyses (~~provide a physically constrained, continuous, global, and homogeneous representation of the atmosphere through a large number of observations (space-borne, air-borne, and ground-based) with short-range forecasts. Although there is no direct observation of atmospheric ice content in ERA5, the specific cloud ice water content (mass of condensate / mass of moist air) (IWC^{ERA5}) ~~comes from the combination of a large amount of global historical observations,~~

advanced modelling and data assimilation systems (https://cds.climate.copernicus.eu/cdsapp!/dataset/reanalysis-era5-pressure-levels-month to the changes in the analysed temperature (and at low levels, humidity) which is mostly driven by the assimilation of temperature-sensitive radiances from satellite instruments (https://cds.climate.copernicus.eu/cdsapp!/dataset/reanalysis-era5-pressure-level tab=form, last access: July 2019). IWC^{ERA5} used in our analysis is representative of non-precipitating ice. Precipitating ice, classified as snow water, is also provided by ERA5 but not used in this study in order to focus only on the injected and non-precipitating ice into the TTL. Furthermore, results from Duncan and Eriksson (2018) have highlighted that ERA5 is able to capture both seasonal and diurnal variability in cloud ice water but the reanalyses exhibit noisier and higher amplitude diurnal variability than borne out by the satellite estimates. The present study uses the IWC^{ERA5} at 100 and 150 hPa averaged over DJF from 2005 to 2016 with one hour one-hour temporal resolution. IWC^{ERA5} is governed by the model microphysics which allows ice supersaturation with respect to ice (100-150% in relative humidity) but not with respect to liquid water. Although microwave radiances at 183 GHz (sensitive to atmospheric scattering induced by ice particles) (Geer et al., 2017) are assimilated, cloud and precipitations are used as control variable in the 4D-Var assimilation system and cannot be adjusted independently in the analysis (Geer et al., 2017). The microwave data have sensitivity to the frozen phase hydrometeors but mainly to larger particles, such as those in the cores of deep convection (Geer et al., 2017), but the sensitivity to cirrus clouds in ERA5 is strongly dependent on microphysical assumptions on the shape and size of the cirrus particles. Indirect feedbacks are also acting on cirrus representation in the model – e.g. changing the intensity of the convection will change the amount of outflow cirrus generated. This is why observations that affects the troposphere by changing for example the stability, the humidity, or the synoptic situation can affect the upper level ice cloud indirectly (Geer et al., 2017). IWC^{ERA5} is used to assess the amount of ice injected in the UT and the TL as estimated by the model developed in Dion et al. (2019) and in the present study. IWC^{ERA5} have been degraded along the vertical at 100 and 150 hPa ($\langle \Delta IWC^{ERA5} \rangle$) consistent consistently with the MLS vertical resolution of IWC^{MLS} (5 and 4 km at 100 and 146 hPa, respectively) using an unitary triangular function , in the absence of IWC averaging kernels by MLS box function (see section **??**). IWC^{ERA5} and $\langle \Delta IWC^{ERA5} \rangle$ will be both considered in this study. IWC^{ERA5}, initially provided in kg kg^{-1}, has been converted into mg m^{-3} using the temperature provided by ERA5 in order to be compared with MLS IWC observations.

2.5 NOAA Winds

Because wind provided by ERA5 is not available at 100 and 150 hPa, our study uses the wind datasets from the National Centers For Environmental Prediction (NCEP) Global Data Assimilation System (GDAS), initialized analyses, provided by the National Oceanic and Atmospheric Administration (NOAA). NOAA provides vertical distribution of daily East-West and North-South wind components in the range between -75 to 107 m s, from 1997 to 2019 (, last access: 8 July 2019). 12 vertical levels are available from 50 to 1000 hPa at global scale. Our study selects the daily mean of wind speed and direction at 100 and 150 hPa in DJF from 2004 to 2017.

3 Methodology

This section summarizes the method developed by **?** to estimate ΔIWC, the amount of ice injected into the UT and the TL. **?** have presented a model relating Prec (as proxy of deep convection) from TRMM to IWC^{MLS} over tropical convective areas during austral convective season DJF. The IWC^{MLS} value measured by MLS during the growing phase of the convection (at x = 01:30 LT or 13:30 LT) is compared to the Prec value at the same time x in order to define the correlation coefficient (C) between Prec and IWC^{MLS}, as follows:

$$C = \frac{Prec_x}{IWC_x^{MLS}} \frac{IWC_x^{MLS}}{Prec_x} \tag{1}$$

The diurnal cycle of IWC estimated ($IWC^{est}(t)$) can be calculated by using C applied to the diurnal cycle of Prec (Prec(t)), where t is the time, as follows:

$$IWC^{est}(t) = Prec(t) \times C \tag{2}$$

The amount of IWC injected up to the UT or the TL (ΔIWC^{Prec}) is defined by the difference between the maximum of IWC^{est} (IWC$^{est}_{max}$) and its minimum (IWC$^{est}_{min}$).

$$\Delta IWC^{Prec} = C \times (Prec_{max} - Prec_{min}) = IWC^{est}_{max} - IWC^{est}_{min} \tag{3}$$

where $Prec_{max}$ and $Prec_{min}$ are the diurnal maximum and minimum of Prec, respectively. Figure **??** illustrates the relationship between the diurnal cycle of Prec and the two MLS measurements at 01:30 LT and 13:30 LT. The growing phase of the convection is defined as the period of increase in precipitation from $Prec_{min}$ to $Prec_{max}$. The amplitude of the diurnal cycle is defined by the difference between $Prec_{max}$ and $Prec_{min}$. In Fig. 1, because the growing phase of the convection illustrated is happening during the afternoon, only the MLS measurement at 13:30 LT is used in the calculation of ΔIWC. IWC at 01:30 LT is not used in that case.

4 Horizontal distribution of ΔIWC estimated from Prec over the MariCont

4.1 Prec from TRMM related to IWC from MLS

In order to identify the main areas of injection of ice in the TL over the MariCont, Figure **??** presents different parameters associated to this area: a) the name of the main islands and seas over the MariCont, b) the elevation (http://www.soda-pro.com/web-services/altitude/srtm-in-a-tile, last access: June 2019), c) the daily mean of Prec at 0.25° × 0.25° horizontal resolution, d) the hour of the diurnal maxima of Prec at 0.25° × 0.25° horizontal resolution, and e) the daily mean

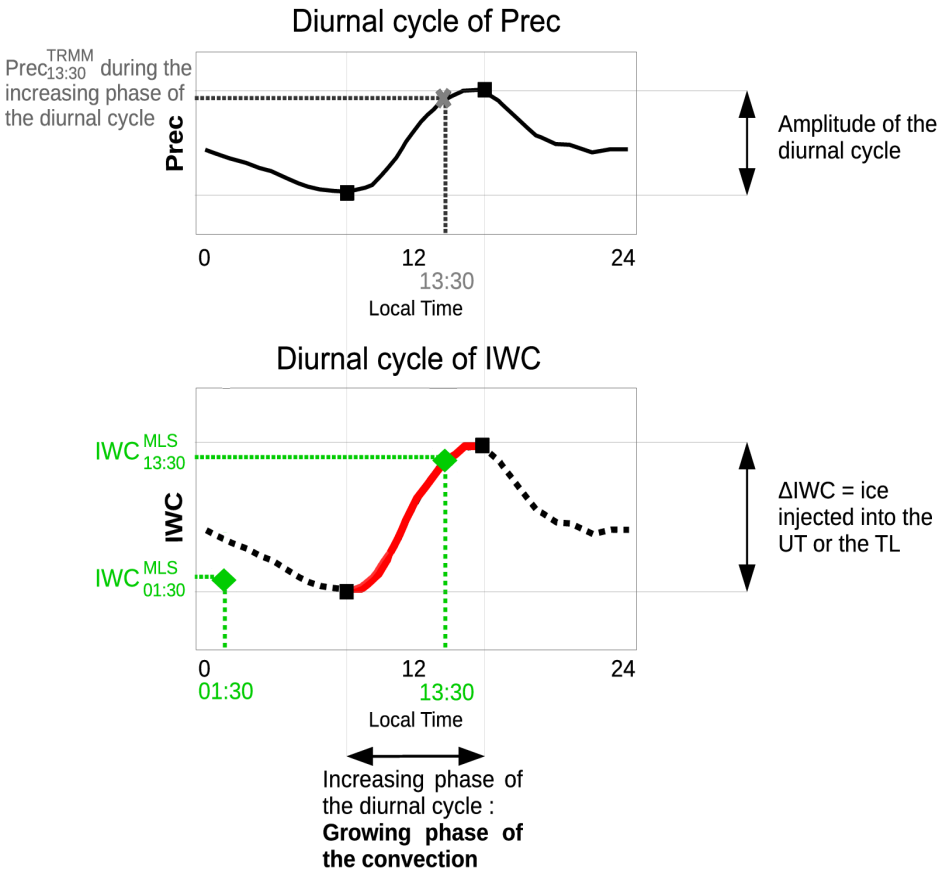

Figure 1. Illustration of the model used to estimate the amount of ice (ΔIWC) injected into the UT or the TL. Diurnal cycle of a proxy of deep convection (Prec) (a), diurnal cycle of ice water content (IWC) estimated from diurnal cycle of the proxy of deep convection (b). In red line, the increasing phase of the diurnal cycle. In black dashed line, the decreasing phase of the diurnal cycle. The green diamonds are the two IWC^{MLS} measurements from MLS. Grey thick cross represents the measurement of Prec during the growing phase of the convection ($Prec_x$), used in the model. Maximum and minimum of the diurnal cycles are represented by black squares. Amplitude of the diurnal cycle is defined by the differences between the maximum and the minimum of the cycle.

$(\bar{IWC} = (IWC_{01:30} + IWC_{13:30}) \times 0.5)$ of IWC^{MLS} at 146 hPa at 2° × 2° horizontal resolution. Several points need to be highlighted. Daily means of Prec over land and coastal parts are higher than over oceans (Fig. **??**c). Areas where the daily mean of Prec is maximum are usually surrounding the highest elevation over land (e.g. over NewGuinea) and near coastal areas (North West of Borneo in the China Sea and South of Sumatra in the Java Sea) (Fig. **??**b and c). ~~**?** explained that high precipitation is mainly concentrated over land in the MariCont because of the strong sea-breeze convergence, combined with~~

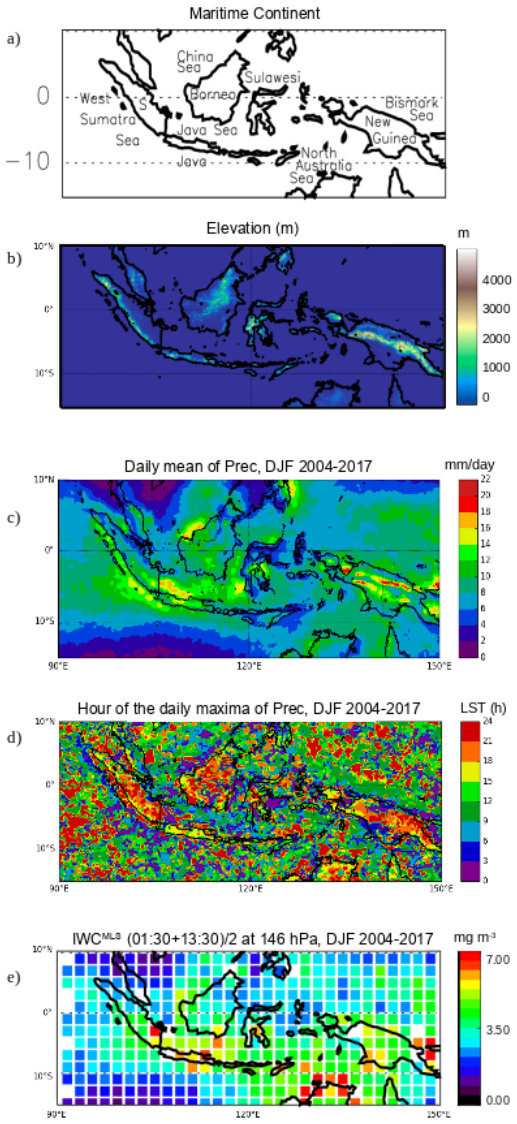

Figure 2. Main islands and seas of the MariCont (S is for Sumatra) (a), elevation from Solar Radiation Data (SoDa) (b); daily mean of Prec measured by TRMM over the Maritime Continent, averaged over the period of DJF 2004-2017 (c), hour (local solar time (LST)) of the diurnal maxima of Prec over the MariCont (d); daily mean (01:30 LT + 13:30 LT)/2 of IWC^{MLS} at 146 hPa from MLS over the MariCont averaged over the period of DJF 2004-2017 (e). ~~Horizontal~~ Observations are presented with a horizontal resolution of $0.25^\circ \times 0.25^\circ$ (b,c and d) and $2^\circ \times 2^\circ$ (e).

~~the mountain–valley winds and cumulus merging processes. The diurnal maximum of Prec over land is observed between~~ The times of the maxima of Prec are over land during the evening (18:00-00:00 LT~~and~~), over coast during the night-morning (00:00-06:00 ~~LT (Fig. **??**d) whereas, over coastal parts, it is in the early morning before 05:~~TL) and over sea during the

morning-noon and even evening depending of the sea considered (09:00-12:00 LT ~~. Over seas, the time of the diurnal maximum varies as a function of the region. Java Sea and North of Australia Sea present maxima around 13~~and 15:~~30 LT while the west Sumatra Sea and the Bismark Sea show maxima around 01~~00-00:~~30 LT~~00 LT). These differences could illustrate the impact of the land/sea breeze within the 24 hours. The sea breeze during the day favours the land convection at the end of the day when land temperature surface is higher than oceanic temperature surface. During the night, the coastline sea surface temperature becomes larger than the land surface temperature and the land breeze favours systematically the convection development over coast. These observations are consistent with results presented in **?**, explaining that high precipitation is mainly concentrated over land in the MariCont because of the strong sea-breeze convergence, but also because of the combination with the mountain–valley winds and cumulus merging processes. Amplitudes of the diurnal cycles of Prec over the MariCont will be detailed as a function of island and sea in section **??**. The location of the largest concentration of IWC (3.5 – 5.0 mg m^{-3}, Fig. **??**e) is consistent with that of Prec ($\sim$ 12 – 16 mm day^{-1}) over the West Sumatra Sea, and over the South of Sumatra island. However, over North Australia seas (including the Timor Sea and the Arafura Sea), we observed large differences between Prec low values (4 – 8 mm day^{-1}) and IWC large concentrations (4 – 7 mg m^{-3}).

4.2 Convective processes compared to IWC measurements

Although TRMM horizontal resolution is 0.25° × 0.25°, we require information at the same resolution as MLS IWC. From the diurnal cycle of TRMM Prec measurements, the duration of the increasing phase of Prec can be known for each 2° × 2° pixel. The duration of the growing phase of the convection can then be defined from Prec over each pixel. Figures **??**a and b present the anomaly (deviation from the mean) of Prec measured by TRMM–3B42 over the MariCont at 01:30 LT and 13:30 LT, respectively, only over pixels when the convection is in the growing phase. The anomaly of IWC measured by MLS over the MariCont is shown in Figs. **??**c and d, over pixels when the convection is in the growing phase at 01:30 LT and 13:30 LT, respectively. ~~Note that some pixels can be present~~ Each pixel of Prec at 01:30 LT or 13:30 LT during the growing phase of the convection deviates by the average of the all Prec at 01:30 LT or 13:30 LT during the growing phase of the convection over the whole MariCont. The gray color denotes pixels for which convection is not ongoing. Some pixels can be presented on both sets of Prec and IWC panels in Figs. ~~**??** only when~~3 when: 1) the onset of the convection is before 01:30 LT and the end is after 13:30 LT or ~~when~~ 2) the onset of the convection is before 13:30 LT and the end is after 01:30 LT. Note that, whithin each 2°x2° pixel, at least 60 measurements of Prec or IWC at 13:30 LT or 01:30 LT over the period 2004-2017 have been selected for the average.

The Prec anomaly at 01:30 LT and 13:30 LT varies between -0.15 and +0.15 mm h~~. At 13:30 LT, the~~ $^{-1}$. The growing phase of the convection ~~is mainly over land while, at 01~~over land is mainly at 13:30 LT~~, the growing phase of the convection is mainly over seas and coastlines. The strongest Prec anomaly~~ . At 13:30 LT, over land, the strongest Prec and IWC anomalies (+0.15 mm h~~) at 13:30 LT is~~ $^{-1}$ and +2.50 mg m^{-3}, respectively) are found over the Java island, ~~while the strongest Prec anomaly at~~ and north of Australia for IWC. At 01:30 LT~~is found over~~ , the growing phase of the convection is found mainly over sea (while the pixels of the land are mostly gray), with maxima of Prec and IWC anomalies over coastlines and seas close to the coasts such as the ~~West Sumatra Sea~~ Java Sea and the Bismark Sea. The IWC anomaly at 13:30 LT and 01:30 LT varies between

-3 and +3 mg m~~. The strongest value of IWC anomaly at 13:30 LT are found over Java, while the strongest values of IWC anomaly at 01:30 LT is found over coastlines and seas close to the coasts, such as the North Australia Sea, Java Sea, China Sea and coast around NewGuinea.~~ $^{-3}$. Three types of areas can be distinguished from Fig. **??**: i) area where Prec and IWC anomalies have the same sign (positive or negative either at 01:30 LT or 13:30 LT) (e.g. over Java, Borneo, Sumatra, Java Sea and coast of Borneo or the China Sea); ii) area where Prec anomaly is positive and IWC anomaly is negative (e.g. over West Sumatra Sea); and iii) area where Prec anomaly is negative and IWC anomaly is positive (e.g. over the North Australia Sea at 01:30 LT). Convective processes associated to these three types of areas over islands and seas of the MariCont are discussed in Sect. 6.

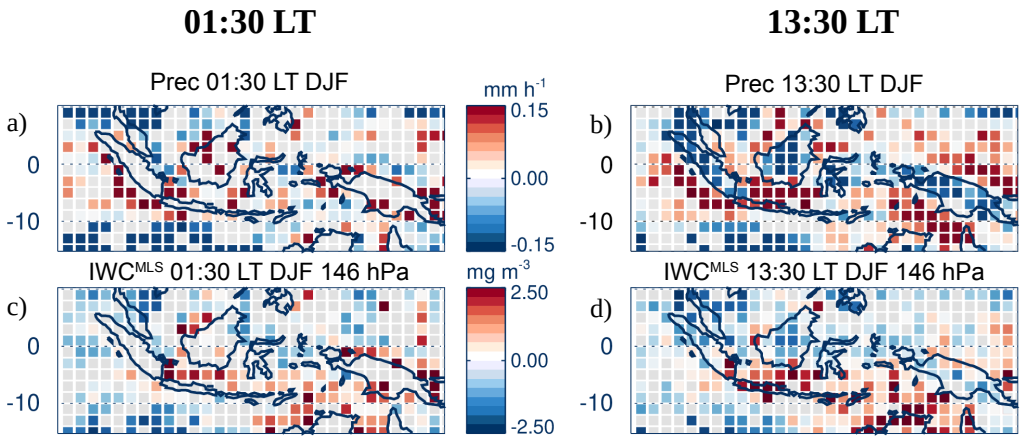

Figure 3. Anomaly (deviation from the mean) of Prec (a-b) and Ice Water Content (IWC^{MLS}) at 146 hPa (c-d), at 01:30 LT (left) and at 13:30 LT (right) over pixels where 01:30 LT and 13:30 LT are during the growing phase of the convection, respectively, averaged over the period of DJF 2004-2017. The gray color denotes pixels for which convection is not ongoing.

4.3 Horizontal distribution of ice injected into the UT and TL estimated from Prec

From the model developed in **?** based on Prec from TRMM–3B42 and IWC from MLS and synthesized in section 2.4, we can calculate the amount of IWC injected (ΔIWC) at 146 hPa (UT, Figure **??**a) and at 100 hPa (TL, Figure **??**b) by deep convection over the MariCont. In the UT, the amount of IWC injected over land is larger (> 10 – 20 mg m^{-3}) than over seas (< 10 mg m^{-3}). South of Sumatra, Sulawesi, North of New Guinea and North of Australia present the largest amounts of ΔIWC over land (15 – 20 mg m^{-3}). Java Sea, China Sea and Bismark Sea present the largest amounts of ΔIWC over seas (7 – 15 mg m^{-3}). West Sumatra Sea and North Australia Sea present low values of ΔIWC (< 2 mg m^{-3}). We can note that the anomalies of Prec and IWC during the growing phase over ~~West Sumatra Sea~~ North Australia Sea at 13:30 LT are positive (~~< 0.15 mg m~~> 0.2 mg m^{-3}, Fig. **??**a and b and > ~~2.50 mg m~~2.5 mg m^{-3}, Fig. **??**c and d, respectively). In the TL, the maxima (up to ~~3 mg m~~3.0 mg

m^{-3}) and minima (down to ~~2~~ 0.2 – ~~3 mg m~~0.3 mg m^{-3}) of ΔIWC are located within the same pixels as in the UT, although 3 ~~– 4~~ to 6 times lower than in the UT. The decrease of ΔIWC with altitude is larger over land (by a factor 6) than over sea (by a factor 3). We can note that the similar pattern between the two layers come from the diurnal cycle of Prec in the calculation of ΔIWC at 146 and 100 hPa. Only the measured value of IWC^{MLS} at 146 and 100 hPa can explain the observed différences in ΔIWC values at these two levels. Thus, similar ΔIWC patterns are expected between the two levels because, according to the model developed in Dion et al. (2019), the deep convection is the main process transporting ice into the UT and the TL during the growing phase of the convection. Convective processes associated to ~~these~~ land and sea are further discussed in Sect. 6.

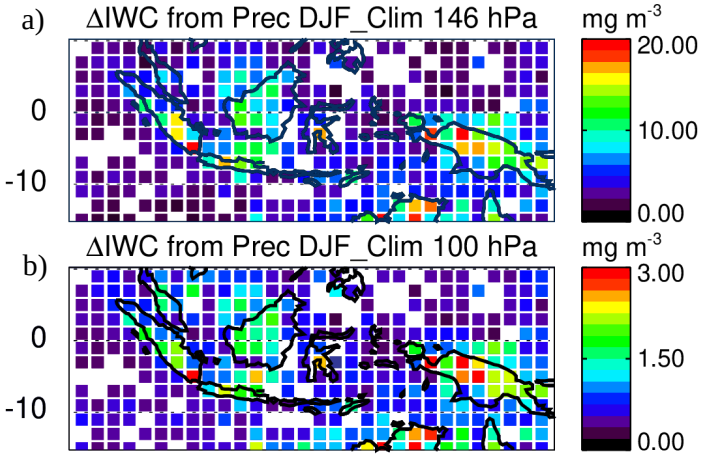

Figure 4. Daily amount of ice injected (ΔIWC) up to the UT (a) and up to the TL (b) estimated from Prec, averaged during DJF 2004-2017.

In order to better understand the impact of deep convection on the strongest ΔIWC injected per pixel ~~into the UT and the TL~~up to the TTL, isolated pixels selected in Fig. ~~4~~ 4a are presented separately in Figure **??**a and f. This Figure shows the diurnal cycles of Prec in four pixels selected for their large ΔIWC in the UT (≥ 15 mg m^{-3}, Fig. **??**b, c, d, e), and the diurnal cycle of Prec in four pixels selected for their low ΔIWC in the UT (but large enough to observe the diurnal cycles of ~~Prec~~ IWC between 2.0 and 5.0 mg m^{-3}, Fig. **??**g, h, i, j). Pixels with low values of ΔIWC over land (Figs. **??**g, h and i) present small amplitude of diurnal cycles of Prec (∼ +0.5 mm h^{-1}), with maxima between 15:00 LT and 20:00 LT and minima around 11:00 LT. The pixel with low value of ΔIWC over sea (Fig. **??**j) presents an almost null amplitude of the diurnal cycle of Prec with low value of Prec all day long (∼ 0.25 mm h^{-1}). Pixels with large values of ΔIWC over land (Fig. **??**b, c, d, e) present longer duration of the increasing phase of the diurnal cycle (from ∼ 09:00 LT to 20:00 – 00:00 LT) than the increasing phase of Prec diurnal cycle over pixels with low values of ΔIWC (from 10:00 LT to 15:00 – 19:00 LT). More precisely, pixels labeled 1 and 2 over New Guinea (Fig. **??**d and e) and the pixel over South of Sumatra (Fig. **??**c) show amplitude of diurnal cycle of Prec reaching 1.0 mm h^{-1}, while the pixel over North Australia (Fig. **??**b) presents lower amplitude of diurnal cycle of Prec (0.5 mm h^{-1}).

IWC measured by MLS during the growing phase of deep convection and the diurnal cycle of IWC estimated from Prec are also shown on Fig. **??**. For pixels with large values of ΔIWC, IWC observed by MLS is between 4.5 and 5.7 mg m^{-3} over North Australia Sea, South Sumatra and New Guinea. For pixels with low values of ΔIWC, IWC observed by MLS is found between 1.9 and 4.7 mg m^{-3}. To summarize, large values of ΔIWC are observed over land in combination to i) longer growing phase of deep convection (> 9 hours) ~~, ii) high value of IWC (> ~4.5 mg m) at 13:30 LT over land and01:30 LT over seas, and~~and/or ~~iii~~ii) large diurnal amplitude of Prec (> 0.5 mm h~~). This shows that ΔIWC is strongly correlated with the shape of the diurnal cycle of Prec.~~$^{-1}$).

In the next section, we estimate ΔIWC using another proxy of deep convection, namely Flash measurements from LIS.

5 Relationship between diurnal cycle of Prec and Flash over MariCont land and sea

Lightning is created into cumulonimbus clouds when the electric potential energy difference is large between the base and the top of the cloud. Lightning can appear at the advanced stage of the growing phase of the convection and during the mature phase of the convection. For these reasons, in this section, we use Flash measured from LIS during DJF 2004-2015 as another proxy of the deep convection in order to estimate ΔIWC (ΔIWC^{Flash}) and check the consistency with ΔIWC obtained with Prec (ΔIWC^{Prec}).

5.1 Flash distribution over the MariCont

Figure **??**a presents the daily mean of Flash in DJF 2004-2015 at 0.25° × 0.25° horizontal resolution. Over land, Flash can reach a maximum of 10~~flashes per day~~$^{-1}$ flashes day^{-1} per pixel while, over seas, Flash are less frequent (∼ 10~~flashes per day~~$^{-3}$ flashes day^{-1} day per pixel). When compared to the distribution of Prec (Fig. **??**c), maxima of Flash are found over the same areas as maxima of Prec (Java, East of Sulawesi coast, Sumatra and North Australia lands). Over Borneo and NewGuinea, coastlines present more Flash (∼10~~flashes per day~~$^{-2}$ flashes day^{-1}) than inland (∼10~~flashes per day~~$^{-3}$ flashes day^{-1}). Differences between Flash and Prec distributions are found over North Australia Sea, with relatively large number of Flash (∼ >10~~flashes per day~~$^{-2}$ flashes day^{-1}) compared to low Prec (4 – 10 mm day^{-1}) (Fig. **??**c), and over NewGuinea where the number of Flash is relatively low (∼10^{-2}- 10~~flashes day~~$^{-3}$ flashes day^{-1}) while Prec is high (∼14 – 20 mm day^{-1}). Figure **??**b shows the hour of the Flash maxima. Over land, the maximum of Flash is between 15:00 LT and 19:00 LT, slightly earlier than the maximum of Prec (Fig. **??**d) observed between 16:00 LT and 24:00 LT. Coastal areas present similar hours of maximum of Prec and Flash, i.e between 00:00 LT and 04:00 LT although, over the West Sumatra Coast, diurnal maxima of both Prec and Flash happen 1–4 hours earlier (from 23:00-24:00 LT) than those of other coasts.

5.2 Prec and Flash diurnal cycles over the MariCont

This section compares the diurnal cycle of Flash with the diurnal cycle of Prec in order to assess the potential for Flash to be used as a proxy of deep convection over land and sea of the MariCont. Diurnal cycles of Prec and Flash over the MariCont land, ~~offshore and coastline~~ coastline and offshore (MariCont_L, MariCont_~~O MariCont-C~~C, MariCont_O, respectively) are

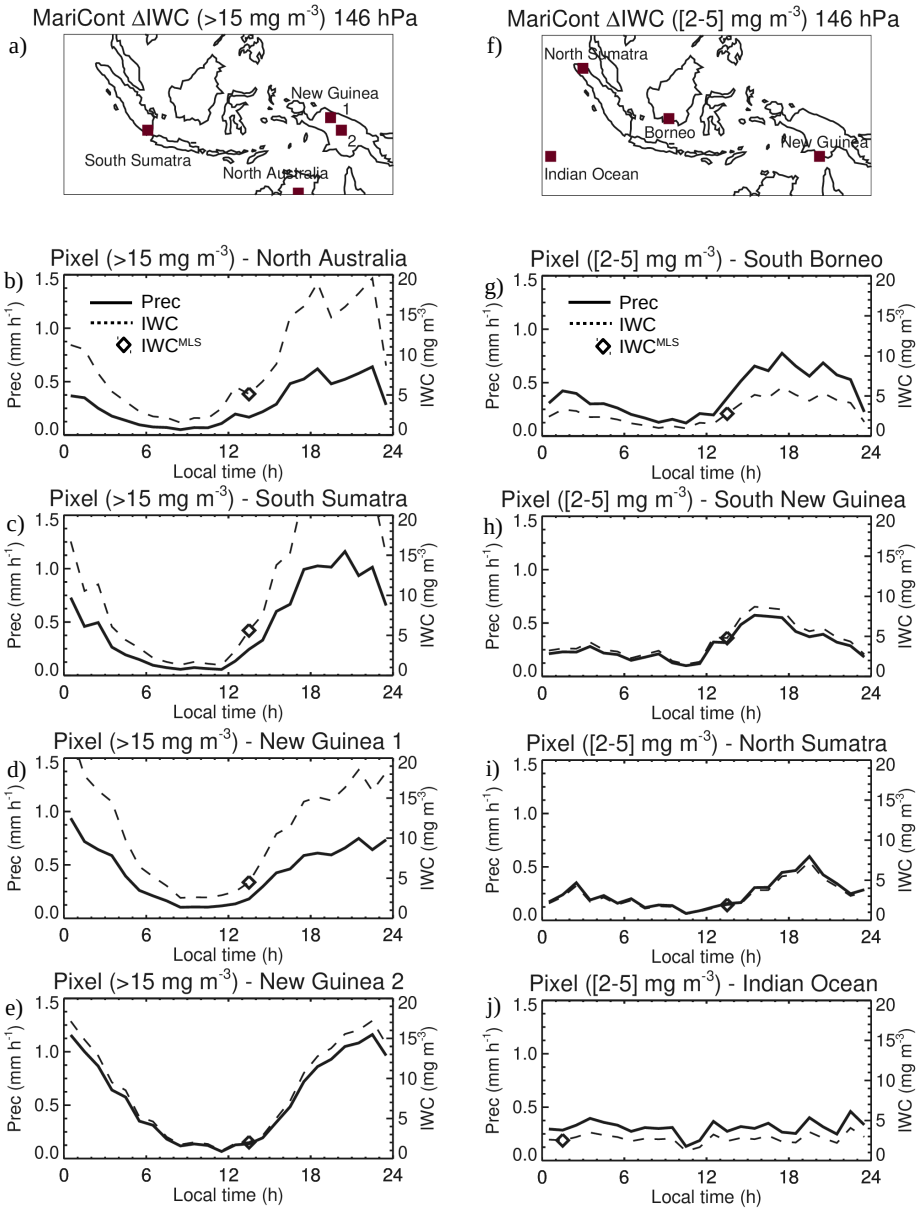

Figure 5. a) and f) location of 2° × 2° pixels where ΔIWC have been found higher than 15 mg m^{-3} (in Fig. 4) and where ΔIWC have been found between 2 and 5 mg m^{-3} (in Fig. 4), respectively. Diurnal cycle of Prec (solid line): (b, c, d, e) over 4 pixels where ΔIWC have been found higher than 15 mg m^{-3} (in Fig. 4), (g, h, i, j) over 4 pixels where ΔIWC have been found between 2 and 5 mg m^{-3} (in Fig. 4), during DJF 2004-2017. The Diamond is IWC^{MLS} measured by MLS during the increasing phase of the convection. The dashed line is the diurnal cycle of IWC estimated from the diurnal cycle of Prec and from IWC^{MLS}.

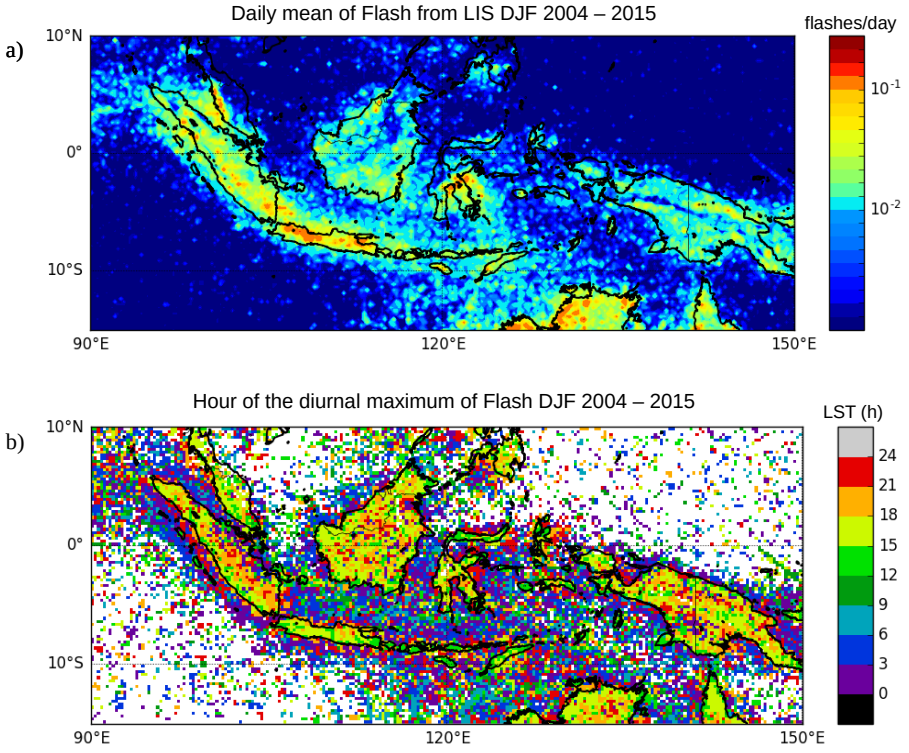

Figure 6. Daily mean of Flash measured by LIS averaged over the period DJF 2004-2015 (a); Hour (local solar time (LST)) of the diurnal maximum of Flash (b).

shown in Figs. **??**a–c, respectively. Within each 0.25° × 0.25° bin, land/coast/ocean ~~/coast~~filters were applied from the Solar Radiation Data (SoDa, http://www.soda-pro.com/web-services/altitude/srtm-in-a-tile). ~~MariCont_C~~ MariCont_C is the average of all coastlines defined as 5 pixels ~~over~~ extending into the sea from the land ~~limits.~~ limit. This choice of 5 pixels has been taken applying some sensitivity tests in order to have the best compromise between a high signal-to-noise ratio and a good representation of the coastal region. The MariCont_O is the average of all offshore pixels defined as sea pixels excluding 10 pixels (2000 km off the land) over the sea from the land coasts, thus coastline pixels are excluded as well as all the coastal influences. MariCont_L is the area of all land pixels. A given 0.25° ×0.25° pixel can contain information from different origins : land/coastlines or sea/coastlines. In that case, we can easily discriminate between land and coastlines or sea and coastlines by applying the land/ocean/coastlines filters. Consequently, this particular pixel will be flagged both as land and coastlines or sea and coastlines

Over land, during the growing phase of the convection, Prec and Flash start to increase at the same time (10:00 LT – 12:00 LT) but Flash reaches a maximum earlier (15:00 LT – 16:00 LT) than Prec (17:00 LT – 18:00 LT). This is consistent with the finding of Liu and Zipser (2008) over the whole tropics. Different maximum times could come from the fact that, while the deep convective activity intensity starts to decrease with the number of flashes, Prec is still high during the dissipating stage of

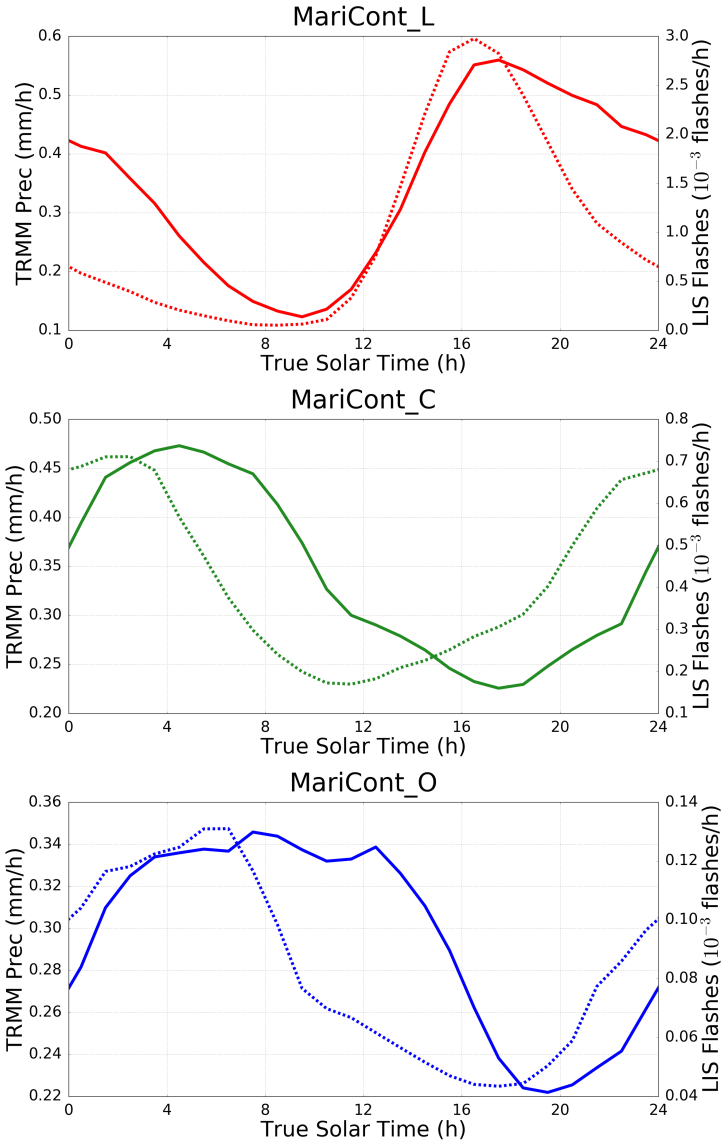

Figure 7. Diurnal cycle of Prec (solid line) and diurnal cycle of Flash (dashed line) over MariCont_L (top), MariCont_~~O~~ C (middle) and MariCont_~~C~~ O (bottom).

the convection and takes longer times to decrease than Flash. Consequently, combining our results with the ones presented in **?**, Flash and Prec can be considered as good proxies of deep convection during the growing phase of the convection over the MariCont_L.

Over ~~offshore areas (Fig. **??**b), minima of diurnal cycle of Prec and diurnal cycle of Flash are in the late afternoon, between 16:00 LT and 17:00 LT (Flash) and 17:00 LT and 18:00 LT (Prec), whilst maxima of diurnal cycle of Prec and Flash are reached in the early morning, between 04:00 LT and 09:00 LT (Flash) and around 08:00 LT – 09:00 LT (Prec). Results over offshore~~

areas are consistent with diurnal cycle of Flash and Prec calculated by ? over the whole tropical ocean, showing the increasing phase of the diurnal cycle of Flash starting 1–2 hours before the increasing phase of the diurnal cycle of Prec. Over coastlines (Fig. ??c), the Prec diurnal cycle is delayed by about + 2 to 7 h with respect to the Flash diurnal cycle. Prec minimum is around 18:00 LT while Flash minimum is around 11:30 LT. Maxima of Prec and Flash are found around 04:00 LT and 02:00 LT, respectively. This means that the increasing phase of Flash is 2-3 h longer than that of Prec. These results are consistent with ? showing a diurnal maximum of precipitation in the early morning between 02:00 LT and 03:00 LT and a diurnal minimum of precipitation around 11:00 LT, over coastal zones of Sumatra. According to Petersen and Rutledge (2001) and ? and ?, coastal zones are areas where precipitation results more from convective activity than from stratiform activity and the amplitude of diurnal maximum of Prec decreases with the distance from the coastline.

Over offshore areas (Fig. ??b), minima of diurnal cycle of Prec and diurnal cycle of Flash are in the late afternoon, between 16:00 LT and 17:00 LT (Flash) and 17:00 LT and 18:00 LT (Prec), whilst maxima of diurnal cycle of Prec and Flash are reached in the early morning, between 06:00 LT and 07:00 LT (Flash) and around 08:00 LT – 09:00 LT (Prec). Results over offshore areas are consistent with diurnal cycle of Flash and Prec calculated by ? over the whole tropical ocean, showing the increasing phase of the diurnal cycle of Flash starting 1–2 hours before the increasing phase of the diurnal cycle of Prec.

The time of transition from maximum to minimum of Prec is always longer than that of Flash. The period after the maximum of Prec is likely more representative of stratiform rainfall than deep convective rainfall. Consistently, over the MariCont ocean, model results from ? have shown that deep the suppression of the deep convection over offshore area in West of Sumatra from the early afternoon due to downwelling wavefront highlighted by deep warm anomalies around noonare coming from a downwelling wavefront which suppresses the convection offshoreduring early afternoon. . According to the authors, later in the afternoon, gravity waves are forced by the stratiform heating profile and propagate slowly offshore. They also highlighted that the diurnal cycle of the offshore convection responds strongly to the gravity wave forcing at the horizontal scale of 4 km.

To summarize, diurnal cycles of Prec and Flash show that:

i) over land, Flash increases proportionally with Prec during the growing phase of the convection,

ii) over offshore areascoastlines, Flash increasing phase is advanced by about 1more than 6–2 7 hours compared to Prec increasing phase,

iii) over coastlinesoffshore areas, Flash increasing phase is advanced by more than 6about 1–7 2 hours compared to Prec increasing phase.

In section ??, we investigate whether this time difference impacts the estimation of ΔIWC over land, coasts, and offshore areas.

5.3 Prec and Flash diurnal cycles and small-scale processes

In this subsection, we study the diurnal cycle of Prec and Flash at $0.25^\circ \times 0.25^\circ$ resolution over areas of deep convective activity over the MariCont. In line with the distribution of large value of Prec (Fig. ??), IWC (Fig. ??) and ΔIWC (Fig. ??), we have selected five islands and five seas over the MariCont. Diurnal cycles of Prec and Flash are presented over land for a) Java, b) Borneo, c) New Guinea, d) Sulawesi and e) Sumatra as shown in Figure ?? and over sea for the a) Java Sea, b) North

Australia Sea (NAusSea), c) Bismark Sea, d) West Sumatra Sea (WSumSea) and e) China Sea as shown in Figure **??**. Diurnal cycles of IWC from ERA5 (IWC^{ERA5}) are also presented in Fig. 8 and 9 and will be discussed in Section 6.

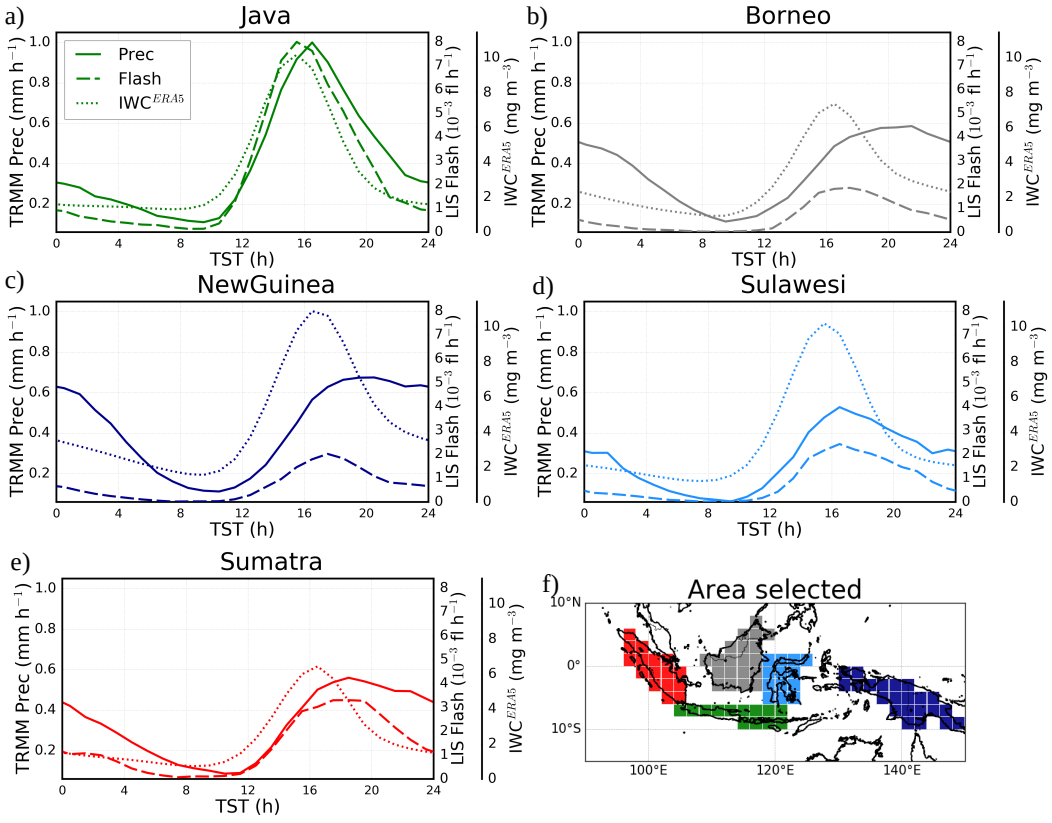

Figure 8. Diurnal cycles of Prec (solid line), Flash (dashed line) and IWC^{ERA5} from ERA5 at 150 hPa (dotted line) over MariCont islands: Java (a), Borneo (b), New Guinea (c), Sulawesi (d) and Sumatra (e) and map of the study zones over land (f).

Over land, the amplitude of the diurnal cycle of Prec is the largest over Java (Fig. **??**a), consistent with **?**, with a maximum reaching 1 mm h^{-1}, while, over the other areas, maxima are between 0.4 and 0.6 mm h^{-1}. Furthermore, over Java, the duration of the increasing phase in the diurnal cycle of Prec is 6-h consistent with that of Flash and elsewhere, the duration of the increasing phase is longer in Prec than in Flash by 1–2 h. The particularity of Java is related to the increasing phase of the diurnal cycle of Prec (6 h), that is faster than over all the other land areas considered in our study (~~8~~ 7 – ~~10 h)and is very consistent with the diurnal cycle of Prec over South America and South Africa (?)~~8 h). The strong and rapid convective growing phase measured over Java might be explained by the fact that the island is narrow with high mountains (up to $\sim$ 2000 m of altitude, as shown in Fig. 2b) reaching the coast. The topography promotes the growth of intense and rapid convective activity. The convection starts around 09:00 LT, rapidly elevating warm air up to the top of the mountains. Around 15:00 LT, air masses cooled in altitude are transported to the sea favoring the dissipating stage of the convection. Sulawesi is also

a small island ~~and presents the same onset of growing phase for the convection as Java, consistent with results presented in Nesbitt and Zipser (2003) and ?~~with high topography as Java. However, the amplitude of the diurnal cycle of Prec and Flash is not as strong as over Java. Other islands, such as Borneo, New Guinea and Sumatra, have high mountains but also large lowland areas. Mountains promote deep convection at the beginning of the afternoon while lowlands help maintain the convective activity through shallow convection and stratiform rainfall (**??**). Deep and shallow convection are then mixed during the slow dissipating phase of the convection (from $\sim$ 16:00 LT to 08:00 LT). However, because Flash are observed only in deep convective clouds, the decreasing phase of Flash diurnal cycles decreases more rapidly than the decreasing phase of Prec. The diurnal maxima of Prec found separately over the 5 islands of the MariCont are much higher than the diurnal maxima of Prec found over tropical land (South America, South Africa and MariCont_L) from **?**: $\sim$ 0.6 – 1.0 mm h^{-1} and $\sim$ 0.4 mm h^{-1}, respectively. However, the duration of the increasing phase of the diurnal cycle of Prec is consistent with the one calculated over tropical land by **?**.

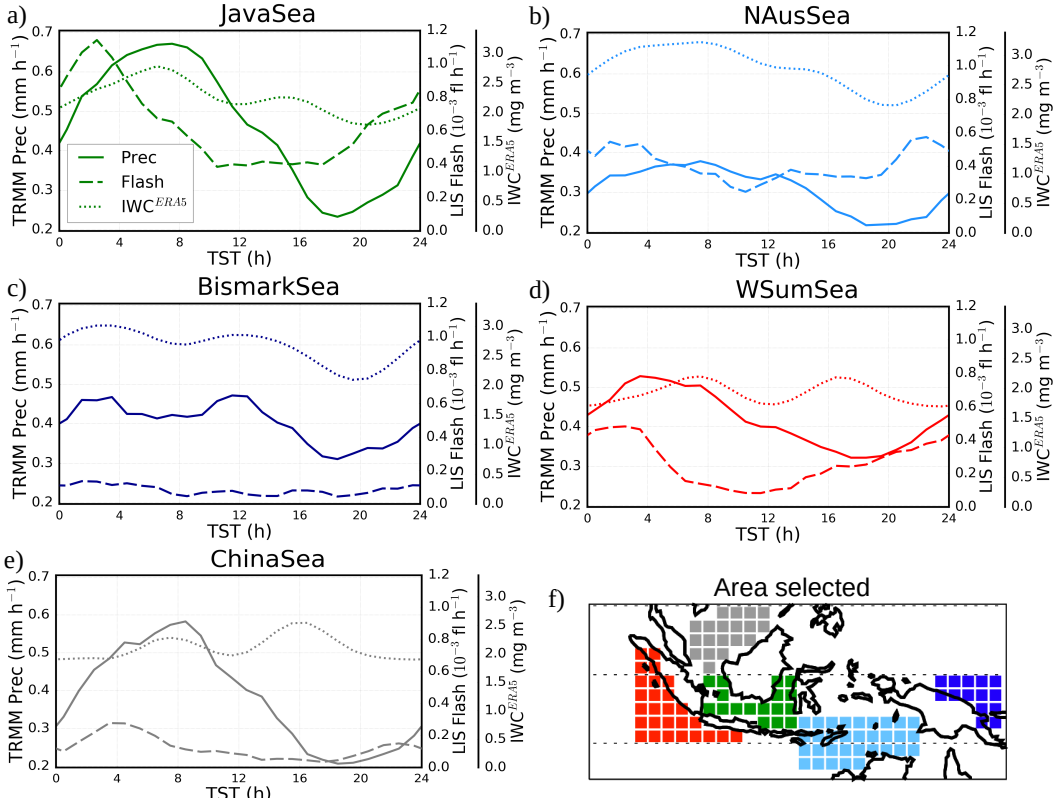

Figure 9. Diurnal cycles of Prec (solid line), Flash (dashed line) and IWC^{ERA5} from ERA5 at 150 hPa (dotted line) over MariCont seas: Java Sea (a), North Australia Sea (NAusSea) (b), Bismark Sea (c), West Sumatra Sea (WSumSea) (d), China Sea (e) and map of the study zones over sea (f).

Over sea, the five selected areas (Fig. **??**a–e) show a diurnal cycle of Prec and Flash either coastline or offshore areas depending onthe area. The diurnal cycle of Prec and Flash over Java Sea is similar to the one over coastlines (Fig. **??**c). Java Sea (Fig. **??**a), an area mainly surrounded by coasts, shows the largest diurnal maximum of Prec ($\sim$ 0.7 mm h^{-1}) and Flash ($\sim$ 1.1 10~~flashes h~~$^{-3}$ flashes h^{-1}) with the longest growing phase. In this area, land and sea breezes observed in coastal areas impact the diurnal cycle of the convection (**?**). During the night, land breeze develops from a temperature gradient between warm sea surface temperature and cold land surface temperature and conversely during the day. Over Java Sea, Prec is strongly impacted by land breezes from Borneo and Java islands (**?**), explaining why Prec and Flash reach largest values during the early morning. By contrast, NAusSea, Bismark Sea and WSumSea (Figs. **??**b, c and d, respectively) present small amplitude of diurnal cycle. In our analysis, these three study zones are the areas including the most offshore pixels. Java Sea and WSumSea present a similar diurnal cycle of Prec and Flash, with Flash growing phase starting about 4 h earlier than that of Prec. China Sea also shows a diurnal maximum of Flash shifted by about 4 hours before the diurnal maximum of Prec, but the time of the diurnal minimum of Prec and Flash is similar. Over ~~NAusSea~~ China Sea and Bismark Sea, the diurnal cycle of Flash shows a ~~very~~ weak amplitude with maxima reaching only 0.1~~flashes h. However, the diurnal minima of Prec and Flash over Bismark Sea are found to be at the same time (~17~~ $\times$0.2 10^{-3} flashes h^{-1}. Furthermore, over the Bismark Sea, while the diurnal minimum in Prec is around 18:00 LT, there are several local minima in Flash (08:00, 14:00 and 18:00 LT). Over NAusSea, the diurnal minimum of Prec is delayed by more than 7 hours compared to the diurnal minimum of Flash.

To summarize, over island, Flash and Prec convective increasing phases start at the same time and increase similarly but the diurnal maximum of Flash is reached 1–2 hours before the diurnal maximum of Prec. Over seas, the duration of the convective increasing phase and the amplitude of the diurnal cycles are not always similar depending on the area considered. The diurnal cycle of Flash is advanced by 4 hours over Java Sea and West Sumatra Sea and by more than 7 hours over North Australia Sea compared to the diurnal cycle of Prec. China Sea and Bismark Sea present the same time of the onset of the Flash and Prec increasing phase. In Section 7, we estimate ΔIWC over the 5 selected island and sea areas from Prec and Flash as a proxy of deep convection.

6 Horizontal distribution of IWC from ERA5 reanalyses

The ERA5 reanalyses provide hourly IWC at 150 and 100 hPa (IWC^{ERA5}). The diurnal cycle of IWC over the MariCont from ERA5 will be used to calculate ΔIWC from ERA5 in order to assess the horizontal distribution and the amount of ice injected in the UT and the TL deduced from our model combining MLS ice and TRMM Prec or MLS ice and LIS flash. Figures **??**a, b, c and d present the daily mean and the hour of the diurnal maxima of IWC^{ERA5} at 150 and 100 hPa. In the UT, the daily mean of IWC^{ERA5} shows a horizontal distribution over the MariCont consistently with that of IWC^{MLS} (Fig. **??**e), except over NewGuinea where IWC^{ERA5} (reaching 6.4 mg m^{-3}) is much stronger than IWC^{MLS} ($\sim$ 4.0 mg m^{-3}). The highest amount of IWC^{ERA5} is located over NewGuinea mountain chain and in the West coast of North Australia (reaching 6.4 mg m^{-3} in the UT and 1.0 mg m^{-3} in the TL). Over islands in the UT and the TL, the hour of the IWC^{ERA5} diurnal maximum is found between 12:00 LT and 15:00 LT over Sulawesi and New Guinea and between 15:00 LT and 21:00 LT over Sumatra, Borneo

and Java, that is close to the hour of the diurnal maximum of Flash over islands (Fig. **??**). Over sea, in the UT and the TL, the hour of the IWC^{ERA5} diurnal maximum is found between 06:00 LT and 09:00 LT over West Sumatra Sea, Java Sea, North Australia Sea, between 06:00 LT and 12:00 LT over China Sea and between 00:00 LT and 03:00 LT over Bismark Sea. There are no significant differences between the hour of the maximum of IWC^{ERA5} in the UT and in the TL.

The diurnal cycles of IWC^{ERA5} at 150 hPa are presented in Figs. **??** and **??** over the selection of islands and seas of the MariCont together with the diurnal cycles of Prec and Flash. Over islands (Fig. **??**), the maximum of the diurnal cycle of IWC^{ERA5} is found between 16:00 LT and 17:00 LT, consistent with the diurnal cycle of Prec and Flash. The duration of the increasing phase of the diurnal cycles of Prec, Flash and IWC^{ERA5} are all consistent to each other ~~, ~ 4~~ (6 – ~~5 h~~8 h). Over sea (Fig. **??**), the maximum of the diurnal cycle of IWC^{ERA5} is mainly found between 07:00 LT and 10:00 LT ~~, consistently with the diurnal cycle of Prec (which is 2 – 3 hours after the diurnal maxima for Flash). Over~~ over Java Sea and North Australia Sea, ~~the diurnal maxima and minima are found at the same hours as the diurnal maxima and minima of Prec~~ consistently with the diurnal cycle of Prec and a second peak is found around 16:00 LT. Thus, the duration of the increasing phase of the diurnal ~~cycle~~ cycles of IWC^{ERA5} is consistent with the one of Prec over these two sea study zones ~~, ~~ (~10 hours), but not with the one of ~~Prec~~Flash. Over Bismark Sea, ~~West Sumatra Sea and China Sea, the diurnal cycles~~ the diurnal maxima of IWC^{ERA5} ~~show two maxima:one at the end of the local morning and the other one during the local afternoon. Over Bismark Sea, these two maxima are consistent with those observed in the diurnal cycle of Prec, consequently the increasing phases of the diurnal cycles of IWC^{ERA5} and Prec are consistent to each other. Over West Sumatra Sea and~~ are found at 04:00 LT with a second peak later at noon. Over West Sumatra Sea, two diurnal maxima are found at 08:00 LT and 17:00 LT. Over China Sea, the ~~two maxima in the diurnal cycle~~ diurnal maximum of IWC^{ERA5} are ~~not observed in the~~ found at 16:00 LT with a second peak at 08:00 LT. These differences in the timing of the maximum of the diurnal cycle of Prec~~and Flash, consequently the increasing phase of IWC^{ERA5} is not consistent with the one of Prec nor the one of Flash.~~ , Flash and IWCERA5 observed at small-scale over sea of the MariCont are not well understood. However, these differences do not impact on the calculation of the ΔIWCPrec, ΔIWCFlash or ΔIWCERA5. Results are presented Section 7.

7 Ice injected over a selection of island and sea areas

7.1 ΔIWC deduced from observations

Figure **??** synthesizes ΔIWC in the UT and the TL over the 5 islands and 5 seas of the MariCont studied in the previous section. Eqs. (1-3) are used to calculate ΔIWC from Prec (ΔIWC^{Prec}) and from Flash (ΔIWC^{Flash}). ~~The~~ As presented in the previous section, Prec and Flash can be used as two proxies of deep convection, with differences more or less accentuated in their diurnal cycles as a function of the region considered. Thus, the observational ΔIWC range calculated between ΔIWC^{Prec} and ΔIWC^{Flash} provides an upper and lower bound of ΔIWC calculated from observational datasets.

In the UT (Fig. **??**a), over islands, ΔIWC calculated over Sumatra, Borneo, Sulawesi and New Guinea varies from ~~4.87 to 6.86 mg m~~4.9 to 6.9 mg m^{-3} whilst, over Java, ΔIWC reaches ~~7.89~~7.9 ~~–8.72 mg m~~8.7 mg m^{-3}. ΔIWC^{Flash} is generally greater than ΔIWC^{Prec} by less than 1.0 mg m~~(41~~$^{-3}$ (((ΔIWC^{Flash}-ΔIWC^{Prec})/ΔIWC^{Flash})×100 ranges from 4 to 22%)

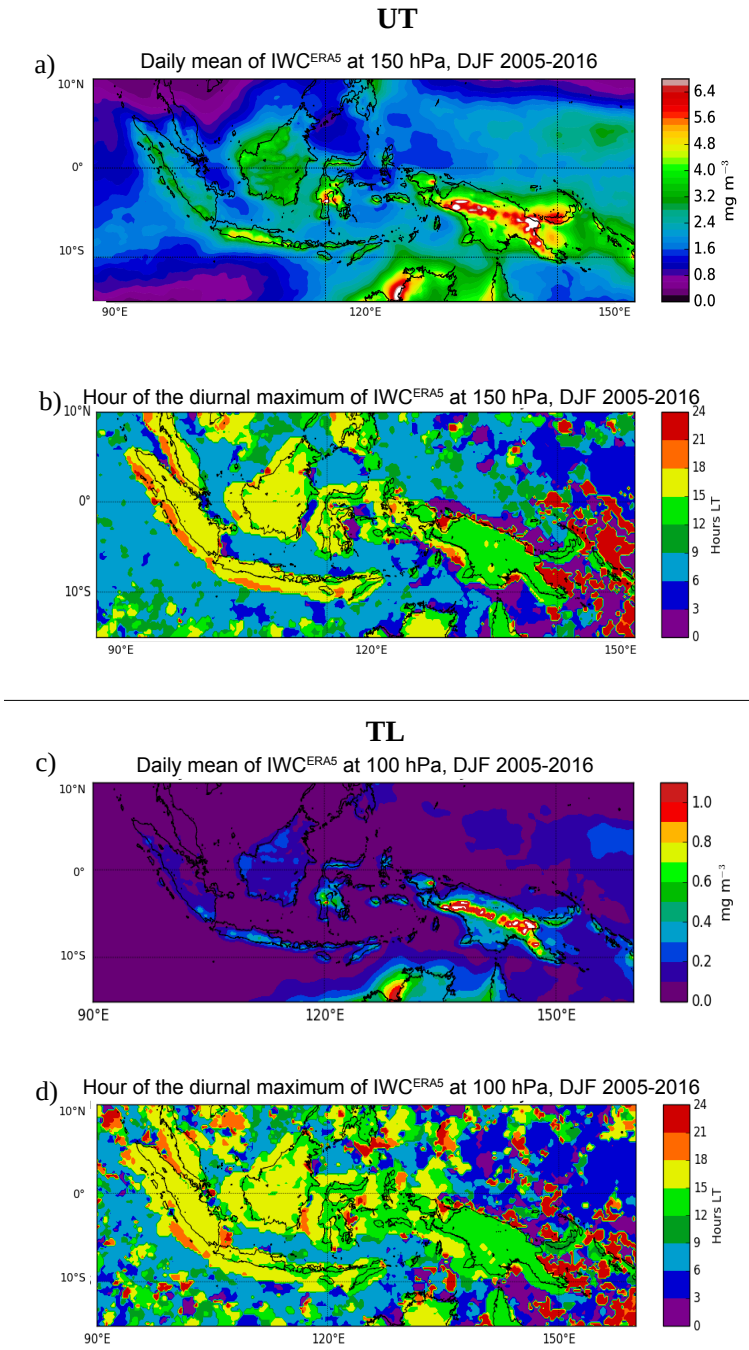

Figure 10. Daily mean of IWC^{ERA5} averaged over the period DJF 2005-2016 at 150 hPa (a) and at 100 hPa (c); Time (hour, local time (LT)) of the diurnal maximum of IWC^{ERA5} at 150 hPa (b) and at 100 hPa (d).

for all the islands, except for ~~New Guinea where the difference reaches 1.40 mg m(20%). Conversely, over Java , ΔIWC^{Prec}~~ Java where is larger than ΔIWC^{Flash} by ~~0.71 mg m(8~~0.7 mg m^{-3} (~~-8~~%). Over sea, ΔIWC varies from ~~1.17 to 4.37 mg m~~1.2 to 4.4 mg m^{-3}. ΔIWC^{Flash} is greater than ΔIWC^{Prec} by 0.6 to ~~2.09 mg m~~2.1 mg m^{-3} (31-50%), except for Java Sea, where ΔIWC^{Prec} is greater than ΔIWC^{Flash} by ~~0.21 mg m(6~~ 0.2 mg m^{-3} (~~-7~~%). Over North Australia Sea, ~~probably because of the 7-hours lagged diurnal cycle of Flash compared to Prec (Fig. **??**),~~ ΔIWC^{Flash} is almost twice as large as than ΔIWC^{Prec} (53%).

In the TL (Fig. **??**b), the observational ΔIWC range is found between ~~0.72 and 1.28 mg m~~0.7 and 1.3 mg m^{-3} over islands and between ~~0.22 and 0.74 mg m~~0.2 and 0.7 mg m^{-3} over seas. The same conclusions apply to the observational ΔIWC range calculated between ΔIWC^{Prec} and ΔIWC^{Flash} in the TL as in the UT with differences less than ~~0.39 mg m~~0.4 mg m^{-3}.

~~At~~ To summarize, independently of the proxies used for the calculation of ΔIWC, and at both altitudes, Java shows the largest injection of ice over the MariCont. Furthermore, it has been shown that both proxies can be used in our model, with more confidence over land: ΔIWC^{Prec} and ΔIWC^{Flash} are consistent to ~~within 4-20 % over islands and 6-50 % over seas~~ each other to within 4-22% over island and 7-53% over sea in the UT and the TL. The largest difference over sea is probably due to the larger contamination of stratiform precipitation included in Prec over sea. ~~Although Flash, is not contaminated by stratiform clouds, it could be a better proxy than Prec over sea but it is unfortunately negligible: less than 10flashes per day (Fig. **??**).~~

7.2 ΔIWC deduced from reanalyses

ΔIWC from ERA5 (ΔIWC^{ERA5}) is calculated in the UT and the TL (z_0 = ~~100 and~~ 150 and 100 hPa, respectively) as the max–min difference in the amplitude of the diurnal cycle. ~~To be consistent~~ Consistently with the MLS observations, we ~~should degrade~~ have degraded the ERA5 vertical resolution to assess the impact of the vertical resolution on ΔIWC^{ERA5}. ~~In the optimal estimation theory (**?**), the vertical distribution of~~ According to Wu et al. (2008), IWC^{ERA5} (IWC^{MLS} estimation derived from MLS represent spatially-averaged quantities within a volume that can be approximated by a box of 300×7×4 km^3 near the pointing tangent height. In order to compare IWC^{MLS} and IWC^{ERA5}~~(z)) should be convolved with the IWC^{MLS} averaging kernels, but this information is not provided by MLS. Instead, we have created a unitary triangular function $\phi(z, z_0, \delta z)$ centered at z_0 with a width at half-maximum of δz.The convolved IWC~~, we degraded: 1) the horizontal resolution of ERA5 from 0.25°×0.25° to 2°×2° (200 km×200 km) and 2) ERA5 data by connecting the vertical profiles of IWC^{ERA5} ~~(z) at z_0 ($\langle IWC^{ERA5}_{z_0} \rangle$) is calculated as:~~with a unitary box function whose width is 5 and 4 km at 100 and 146 hPa, respectively.

$$\langle IWC^{ERA5}_{z_0} \rangle = \int \phi(z, z_0, \delta z) IWC^{ERA5}(z) dz$$

Consistently with **?**, we have fixed δz = 4 and 5 km at z_0 = 146 and 100 hPa, respectively. The ice injected from ERA5 at z_0 = 146 and 100 hPa with degraded vertical resolution ($\langle \Delta IWC^{ERA5}_{z_0} \rangle$) is thus calculated from $\langle IWC^{ERA5}_{z_0} \rangle$.

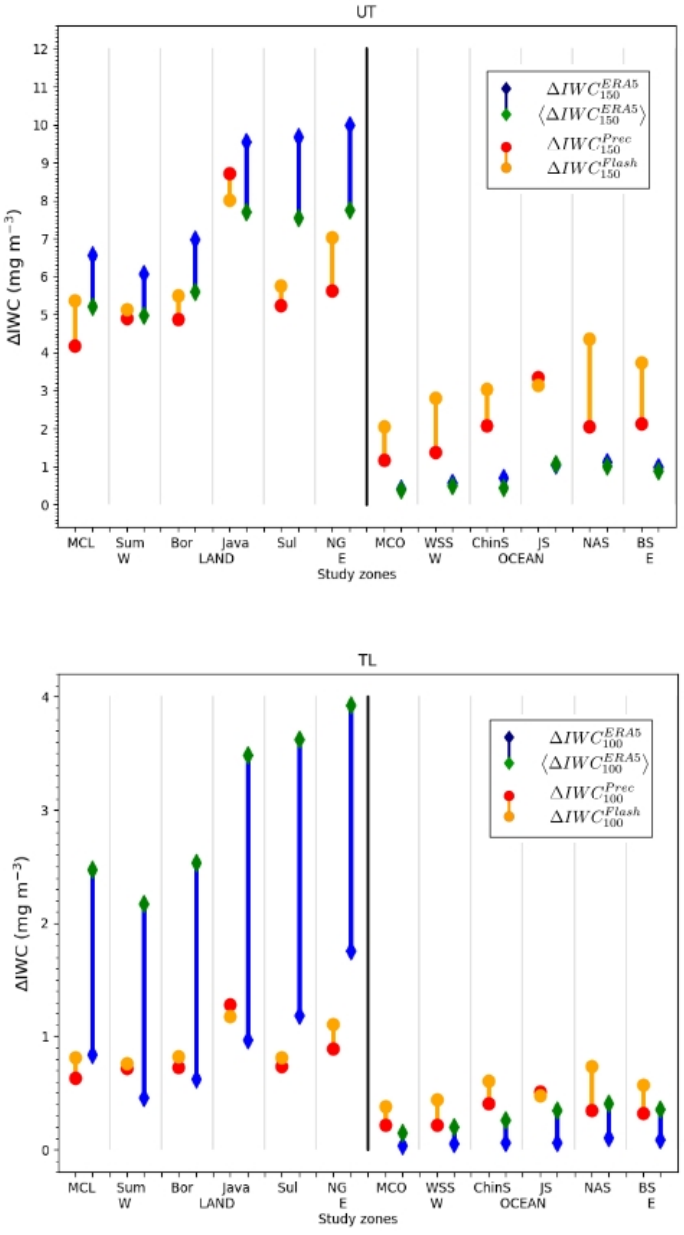

Figure 11. a) ΔIWC (mg m^{-3}) estimated from Prec (red) and Flash (orange) at 146 hPa and ΔIWC estimated from ERA5 at the level 150 hPa and at the level 150 hPa degraded in the vertical, over islands and seas of the MariCont: MariCont_L (MCL) and MariCont_O (MCO); from West (W) to East (E) over land, Sumatra (Sum), Borneo (Bor), Java, Sulawesi (Sul) and New Guinea (NG); and over seas, West Sumatra Sea (WSS), China Sea (ChinS), Java Sea (JS), North Australia Sea (NAS) and Bismark Sea (BS). b), Same as a) but for 100 hPa.

Figure ?? shows ΔIWC^{ERA5} and $\langle \Delta IWC^{ERA5}_{z_0} \rangle$ at z_0 = 150 and 100 hPa, over the island and the sea study zones. In the UT (Fig. ??a), over islands, ΔIWC^{ERA5}_{150} and $\langle \Delta IWC^{ERA5}_{150} \rangle$ calculated over Sumatra and Borneo vary from ~~4.75 to 6.97 mg m(~22 %of variability per study zones~~4.9 to 7.0 mg m^{-3} (the relative variation calculated as ((ΔIWC^{ERA5}-$\langle \Delta IWC^{ERA5} \rangle$)/$\Delta IWC^{ERA5}$)×100 is 18-19 %) whilst ΔIWC^{ERA5}_{150} and $\langle \Delta IWC^{ERA5}_{150} \rangle$ over Java, Sulawesi and New Guinea reach ~~7.41~~7.5 ~~–9.97 mg m~~10.0 mg m^{-3} (~~23 ~~19-22 % of variability per study ~~zones~~zone). Over sea, ΔIWC^{ERA5}_{150} and $\langle \Delta IWC^{ERA5}_{150} \rangle$ vary from 0.35 to ~~1.11 mg m~~1.1 mg m^{-3} (9 – 32 % of variability per study ~~zones~~zone). Over island and sea, ΔIWC^{ERA5}_{150} is greater than $\langle \Delta IWC^{ERA5}_{150} \rangle$. The small differences between ΔIWC^{ERA5}_{150} and $\langle \Delta IWC^{ERA5}_{150} \rangle$ over island and sea in the UT support the fact that the vertical resolution at 150 hPa has a low impact on the estimated ΔIWC.

In the TL, over land, ΔIWC^{ERA5}_{100} and $\langle \Delta IWC^{ERA5}_{100} \rangle$ vary from ~~0.46 to 3.65 mg m~~0.5 to 3.7 mg m^{-3} (~68% of variability per study ~~zones~~zone) with $\langle \Delta IWC^{ERA5}_{100} \rangle$ being ~~lower~~ larger than ΔIWC^{ERA5}_{100} by less than ~~2.12 mg m~~2.1 mg m^{-3}. Over sea, ΔIWC^{ERA5}_{100} and $\langle \Delta IWC^{ERA5}_{100} \rangle$ vary from ~~0.04 to 0.36 mg m~~0.05 to 0.4 mg m^{-3} (~71 % of variability per study ~~zones~~zone) with ΔIWC^{ERA5}_{100} lower than $\langle \Delta IWC^{ERA5}_{100} \rangle$ by less than ~~0.25 mg m~~0.2 mg m^{-3}. The large differences between ΔIWC^{ERA5}_{100} and $\langle \Delta IWC^{ERA5}_{100} \rangle$ over island and sea in the TL support the fact that the vertical resolution at 100 hPa has a high impact on the estimation of ΔIWC.

7.3 Synthesis

The comparison between the observational ΔIWC range and the reanalysis ΔIWC range is presented in Fig. ??. In the UT, over land, observation and reanalysis ΔIWC ranges overlap (agree to within ~~0 – 0.64 mg m(8 %),~~ 0.1 to 1.0 mg m^{-3}), which highlights the robustness of our model over land, except over Sulawesi ~~with differences of 1.63 mg m(23%~~and New Guinea, where the observational ΔIWC range and the reanalysis ΔIWC range differ by 1.7 and 0.7 mg m^{-3}, respectively). Over sea, the observational ΔIWC range is systematically greater than the reanalysis ΔIWC range by ~ ~~1.00~~ 1.0 – ~~2.19 mg m~~2.2 mg m^{-3} (75 %), showing a systematic positive bias and a too large variability range in our model over sea compared to ERA5. Combining observational and reanalysis ranges, the total ΔIWC variation range is estimated in the UT between ~~4.17 and 9.97 mg m~~4.2 and 10.0 mg m^{-3} (~ 20 % of variability per study ~~zones~~zone) over land and between ~~0.35 and 4.37 mg m~~0.3 and 4.4 mg m^{-3} (~ 30 % of variability per study ~~zones~~zone) over sea ~~, and~~and, in the TL, between ~~0.63 and 3.65 mg m~~0.6 and 3.9 mg m^{-3} (~ 70 % of variability per study ~~zones~~zone) over land, and between ~~0.04 and 0.74 mg m~~0.1 and 0.7 mg m^{-3} (~ 80 % of variability per study ~~zones~~zone) over sea.

The ~~amount~~ amounts of ice injected in the UT deduced from observations and reanalysis are consistent to each other over MariCont_L, Sumatra, Borneo and Java, with significant differences ~~between observations and reanalyses~~ over Sulawesi, New Guinea ~~and MariCont_O~~(within 1.7 to 0.7 mg m^{-3}, respectively) and all individual offshore study zones (within 0.7 to 2.1 mg m^{-3}). The impact of the vertical resolution on the estimation of ΔIWC in the TL is certainly non negligible, with larger ΔIWC variability range in the TL (70 – 80 %) than in the UT (20 – 30 %). At both levels, observational and reanalyses ΔIWC estimated over land is more than twice as large as ΔIWC estimated over sea. Finally, whatever the level considered, although Java has shown particularly high values in the observational ΔIWC range compared to other study zones, the reanalysis ΔIWC range shows that Sulawesi and NewGuinea would also be able to reach similar high values of ΔIWC as Java. ~~Whatever the~~

datasets used, the vertical distribution of ΔIWC in the TTL has shown a gradient of ~ 6 mg mbetween the UT and the TL over land compared to a gradient of ~ 2 mg mbetween the UT and the TL over ocean.

8 Discussion on small-scale convective processes impacting ΔIWC over a selection of areas

Our results have shown that, in all the datasets used, Java island and Java Sea are the two areas with the largest amount of ice injected up to the UT and the TL over the MariCont land and sea, respectively. In this section, processes impacting ΔIWC in the different study zones are discussed.

8.1 Java island, Sulawesi and New Guinea

Sulawesi, New Guinea and particularly Java island have been shown as the areas of the largest ΔIWC in the UT and TL. **?** have used high resolution observations and regional climate model simulations to show the three main processes impacting the diurnal cycle of rainfall over the Java island. The main process explaining the rapid and strong peak of Prec during the afternoon over Java (Fig. **??**a) is the sea-breeze convergence around midnight. This convergence caused by sea-breeze phenomenon increases the deep convective activity and impacts on the diurnal cycle of Prec and on the IWC injected up to the TL by amplifying their quantities. The second process is the mountain-valley wind converging toward the mountain peaks, and reinforcing the convergence and the precipitation. The land breeze becomes minor compared to the mountain-valley breeze and this process is amplified with the mountain altitude. As shown in Fig. **??**b, NewGuinea has the highest mountain chain of the MariCont. The third process shown by **?** is precipitation that is amplified by the cumulus merging processes which is more important over small islands such as Java (or Sulawesi) than over large islands such as Borneo or Sumatra. Another process is the interaction between sea-breeze and precipitation-driven cold pools that generates lines of strong horizontal moisture convergence (**?**). Thus, IWC is increasing proportionally with Prec consistent with the results from **?** and rapid convergence combined with deep convection transports elevated amounts of IWC at 13:30 LT (Fig. **??**) producing high ΔIWC during the growing phase of the convection (Fig. **??** and Fig. **??**) over Java.

8.2 West Sumatra Sea

In section **??**, it has been shown that the West Sumatra Sea is an area with positive anomaly of Prec during the growing phase of the convection but negative anomaly of IWC, which differs from other places. These results suggest that Prec is representative not only of convective precipitation but also of stratiform precipitation. The diurnal cycle of ~~Prec~~ stratiform and convective precipitations over West Sumatra Sea has been studied by **?** using 3 years of TRMM precipitation radar (PR) datasets, following the ~~2A23 Algorithm (?) separating stratiform from convective rainfall type. ?~~ 2A23Algorithm (Awaka, 1998). The authors have shown that rainfall over Sumatra is characterized by convective activity with a diurnal maximum between 15:00 and 22:00 LT ~~,~~ while, over the West Sumatra Sea, the rainfall type is convective and stratiform, with a diurnal maximum during the early morning (as observed in Fig. **??**). Furthermore, their analyses have shown a strong diurnal cycle of 200-hPa wind, humidity and stability, consistent with the PR over Sumatra West Sea and Sumatra ~~island~~Island. Stratiform and convective clouds are

both at the origin of heavy rainfall in the tropics (**??**) and in the West Sumatra Sea, but stratiform clouds are mid-altitude clouds in the troposphere and do not transport ice up to the tropopause.~~Flash measured~~ Thus, over the West Sumatra Sea~~would thus be a better proxy of deep convection in order to estimate~~ , the calculation of ΔIWC ~~than Prec because Prec is contaminated by stratiform rainfall~~estimated from Prec is possibly overestimated because Prec include a non-negligible amount of stratiform precipitation over this area.

8.3 North Australia Sea and seas with nearby islands

~~Comparisons~~

The comparisons between Figs. ~~??c and ??a~~ 2c and 6a have shown strong daily mean of Flash (10−2 –10~~flashes day~~−1 flashes day−1) but low daily mean of Prec (~~2~~ 2.0 – ~~8 mm day~~8.0 mm day−1) over the North Australia Sea. ~~Consequently, results in Fig. ?? have shown~~ Additionally, Fig. 11 shows that the strongest differences between ΔIWC^{Prec} and ΔIWC^{Flash} are found over the North Australia Sea, with ΔIWC^{Flash} greater than ΔIWC^{Prec} by ~~2.32 mg m~~2.3 mg m−3 in the UT and by ~~0.39 mg m~~0.4 mg m−2 in the TL (53% of variability ~~). Convective systems of the North Australian land and seas have been studied by ?. The North Australia Sea, mainly composed of the Arafura Sea and the Timor Sea, has~~ between ΔIWC^{Flash} and ΔIWC^{Prec}). These results imply that the variability range in our model is too large and highlight the difficulty to estimate ΔIWC over this study zone. Furthermore, as for Java Sea or Bismarck Sea, North Australia Sea has the particularity to be surrounding by several islands. According to the study from **?**, the ~~strongest convective activity during the DJF season (monsoon months) (?). During this season, isolated pulse convection and many mesoscale convective systems (MCSs) are active, such as the famous "Hector" storm over the Tiwi Islands, North of Darwin (??), squall lines (?) and cloud line (?). ?, identifying clouds from IR imagery, have shown that the number of clouds over the North Australia Sea~~ cloud size is the largest during the afternoon ~~but the size of the cloud is larger in the early morning. Although the number of clouds is low near 01:30 LT, the deepest daily convective activity during the early morning is at the origin of the strong relative value of IWC amount at 01:30 LT (see Fig. ??). Their studies have also shown that the diurnal maximum of number of clouds and cloud sizes over coastal part near NewGuinea is observed during the night , marked by land breeze convergence and gravity waves. Thus, nighttime convective systems over coasts propagate through the North Australia Sea and reinforce the IWC amount in the UT in the~~ over the North Australia land, during the night over North Australia coastline and during the early morning over ~~sea. Figure ?? presents the daily average of horizontal wind in the UT at 150 hPa and in the TL at 100 hPa over the period DJF 2004-2017. The wind direction at both altitudes is Westward, from North Australia land to the North Australia Sea. Thus, we suggest that because 1) the diurnal maximum of deep convection over North Australia land is found during the afternoon (?), and 2) the wind prevalence is from the North Australia land to sea, air masses charged with ice are advected from the North Australia land to~~ the North Australia ~~coastlines and seas at both altitudes. Thus, ΔIWC is injected during the day over the North Australia land in the UT and the TL and would be transported over the sea from the evening to the night and the early morning.~~ sea. These results suggest that deep convective activity moves from the land to the sea during the night. Over the North Australia Sea, it seems that the deep convective clouds are mainly composed by storms with lightning but precipitationd are weak or do not reach the surface and evaporating before.

~~Daily mean of wind speed and direction at 150 hPa (UT) a), and at 100 hPa (TL) b), from NOAA averaged during DJF 2004-2017 over the MariCont. The arrows with arbitrary length unit represent the wind direction.~~

9 Conclusions

The present study has combined observations of ice water content (IWC) measured by the Microwave Limb Sounder (MLS), precipitation (Prec) from the algorithm 3B42 of the Tropical Rainfall Measurement Mission (TRMM), the number of flashes (Flash) from the Lightning Imaging Sensor (LIS) of TRMM with IWC provided by the ERA5 reanalyses in order to estimate the amount of ice injected (ΔIWC) in the upper troposphere (UT) and the tropopause level (TL) over the MariCont, from the method proposed in a companion paper (**?**). ΔIWC is firstly calculated using the IWC measured by MLS (IWC^{MLS}) in DJF from 2004 to 2017 at the temporal resolution of 2 observations per day and Prec from TRMM-3B42 during the same period, to obtain a 1-hour resolution diurnal cycle. In the model used (**?**), Prec is considered as a proxy of deep convection impacting ice (ΔIWC^{Prec}) in the UT and the TL. While **?** have calculated ΔIWC^{Prec} over large convective study zones in the tropics, we show the spatial distribution of ΔIWC^{Prec} into the UT and the TL at 2° × 2° horizontal resolution over the MariCont, highlighting local areas of strong injection of ice up to 20 mg m^{-3} in the UT and up to 3 mg m^{-3} in the TL. ΔIWC injected in the UT and the TL has also been evaluated by using another proxy of deep convection: Flash measured by TRMM-LIS. Diurnal cycle of Flash has been compared to diurnal cycle of Prec, showing consistencies in 1) the spatial distribution of Flash and Prec over the MariCont (maxima of Prec and Flash located over land and coastline), and 2) their diurnal cycles over land (similar onset and duration of the diurnal cycle increasing phase). Differences have been mainly observed over sea and coastline areas, with the onset of the diurnal cycle increasing phase of Prec delayed by several hours depending on the considered area (from 2 to 7 h) compared to Flash. ΔIWC calculated by using Flash as a proxy of deep convection (ΔIWC^{Flash}) is compared to ΔIWC^{Prec} over five islands and five seas of the MariCont to establish an observational ΔIWC range over each study zone. ΔIWC is also estimated from IWC provided by the ERA5 reanalyses (ΔIWC^{ERA5} and IWC^{ERA5}, respectively) at 150 and 100 hPa over the study zones. We have also degraded the vertical resolution of IWC^{ERA5} to be consistent with that of IWC^{MLS} observations: 4 km at 146 hPa and 5 km at 100 hPa. The ΔIWC ranges calculated from observations and reanalyses were evaluated over the selected study zones (island and sea).

With the study of ΔIWC^{Prec}, results show that the largest amounts of ice injected in the UT and TL per 2° × 2° pixels are related to i) an amplitude of Prec diurnal cycle larger than 0.5 mm h^{-1}, ii) values of IWC measured during the growing phase of the convection larger than 4.5 mg m^{-3} and iii) duration of the growing phase of the convection longer than 9 hours. The largest ΔIWC^{Prec} has been found over areas where the convective activity is the deepest. The observational ΔIWC range calculated between ΔIWC^{Prec} and ΔIWC^{Flash} has been found to be within 4 – ~~20~~ 22 % over land and to within ~~6~~ 7 – ~~50~~ 53 % over sea. The largest differences between ΔIWC^{Prec} and ΔIWC^{Flash} over sea might be due to the combination of the presence of stratiform precipitation included into Prec and the very low values of Flash over seas (<10~~flashes day~~$^{-2}$ flashes day^{-1}). The diurnal cycle of IWC^{ERA5} at 150 hPa is more consistent with that of Prec and Flash over land than over ocean. Finally, the observational ΔIWC range has been shown to be consistent with the reanalysis ΔIWC range to within 23 % over

land and to within ~~75~~ 30-50 % over sea in the UT and to within 49 % over land and to within 39 % over sea in the TL. Thus, thanks to the combination between the observational and reanalysis ΔIWC ranges, the total ΔIWC variation range has been found in the UT to be between ~~4.17 and 9.97 mg m~~4.2 and 10.0 mg m^{-3} (to within 20 % per study zones) over land and between ~~0.35 and 4.37 mg m~~0.3 and 4.4 mg m^{-3} (to within 30 % per study zones) over sea and, in the TL, between ~~0.63 and 3.65 mg m~~0.6 and 3.9 mg m^{-3} (to within 70 % per study zones) over land and between ~~0.04 and 0.74 mg m~~0.1 and 0.7 mg m^{-3} (to within 80% per study zones) over sea. The ΔIWC variation range in the TL is larger than that in the UT highlighting the stronger impact of the vertical resolution in the observations in the TL compared to the UT.

The study at small scale over islands and seas of the MariCont has shown that ΔIWC from ERA5, Prec and Flash in the UT agree to within 0 – ~~0.64 mg m~~0.6 mg m^{-3} (8%) over MariCont_L, Sumatra, Borneo and Java with the largest values obtained over Java. However, while Java presents the largest amount of ΔIWC^{Prec} and ΔIWC^{Flash} in the UT and the TL (larger by about 1.0 mg m^{-3} in the UT and about ~~0.25 mg m~~0.3 mg m^{-3} in the TL than other land study zones), New Guinea and Sulawesi reach similar ranges of values of ice injected with ERA5 than

Java in the UT and even larger ranges of values as Java in the TL. Processes related to the strongest amount of ΔIWC injected into the UT and the TL have been identified as the combination of sea-breeze, mountain-valley breeze and merged cumulus, such as over NewGuinea and accentuated over small islands with high topography such as Java or Sulawesi. ~~Over sea areas, ΔIWC is a combination between the vertical transport of air masses by deep convection during night and early morning over offshore sea and by the westward horizontal transport of air masses near the tropopause, coming from land through coastline areas, during the end of the afternoon and at night (such as in North of Australia seas).~~

Author contributions. IAD analysed the data, formulated the model and the method combining MLS, TRMM and LIS data and took primary responsibility for writing the paper. CD has treated the LIS data, provided the Figures with Flash datasets, gave advices on data processing and contributed to the Prec and Flash comparative analysis. PR strongly contributed to the design of the study, the interpretation of the results and the writing of the paper. PR, FC, PH and TD provided comments on the paper and contributed to its writing.

Acknowledgements. We thank the National Center for Scientific Research (CNRS) and the Excellence Initiative (Idex) of Toulouse, France to fund this study and the project called Turbulence Effects on Active Species in Atmosphere (TEASAO – http://www.legos.obs-mip.fr/projets/axes-transverses-processus/teasao, Peter Haynes Chair of Attractivy). We would like to thank the teams that have provided the MLS data (https://disc.gsfc.nasa.gov/datasets/ML2IWC_V004, last access: June 2019), the TRMM data (https://pmm.nasa.gov/data-access/downloads/trmm), the LIS data (https://ghrc.nsstc.nasa.gov/lightning/data/data_lis_trmm.html, last access: June 2019), the ERA5 Reanalysis data (https://cds.climate.copernicus.eu/cdsapp/dataset/reanalysis\protect\discretionary{\char\hyphenchar\font}{}{}era5, last access: June 2019), and the NCEP Reanalysis data provided by the NOAA/OAR/ESRL PSD, Boulder, Colorado, USA, (https://www.esrl.noaa.gov/psd/, last access: June 2019).

References

J. Awaka. Algorithm 2A23—Rain type classification. In Proc. Symp. on the Precipitation Observation from Non-Sun Synchronous Orbit, pages 215–220, 1998.

R. E. Carbone, J. W. Wilson, T. D. Keenan, and J. M. Hacker. Tropical island convection in the absence of significant topography. part i: Life cycle of diurnally forced convection. Monthly weather review, 128(10):3459–3480, 2000.

L. Chappel. Assessing severe thunderstorm potential days and storm types in the tropics. In Presentation at the International Workshop on the Dynamics and Forecasting of Tropical Weather Systems, Darwin, 22-26 January 2001, 2001.

T. Dauhut, J.-P. Chaboureau, J. Escobar, and P. Mascart. ~~Giga-les~~ Giga-LES of hector the convector and its two tallest updrafts up to the stratosphere. Journal of the Atmospheric Sciences, 73(12):5041–5060, 2016.

T. Dauhut, J.-P. Chaboureau, P. Mascart, and T. Lane. The overshoots that hydrate the stratosphere in the tropics. In EGU General Assembly Conference Abstracts, volume 20, page 9149, 2018.

I.-A. Dion, P. Ricaud, P. Haynes, F. Carminati, and T. Dauhut. Ice injected into the tropopause by deep convection–part 1: In the austral convective tropics. Atmospheric Chemistry and Physics, 19(9):6459–6479, 2019.

S. Fueglistaler, A. E. Dessler, T. J. Dunkerton, I. Folkins, Q. Fu, and P. W. Mote. Tropical tropopause layer. Reviews of Geophysics, 47(1), 2009a. doi: 10.1029/2008RG000267. URL https://agupubs.onlinelibrary. wiley.com/doi/abs/10.1029/2008RG000267.

A. J. Geer, F. Baordo,N. Bormann, P. Chambon, S. J. English, M. Kazumori, ... C. Lupu. The growing impact of satellite observations sensitive to humidity, cloud and precipitation. Quarterly Journal of the Royal Meteorological Society, 143(709), 3189-3206, 2017.

R. Goler, M. J. Reeder, R. K. Smith, H. Richter, S. Arnup, T. Keenan, P. May, and J. Hacker. Low-level convergence lines over ~~northeastern~~ North Eastern australia. part i: The ~~north australian~~ North Australian cloud line. Monthly weather review, 134(11):3092–3108, 2006.

H. Hatsushika and K. Yamazaki. Interannual variations of temperature and vertical motion at the tropical tropopause associated with ~~enso~~ENSO. Geophysical research letters, 28(15):2891–2894, 2001.

H. Hersbach. Operational global reanalysis: progress, future directions and ~~syn- ergies~~ synergies with NWP. European Centre for Medium Range Weather Forecasts, 2018.

R. A. Houze and A. K. Betts. Convection in gate. Reviews of Geophysics, 19(4): 541–576, 1981.

G. J. Huffman, D. T. Bolvin, E. J. Nelkin, D. B. Wolff, R. F. Adler, G. Gu, Y. Hong, K. P. Bowman, and E. F. Stocker. The ~~trmm multisatellite precipitation analy- sis (tmpa): Quasi-global~~TRMM multisatellite precipitation analysis (TMPA): quasi-global, multiyear, combined-sensor precipitation estimates at fine scales. Journal of hydrometeorology, 8(1):38–55, 2007.

E. J. Jensen, A. S. Ackerman, J. A. Smith (2007). Can overshooting convection dehydrate the tropical tropopause layer?. Journal of Geophysical Research: Atmospheres, 112(D11), 2007.

C. Liu and E. J. Zipser. Global distribution of convection penetrating the tropical tropopause. Journal of Geophysical Research: Atmospheres, 110(D23), 2005.

C. Liu and E. J. Zipser. Diurnal cycles of precipitation, clouds, and lightning in the tropics from 9 years of TRMM observations. Geophys. Res. Lett., 35, L04819, doi:10.1029/2007GL032437, 2008.

Livesey, N.J., Read,W.G., Wagner, P.A., Froidevaux, L., Lambert, A., Manney, G.L., Millan, L.F., Pumphrey,H.C., Santee, M.L., Schwartz, M.J., Wang, S., Fuller, R.A., Jarnot, R.F., Knosp, B.W.,Martinez, E., and Lay, R.R., Version 4.2x Level 2 data quality and description doc-ument, Tech. Rep. JPL D-33509 Rev. D, Jet Propulsion Laboratory, available at:http://mls.jpl.nasa.gov (last access: 01 09 2019), 2018.

P. Lopez. Direct 4D-Var assimilation of NCEP stage IV radar and gauge precipitation data at ECMWF. Monthly Weather Review, 139(7), 2098-2116, 2011.

B. S. Love, A. J. Matthews, and G. M. S. Lister. The diurnal cycle of precipitation over the maritime continent in a high-resolution atmospheric model. Quarterly Journal of the Royal Meteorological Society, 137(657):934–947, 2011.

L. Millán, W. Read, Y. Kasai, A. Lambert, N. Livesey, J. Mendrok, H. Sagawa, T. Sano, M. Shiotani, and D. L. Wu. Smiles ice cloud products. Journal of Geophysical Research: Atmospheres, 118(12):6468–6477, 2013.

S. Mori, H. Jun-Ichi, Y. I. Tauhid, M. D. Yamanaka, N. Okamoto, F. Murata, N. Sakurai, H. Hashiguchi, and T. Sribimawati. Diurnal land–sea rainfall peak migration over ~~sumatera island, indonesian maritime continent~~Sumatera island, Indonesian Maritime Continent, observed by ~~trmm~~ TRMM satellite and intensive rawinsonde soundings. Monthly Weather Review, 132(8):2021–2039, 2004.

S. W. Nesbitt and E. J. Zipser. The diurnal cycle of rainfall and convective inten- sity according to three years of trmm measurements. Journal of Climate, 16 (10):1456–1475, 2003.

W. A. Petersen, and S. A. Rutledge. Regional variability in tropical convection: Observations from TRMM. Journal of Climate, 14(17), 3566-3586, 2001.

M. Pope, C. Jakob, and M. J. Reeder. Convective systems of the north australian monsoon. Journal of Climate, 21(19):5091–5112, 2008.

J.-H. Qian. Why precipitation is mostly concentrated over islands in the maritime continent. Journal of the Atmospheric Sciences, 65(4):1428–1441, 2008.

C. S. Ramage. Role of a tropical "maritime continent" in the atmospheric ~~circu- lation~~circulation. Mon. Wea. Rev, 96(6):365–370, 1968.

W. J. Randel, F. Wu, H. Voemel, G. E. Nedoluha, and P. Forster. Decreases in stratospheric water vapor after 2001: Links to changes in the tropical tropopause and the brewer-dobson circulation. Journal of Geophysical Re- search: Atmospheres, 111(D12), 2006a.

W.J. Randel and E.J. Jensen. Physical processes in the tropical tropopause layer and their roles in a changing climate. Nature Geoscience, 6:169, 2013. doi: 10.1038/ngeo1733. URL https://doi.org/10.1038/ngeo1733.

S. C. Sherwood. A stratospheric "drain" over the maritime continent. Geophysical research letters, 27(5):677–680, 2000.

A. Stenke and V. Grewe. Simulation of stratospheric water vapor trends: impact on stratospheric ozone chemistry. Atmospheric Chemistry and Physics, 5(5): 1257–1272, 2005.

G. L. Stephens and T. J. Greenwald. The earth's radiation budget and its rela- tion to atmospheric hydrology: 2. observations of cloud effects. Journal of Geophysical Research: Atmospheres, 96(D8):15325–15340, 1991.

G.-Y. Yang and J. Slingo. The diurnal cycle in the tropics. Monthly Weather Review, 129(4):784–801, 2001. 129<0784:TDCITT>2.0.CO;2. doi: 10.1175/1520-0493(2001) URL https://doi.org/10.1175/1520-0493(2001)129<0784:TDCITT>2.0.CO;2.

J. W. Waters, L. Froidevaux, R. S. Harwood, R. F. Jarnot, H. M. Pickett, W. G. Read, ... and J. R. Holden (2006). The earth observing system microwave limb sounder (EOS MLS) on the Aura satellite. IEEE Transactions on Geoscience and Remote Sensing, 44(5), 1075-1092.

Ice injected into the tropopause by deep convection – Part 2: Over the Maritime Continent

Dion Iris-Amata[1], Dallet Cyrille[1], Ricaud Philippe[1], Carminati Fabien[2], Haynes Peter[3], and Dauhut Thibaut[4]

[1]CRNM, Meteo-France - CNRS, Toulouse, 31057, France
[2]Met Office, Exeter, Devon, EX1 3PB, UK
[3]DAMTP, University of Cambridge, Cambridge, CB3 0WA, UK
[4]Max Planck Institute for Meteorology, Hamburg, Germany

Correspondence: Iris-Amata Dion (iris.dion@meteo.fr)

Abstract. The amount of ice injected up to the tropical tropopause layer has a strong radiative impact on climate. In the tropics, the Maritime Continent (MariCont) region presents the largest injection of ice by deep convection into the upper troposphere (UT) and tropopause level (TL) (from results presented in the companion paper Part 1). This study focuses on the MariCont region and aims to assess the processes, the areas and the diurnal amount and duration of ice injected by deep convection over islands and over seas using a 2° × 2° horizontal resolution during the austral convective season of December, January and February. The model presented in the companion paper is used to estimate the amount of ice injected (ΔIWC) up to the TL by combining ice water content (IWC) measured twice a day in tropical UT and TL by the Microwave Limb Sounder (MLS; Version 4.2), from 2004 to 2017, and precipitation (Prec) measurement from the Tropical Rainfall Measurement Mission (TRMM; Version 007) at high temporal resolution (1 hour). The horizontal distribution of ΔIWC estimated from Prec (ΔIWC^{Prec}) is presented at 2° × 2° horizontal resolution over the MariCont. ΔIWC is also evaluated by using the number of lightning events (Flash) from the TRMM-LIS instrument (Lightning Imaging Sensor, from 2004 to 2015 at 1-h and 0.25°×0.25°resolutions). ΔIWC^{Prec} and ΔIWC estimated from Flash (ΔIWC^{Flash}) are compared to ΔIWC estimated from the ERA5 reanalyses (ΔIWC^{ERA5}) degrading the vertical resolution to that of MLS observations ($\langle \Delta IWC^{ERA5} \rangle$). Our study shows that, while the diurnal cycles of Prec and Flash are consistent to each other in timing and phase over lands and different over offshore and coastal areas of the MariCont, the observational ΔIWC range between ΔIWC^{Prec} and ΔIWC^{Flash} is small (they agree to within 4 – ~~20~~22% over land and to within ~~6~~ 7 – ~~50~~53% over ocean) in the UT and TL. The reanalysis ΔIWC range between ΔIWC^{ERA5} and $\langle \Delta IWC^{ERA5} \rangle$ has been also found to be small in the UT (~~22~~ 4 – ~~32~~ 29 %) but large in the TL (~~68~~ 55 – ~~71~~ 78 %), highlighting the stronger impact of the vertical resolution on the TL than in the UT. Combining observational and reanalysis ΔIWC ranges, the total ΔIWC range is estimated in the UT between ~~4.17 and 9.97 mg m~~4.2 and 10.0 mg m^{-3} (20 % of variability per study zone) over land and between ~~0.35 and 4.37 mg m~~0.3 and 4.4 mg m^{-3} (30% of variability per study zone) over sea, and, in the TL, between ~~0.63 and 3.65 mg m~~0.6 and 3.9 mg m^{-3} (70% of variability per study zone) over land and between ~~0.04 and 0.74 mg m~~0.1 and 0.7 mg m^{-3} (80% of variability per study zone) over sea. Finally, from IWC^{ERA5}, Prec and Flash, this study highlights 1) ΔIWC over land has been found larger than ΔIWC over sea with a limit at 4.0 mg m^{-3} in the UT between minimum of ΔIWC estimated over land and maximum of ΔIWC estimated over

sea, and 2) small islands with high topography present the strongest amounts of ΔIWC such as the Java Island, the ~~Java Island is the~~ area of the largest ΔIWC in the UT (~~7.89~~ 7.7 – ~~8.72 mg m~~9.5 mg m^{-3} daily mean).

1 Introduction

In the tropics, water vapour (WV) and ice cirrus clouds near the cold point tropopause (CPT) have a strong radiative effect on climate (**?**) and an indirect impact on stratospheric ozone (**?**). WV and water ice crystals are transported up to the tropopause layer by two main processes: a three-dimensional large-scale slow process (3-m month $^{-1}$), and a small scale fast convective process (diurnal timescale) (e.g. **??**). Many studies have already shown the impact of convective processes on the hydration of the atmospheric layers from the upper troposphere (UT) to the lower stratosphere (LS) ~~(e.g. **???**)~~(e.g. **????**). However, the amount of total water (WV and ice) transported by deep convection up to the tropical UT and LS is still not well understood. The vertical distribution of total water in those layers is constrained by thermal conditions of the CPT (**?**). During deep convective events, **?** have shown that air masses transported up to 146 hPa in the UT and up to 100 hPa in the tropopause layer (TL) have ice to total water ratios of more than 50% and 70%, respectively, and that ice in the UT is strongly spatially correlated with the diurnal increases of deep convection, while WV is not. **?** hence focused on the ice phase of total water to estimate the diurnal amount of ice injected into the UT and the TL over convective tropical areas, showing that it is larger over land than over ocean, with maxima over land of the Maritime Continent (MariCont), the region including Indonesian islands. For these reasons, the present study is focusing on the MariCont region in order to better understand small-scale processes impacting the diurnal injection of ice up to the TL.

A method to estimate the amount of ice injected into the UT and up to the TL over convective areas and during convective seasons has been proposed by **?**. This method provides an estimation of the amplitude of the diurnal cycle of ice in those layers using the twice daily Ice Water Content (IWC) measurements from the Microwave Limb Sounder (MLS) instrument and the full diurnal cycle of precipitation (Prec) measured by the Tropical Rainfall Measurement Mission (TRMM) instrument, at one hour resolution. The method first focuses on the increasing phase of the diurnal cycle of Prec (peak to peak from the diurnal Prec minimum to the diurnal Prec maximum) and shows that the increasing phase of Prec is consistent in time and in amplitude with the increasing phase of the diurnal cycle of deep convection, over tropical convective zones and during convective season. The amount of ice (ΔIWC) injected into the UT and the TL is estimated by relating IWC measured by MLS during the growing phase of the deep convection to the increasing phase of the diurnal cycle of Prec. **?** conclude that deep convection over the MariCont region is the main process impacting the increasing phase of the diurnal cycle of ice in those layers.

The MariCont region is one of the main convective ~~centers~~ center in the tropics with the wettest troposphere and the coldest and driest tropopause (**???**). **?** have shown that over the Indonesian area, the phase of the convective activity diurnal cycle drifts from land to coastlines and to offshore areas. Even though authors have done a comprehensive work around the study

of the diurnal cycle of precipitation and convection over the MariCont, the diurnal cycle of ice injected by deep convection up to the TL over this region is still not well understood. **?** have tentatively evaluated the upper tropospheric diurnal cycle of ice from Superconducting Submillimeter-Wave Limb-Emission Sounder (SMILES) measurements over the period 2009-2010 but without differentiating land and sea over the MariCont, which caused their analysis to show little diurnal variation over that region. **?** have 1) highlighted that the MariCont must be considered as two separate areas: the MariCont land (MariCont_L) and the MariCont ocean (MariCont_O), with two distinct diurnal cycles of the Prec and 2) estimated the amount of ice injected in the UT and the TL. Over these two domains, it has also been shown that convective processes are stronger over MariCont_L than over MariCont_O. Consequently, the amount of ice injected in the UT and the TL is greater over MariCont_L than over MariCont_O. ~~Considering a higher horizontal resolution over small islands and seas~~

Building upon the results of **?**, the present study aims to improve the methodology of Dion et al. (2019) by i) studying smaller study zones than in Dion et al. (2019) and by distinguishing island and sea of the MariCont~~and investigating other~~ , ii) assessing the sensitivity of model to different proxies of deep convection ~~, the authors were expected a better characterisation of the~~ and iii) assessing the amount of ice injected ~~up to the TTL. Building upon the results of **?**, the present study is addressing the evaluation of~~ in the UT and the TL inferred by our model to that of ERA5 reanalyses. Based on space-borne observations and meteorological reanalyses, ΔIWC ~~at a~~ is assessed at a horizontal resolution of $2° \times 2°$ over 5 islands (Sumatra, Borneo, Java, Sulawesi and New Guinea) and 5 seas (West Sumatra Sea, Java Sea, China Sea, North Australia Sea, and Bismark Sea) of the MariCont during convective season (December, January and February, hereafter DJF) from 2004 to 2017. ΔIWC will be first estimated from Prec measured by TRMM-3B42. A sensitivity study of ΔIWC based on the number of flashes (Flash) detected by the TRMM Lightning Imaging Sensor (TRMM-LIS), an alternative proxy for deep convection as shown by Liu and Zipser (~~2009~~2008), is also proposed. Finally, we will use IWC calculated by the ERA5 reanalyses from 2005 to 2016 to estimate ΔIWC in the UT and the TL over each study zone and compare it to ΔIWC estimated from Prec and Flash.

The observational datasets used in our study are presented in Sect. 2. Method is recalled in Sect. 3. The amount of ice (ΔIWC) injected up to the TL estimated from Prec is evaluated in Sect. 4. Diurnal cycles of Prec and Flash are compared to each other over different areas of the MariCont in Sect. 5. Results of the estimated ΔIWC injected up to the UT and the TL over five islands and five seas of the MariCont are presented and compared with the ERA5 reanalyses in Sect. 6. Results are discussed in Sect. 7, and conclusions are drawn in Sect. 8. This paper contains many abbreviations and acronyms. To facilitate reading, they are compiled in the Acronyms list.

2 Datasets

This section presents the instruments and the reanalyses used for this study.

2.1 MLS Ice Water Content

The Microwave Limb Sounder (MLS, ~~Version~~ data processing algorithm version 4.2) instrument on board NASA's Earth Observing System (EOS) Aura platform ~~(?)~~ (??) launched in 2004 provides ice water content (IWC^{MLS}, mg m~~) measurementsat~~

$^{-3}$) measurements. MLS provides IWC^{MLS} are given at 6 levels in the UTLS (82, 100, 121, 146~~hPa (in the UT)~~, 177 and ~~at~~ 215). However, we have chosen to study only two levels: an upper and a lower level of the TTL. Because the level at 82 hPa does not provide enough significant measurements of IWC to have a good signal-to-noise, we have selected 2 levels: 1) at 100 hPa ~~(in the TL)~~as the upper level of the TTL (named TL for tropopause level), and 2) at 146 hPa as the lower level of the TTL (named UT for upper troposphere). MLS follows a sun-synchronous near-polar orbit, completing 233 revolution cycles every 16 days, with daily global coverage every 14 orbits. The instrument is crossing twice a day the equator at fixed time, measuring IWC^{MLS} at 01:30 local time (LT) and 13:30 LT. The horizontal resolution of IWC^{MLS} measurements is $\sim$ 300 and 7 km along and across the track, respectively. The vertical resolution of IWC^{MLS} is 4 and 5 km at 146 and 100 hPa, respectively. ~~Since the averaging kernels of IWC^{MLS} are not provided by MLS , we will use an unitary triangular function centered at 146 and 100 hPa, having a width at half-maximum of 4 and 5 km, respectively, to represent the averaging Kernels of MLS IWC at 146 and 100 hPa (see section ??~~Although optimal estimation is used to retrieve almost all other MLS products, a cloud-induced radiance technique is used to validate the MLS IWC (Wu et al., 2008; Wu et al., 2009). In our study, high ~~spatial~~ horizontal resolution is now possible because we consider 13 years of MLS data, allowing to average the IWC^{MLS} measurements within the bins of horizontal resolution of 2° ×2° ($\sim$ 230 km). We select IWC^{MLS} during all austral convective seasons DJF between 2004 and 2017. The IWC measurements were filtered following the recommendations of the MLS team described in **?**. The resolutions of IWC^{MLS} (horizontal along the path, horizontal perpendicular to the path, vertical) measured at 146 and 100 hPa are 300×7×4 km and 250×7×5 km, respectively. The precision of the measurement is 0.10 mg m^{-3} at 146 hPa and 0.25 to 0.35 mg m^{-3} at 100 hPa. The accuracy is 100% for values less than 10 mg m^{-3} at both levels and the valid range is 0.02-50.0 mg m^{-3} at 146 hPa and 0.1-50.0 mg m^{-3} at 100 hPa (Wu et al., 2008).

2.2 TRMM-3B42 Precipitation

The Tropical Rainfall Measurement Mission (TRMM) was launched in 1997 and provided measurements of Prec until 2015. TRMM is composed of five instruments, three of them are complementary sensor rainfall suite (PR, TMI, VIRS). TRMM had an almost circular orbit at 350 km altitude height performing a complete revolution in one and a half hour. The 3B42 algorithm product (TRMM-3B42) (version V7) has been created to estimate the precipitation and extend the precipitation product through 2019. ~~Thus, the~~ TRMM-3B42 ~~, a Prec dataset is based on TRMM observations~~ is a multi-satellite precipitation analysis composing a Global Precipitation Measurement (GPM) Mission. TRMM-3B42 is computed from the various precipitation-relevant satellite passive Microwave (PMW) sensors using GPROF2017 computed at the Precipitation Processing System (PPS) (e.g., GMI, DPR, Ku, Ka, Special Sensor Microwave Imager/Sounder [SSMIS], etc.) and including TRMM measurements from 1997 to 2015 ~~and provides Prec data from 1997 to 2019~~ (Huffman et al., 2007, 2010; and Huffman and Bolvin, 2018). Work is currently underway with NASA funding to develop more appropriate estimators for random error, and to introduce estimates of bias error (Huffman and Bolvin, 2018). Prec data are provided at a 0.25° × 0.25° ($\sim$ 29.2 km) horizontal resolution, extending from 50° S to 50° N (https://pmm.nasa.gov/data-access/downloads/trmm, last access: April 2019). Prec from TRMM-3B42 products depends on input from microwave and IR sensors (**?**) and does not differentiate between stratiform and convective precipitation. In our study, Prec from TRMM-3B42 is selected over the austral convective seasons (DJF) from 2004 to 2017

and averaged to a horizontal grid of 2° ×2° to be compared to IWC^{MLS}. ~~As the TRMM orbit precesses,~~ The granule temporal coverage of TRMM-3B42 data is 3 hours, but the temporal resolution of individual measurements is 1 minute. Thus, it is statistically possible to degrade the resolution to 1 hour. TRMM-3B42 are provided in Universal Time that we converted into local time (LT). Details of the ~~diurnal cycle of Prec averaged over the study period is calculated with a 1-h temporal resolution~~binning methodology of TRMM-3B42 is provided by Huffman and Bolvin (2018).

2.3 TRMM-LIS number of Flashes

The Lightning Imaging Sensor (LIS) aboard of the TRMM satellite measures several parameters relative to lightning. According to Christian et al. (2000), LIS used a Real-Time Event Processor (RTEP) that discriminates lightning event from Earth albedo light. ~~The instrument in itself was composed of a grid of 128 × 128 detectors allowing to observe a point within 90 seconds with a temporal resolution of 2 milliseconds.~~ A lightning event corresponds to the detection of a light anomaly on a pixel representing the most fundamental detection of the sensor. After a spatial and temporal processing, the sensor was able to characterize a flash from several detected events. The instrument detects lightning with storm-scale resolution of 3-6 km (3 km at nadir, 6 km at limb) over a large region (550-550 km) of the Earth's surface. LIS horizontal resolution is provided at 0.25°×0.10°. A significant amount of software filtering has gone into the production of science data to maximize the detection efficiency and confidence level. Thus, each datum is a lightning signal and not noise. Furthermore, the weak lightning signals that occur during the day are hard to detect because of background illumination. A real-tile event processor removes the background signal to enable the system and detect weak lightning and achieve a 90% detection efficiency during the day. LIS is thus able to provide the number of flashes (Flash) measured. The ~~LIS~~ TRMM LIS detection efficiency ranges from 69% near noon to 88% at night. The LIS instrument performed measurements between 1 January 1998 and 8 April 2015. To be as consistent as possible to the MLS and TRMM-3B42 period of study, we are using LIS measurements during DJF from 2004 to 2015. ~~LIS spatial resolution varies between 3 km at nadir and 6 km off-nadir.~~ The observation range of the sensor is between 38° N and 38° S. As LIS is on the TRMM platform, with an orbit that precesses, Flash from LIS can be averaged to obtain the full 24-h diurnal cycle of Flash over the study period with a 1-h temporal resolution. In our study, Flash measured by LIS is studied at 0.25° × 0.25° horizontal resolution to be compared to Prec from TRMM-3B42.

2.4 ERA5 Ice Water Content

The European Centre for Medium-range Weather Forecasts (ECMWF) Reanalysis 5, known as ERA5, replaces the ERA-Interim reanalyses as the fifth generation of the ECMWF reanalysis providing global climate and weather for the past decades (from 1979) (**?**). ERA5 provides hourly estimates for a large number of atmospheric, ocean and land surface quantities and covers the Earth on a 30 km grid with 137 levels from the surface up to a height of 80 km. ~~Cloud ice water content from~~ Reanalyses such as ERA5 ~~reanalyses (~~provide a physically constrained, continuous, global, and homogeneous representation of the atmosphere through a large number of observations (space-borne, air-borne, and ground-based) with short-range forecasts. Although there is no direct observation of atmospheric ice content in ERA5, the specific cloud ice water content (mass of condensate / mass of moist air) (IWC^{ERA5}) ~~comes from the combination of a large amount of global historical observations,~~

advanced modelling and data assimilation systems (https://cds.climate.copernicus.eu/cdsapp!/dataset/reanalysis-era5-pressure-levels-month to the changes in the analysed temperature (and at low levels, humidity) which is mostly driven by the assimilation of temperature-sensitive radiances from satellite instruments (https://cds.climate.copernicus.eu/cdsapp!/dataset/reanalysis-era5-pressure-level tab=form, last access: July 2019). IWC^{ERA5} used in our analysis is representative of non-precipitating ice. Precipitating ice, classified as snow water, is also provided by ERA5 but not used in this study in order to focus only on the injected and non-precipitating ice into the TTL. Furthermore, results from Duncan and Eriksson (2018) have highlighted that ERA5 is able to capture both seasonal and diurnal variability in cloud ice water but the reanalyses exhibit noisier and higher amplitude diurnal variability than borne out by the satellite estimates. The present study uses the IWC^{ERA5} at 100 and 150 hPa averaged over DJF from 2005 to 2016 with one hour one-hour temporal resolution. IWC^{ERA5} is governed by the model microphysics which allows ice supersaturation with respect to ice (100-150% in relative humidity) but not with respect to liquid water. Although microwave radiances at 183 GHz (sensitive to atmospheric scattering induced by ice particles) (Geer et al., 2017) are assimilated, cloud and precipitations are used as control variable in the 4D-Var assimilation system and cannot be adjusted independently in the analysis (Geer et al., 2017). The microwave data have sensitivity to the frozen phase hydrometeors but mainly to larger particles, such as those in the cores of deep convection (Geer et al., 2017), but the sensitivity to cirrus clouds in ERA5 is strongly dependent on microphysical assumptions on the shape and size of the cirrus particles. Indirect feedbacks are also acting on cirrus representation in the model – e.g. changing the intensity of the convection will change the amount of outflow cirrus generated. This is why observations that affects the troposphere by changing for example the stability, the humidity, or the synoptic situation can affect the upper level ice cloud indirectly (Geer et al., 2017). IWC^{ERA5} is used to assess the amount of ice injected in the UT and the TL as estimated by the model developed in Dion et al. (2019) and in the present study. IWC^{ERA5} have been degraded along the vertical at 100 and 150 hPa ($\langle \Delta IWC^{ERA5} \rangle$) consistent consistently with the MLS vertical resolution of IWC^{MLS} (5 and 4 km at 100 and 146 hPa, respectively) using an unitary triangular function , in the absence of IWC averaging kernels by MLS box function (see section **??**). IWC^{ERA5} and $\langle \Delta IWC^{ERA5} \rangle$ will be both considered in this study. IWC^{ERA5}, initially provided in kg kg^{-1}, has been converted into mg m^{-3} using the temperature provided by ERA5 in order to be compared with MLS IWC observations.

2.5 NOAA Winds

Because wind provided by ERA5 is not available at 100 and 150 hPa, our study uses the wind datasets from the National Centers For Environmental Prediction (NCEP) Global Data Assimilation System (GDAS), initialized analyses, provided by the National Oceanic and Atmospheric Administration (NOAA). NOAA provides vertical distribution of daily East-West and North-South wind components in the range between -75 to 107 m s, from 1997 to 2019 (, last access: 8 July 2019). 12 vertical levels are available from 50 to 1000 hPa at global scale. Our study selects the daily mean of wind speed and direction at 100 and 150 hPa in DJF from 2004 to 2017.

3 Methodology

This section summarizes the method developed by **?** to estimate ΔIWC, the amount of ice injected into the UT and the TL. **?** have presented a model relating Prec (as proxy of deep convection) from TRMM to IWC^{MLS} over tropical convective areas during austral convective season DJF. The IWC^{MLS} value measured by MLS during the growing phase of the convection (at x = 01:30 LT or 13:30 LT) is compared to the Prec value at the same time x in order to define the correlation coefficient (C) between Prec and IWC^{MLS}, as follows:

$$C = \frac{Prec_x}{IWC_x^{MLS}} \frac{IWC_x^{MLS}}{Prec_x} \tag{1}$$

The diurnal cycle of IWC estimated ($IWC^{est}(t)$) can be calculated by using C applied to the diurnal cycle of Prec (Prec(t)), where t is the time, as follows:

$$IWC^{est}(t) = Prec(t) \times C \tag{2}$$

The amount of IWC injected up to the UT or the TL (ΔIWC^{Prec}) is defined by the difference between the maximum of IWC^{est} (IWC$^{est}_{max}$) and its minimum (IWC$^{est}_{min}$).

$$\Delta IWC^{Prec} = C \times (Prec_{max} - Prec_{min}) = IWC^{est}_{max} - IWC^{est}_{min} \tag{3}$$

where $Prec_{max}$ and $Prec_{min}$ are the diurnal maximum and minimum of Prec, respectively. Figure **??** illustrates the relationship between the diurnal cycle of Prec and the two MLS measurements at 01:30 LT and 13:30 LT. The growing phase of the convection is defined as the period of increase in precipitation from $Prec_{min}$ to $Prec_{max}$. The amplitude of the diurnal cycle is defined by the difference between $Prec_{max}$ and $Prec_{min}$. In Fig. 1, because the growing phase of the convection illustrated is happening during the afternoon, only the MLS measurement at 13:30 LT is used in the calculation of ΔIWC. IWC at 01:30 LT is not used in that case.

4 Horizontal distribution of ΔIWC estimated from Prec over the MariCont

4.1 Prec from TRMM related to IWC from MLS

In order to identify the main areas of injection of ice in the TL over the MariCont, Figure **??** presents different parameters associated to this area: a) the name of the main islands and seas over the MariCont, b) the elevation (http://www.soda-pro.com/web-services/altitude/srtm-in-a-tile, last access: June 2019), c) the daily mean of Prec at 0.25° × 0.25° horizontal resolution, d) the hour of the diurnal maxima of Prec at 0.25° × 0.25° horizontal resolution, and e) the daily mean

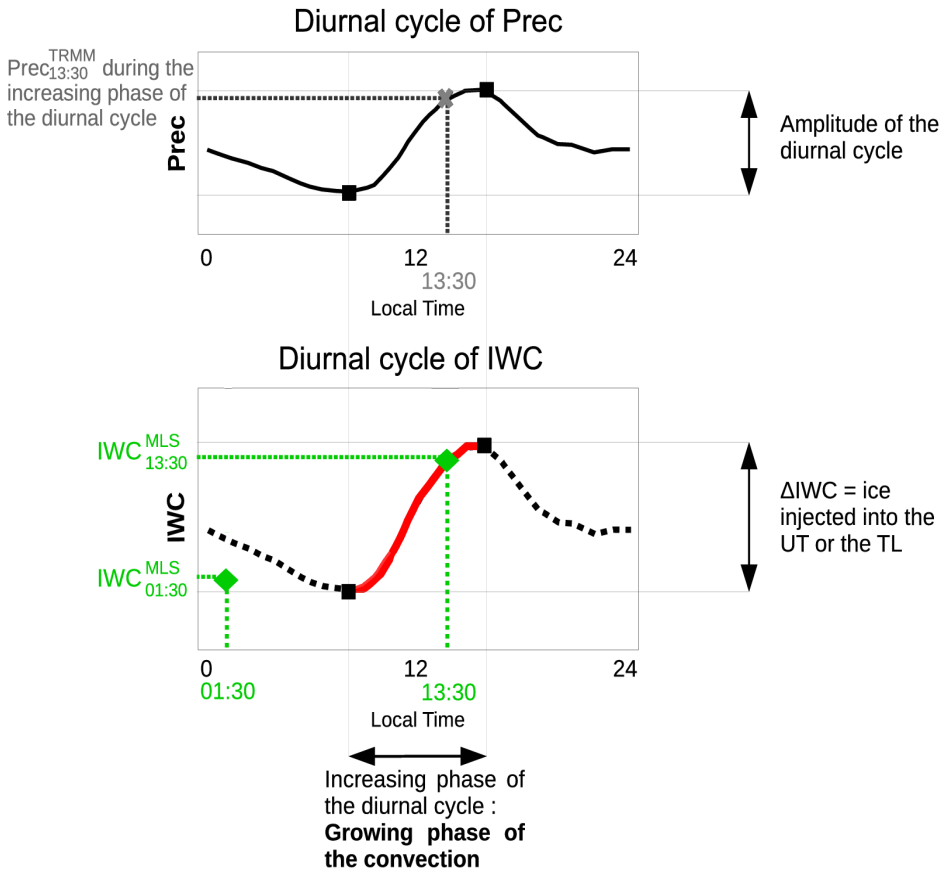

Figure 1. Illustration of the model used to estimate the amount of ice (ΔIWC) injected into the UT or the TL. Diurnal cycle of a proxy of deep convection (Prec) (a), diurnal cycle of ice water content (IWC) estimated from diurnal cycle of the proxy of deep convection (b). In red line, the increasing phase of the diurnal cycle. In black dashed line, the decreasing phase of the diurnal cycle. The green diamonds are the two IWC^{MLS} measurements from MLS. Grey thick cross represents the measurement of Prec during the growing phase of the convection ($Prec_x$), used in the model. Maximum and minimum of the diurnal cycles are represented by black squares. Amplitude of the diurnal cycle is defined by the differences between the maximum and the minimum of the cycle.

$(\bar{IWC} = (IWC_{01:30} + IWC_{13:30}) \times 0.5)$ of IWC^{MLS} at 146 hPa at 2° × 2° horizontal resolution. Several points need to be highlighted. Daily means of Prec over land and coastal parts are higher than over oceans (Fig. **??**c). Areas where the daily mean of Prec is maximum are usually surrounding the highest elevation over land (e.g. over NewGuinea) and near coastal areas (North West of Borneo in the China Sea and South of Sumatra in the Java Sea) (Fig. **??**b and c). ~~**?** explained that high precipitation is mainly concentrated over land in the MariCont because of the strong sea-breeze convergence, combined with~~

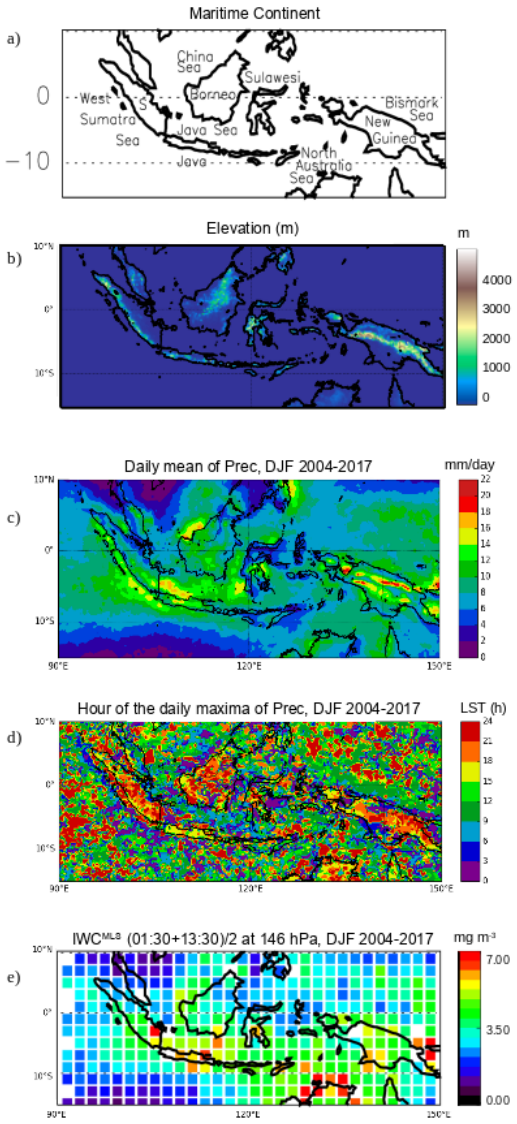

Figure 2. Main islands and seas of the MariCont (S is for Sumatra) (a), elevation from Solar Radiation Data (SoDa) (b); daily mean of Prec measured by TRMM over the Maritime Continent, averaged over the period of DJF 2004-2017 (c), hour (local solar time (LST)) of the diurnal maxima of Prec over the MariCont (d); daily mean (01:30 LT + 13:30 LT)/2 of IWC^{MLS} at 146 hPa from MLS over the MariCont averaged over the period of DJF 2004-2017 (e). ~~Horizontal~~ Observations are presented with a horizontal resolution of $0.25^\circ \times 0.25^\circ$ (b,c and d) and $2^\circ \times 2^\circ$ (e).

~~the mountain–valley winds and cumulus merging processes. The diurnal maximum of Prec over land is observed between~~ The times of the maxima of Prec are over land during the evening (18:00-00:00 LT~~and~~), over coast during the night-morning (00:00-06:00 ~~LT (Fig. **??**d) whereas, over coastal parts, it is in the early morning before 05:~~TL) and over sea during the

morning-noon and even evening depending of the sea considered (09:00-12:00 LT ~~. Over seas, the time of the diurnal maximum varies as a function of the region. Java Sea and North of Australia Sea present maxima around 13~~and 15:~~30 LT while the west Sumatra Sea and the Bismark Sea show maxima around 01~~00-00:~~30 LT~~00 LT). These differences could illustrate the impact of the land/sea breeze within the 24 hours. The sea breeze during the day favours the land convection at the end of the day when land temperature surface is higher than oceanic temperature surface. During the night, the coastline sea surface temperature becomes larger than the land surface temperature and the land breeze favours systematically the convection development over coast. These observations are consistent with results presented in **?**, explaining that high precipitation is mainly concentrated over land in the MariCont because of the strong sea-breeze convergence, but also because of the combination with the mountain–valley winds and cumulus merging processes. Amplitudes of the diurnal cycles of Prec over the MariCont will be detailed as a function of island and sea in section **??**. The location of the largest concentration of IWC (3.5 – 5.0 mg m^{-3}, Fig. **??**e) is consistent with that of Prec ($\sim$ 12 – 16 mm day^{-1}) over the West Sumatra Sea, and over the South of Sumatra island. However, over North Australia seas (including the Timor Sea and the Arafura Sea), we observed large differences between Prec low values (4 – 8 mm day^{-1}) and IWC large concentrations (4 – 7 mg m^{-3}).

4.2 Convective processes compared to IWC measurements

Although TRMM horizontal resolution is 0.25° × 0.25°, we require information at the same resolution as MLS IWC. From the diurnal cycle of TRMM Prec measurements, the duration of the increasing phase of Prec can be known for each 2° × 2° pixel. The duration of the growing phase of the convection can then be defined from Prec over each pixel. Figures **??**a and b present the anomaly (deviation from the mean) of Prec measured by TRMM–3B42 over the MariCont at 01:30 LT and 13:30 LT, respectively, only over pixels when the convection is in the growing phase. The anomaly of IWC measured by MLS over the MariCont is shown in Figs. **??**c and d, over pixels when the convection is in the growing phase at 01:30 LT and 13:30 LT, respectively. ~~Note that some pixels can be present~~ Each pixel of Prec at 01:30 LT or 13:30 LT during the growing phase of the convection deviates by the average of the all Prec at 01:30 LT or 13:30 LT during the growing phase of the convection over the whole MariCont. The gray color denotes pixels for which convection is not ongoing. Some pixels can be presented on both sets of Prec and IWC panels in Figs. ~~**??** only when~~3 when: 1) the onset of the convection is before 01:30 LT and the end is after 13:30 LT or ~~when~~ 2) the onset of the convection is before 13:30 LT and the end is after 01:30 LT. Note that, whithin each 2°x2° pixel, at least 60 measurements of Prec or IWC at 13:30 LT or 01:30 LT over the period 2004-2017 have been selected for the average.

The Prec anomaly at 01:30 LT and 13:30 LT varies between -0.15 and +0.15 mm h~~. At 13:30 LT, the~~ $^{-1}$. The growing phase of the convection ~~is mainly over land while, at 01~~over land is mainly at 13:30 LT~~, the growing phase of the convection is mainly over seas and coastlines. The strongest Prec anomaly~~ . At 13:30 LT, over land, the strongest Prec and IWC anomalies (+0.15 mm h~~) at 13:30 LT is~~ $^{-1}$ and +2.50 mg m^{-3}, respectively) are found over the Java island, ~~while the strongest Prec anomaly at~~ and north of Australia for IWC. At 01:30 LT~~is found over~~ , the growing phase of the convection is found mainly over sea (while the pixels of the land are mostly gray), with maxima of Prec and IWC anomalies over coastlines and seas close to the coasts such as the ~~West Sumatra Sea~~ Java Sea and the Bismark Sea. The IWC anomaly at 13:30 LT and 01:30 LT varies between

-3 and +3 mg m~~. The strongest value of IWC anomaly at 13:30 LT are found over Java, while the strongest values of IWC anomaly at 01:30 LT is found over coastlines and seas close to the coasts, such as the North Australia Sea, Java Sea, China Sea and coast around NewGuinea.~~ $^{-3}$. Three types of areas can be distinguished from Fig. **??**: i) area where Prec and IWC anomalies have the same sign (positive or negative either at 01:30 LT or 13:30 LT) (e.g. over Java, Borneo, Sumatra, Java Sea and coast of Borneo or the China Sea); ii) area where Prec anomaly is positive and IWC anomaly is negative (e.g. over West Sumatra Sea); and iii) area where Prec anomaly is negative and IWC anomaly is positive (e.g. over the North Australia Sea at 01:30 LT). Convective processes associated to these three types of areas over islands and seas of the MariCont are discussed in Sect. 6.

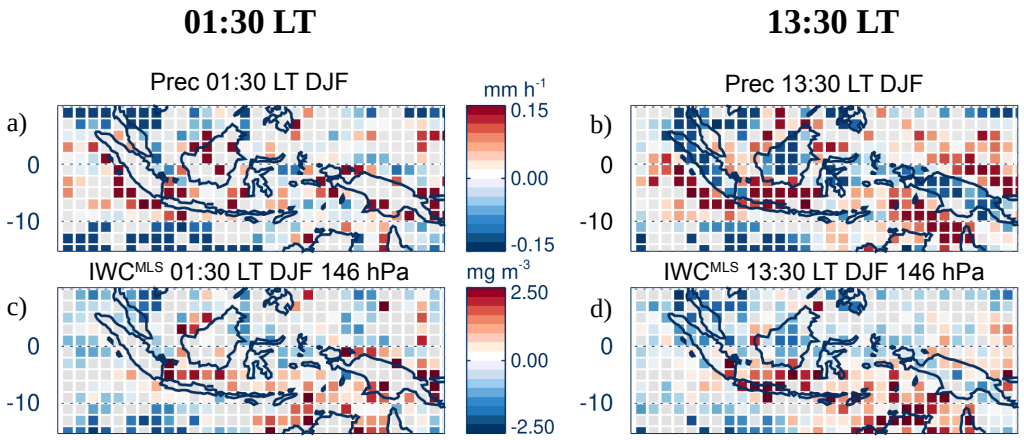

Figure 3. Anomaly (deviation from the mean) of Prec (a-b) and Ice Water Content (IWC^{MLS}) at 146 hPa (c-d), at 01:30 LT (left) and at 13:30 LT (right) over pixels where 01:30 LT and 13:30 LT are during the growing phase of the convection, respectively, averaged over the period of DJF 2004-2017. The gray color denotes pixels for which convection is not ongoing.

4.3 Horizontal distribution of ice injected into the UT and TL estimated from Prec

From the model developed in **?** based on Prec from TRMM–3B42 and IWC from MLS and synthesized in section 2.4, we can calculate the amount of IWC injected (ΔIWC) at 146 hPa (UT, Figure **??**a) and at 100 hPa (TL, Figure **??**b) by deep convection over the MariCont. In the UT, the amount of IWC injected over land is larger (> 10 – 20 mg m^{-3}) than over seas (< 10 mg m^{-3}). South of Sumatra, Sulawesi, North of New Guinea and North of Australia present the largest amounts of ΔIWC over land (15 – 20 mg m^{-3}). Java Sea, China Sea and Bismark Sea present the largest amounts of ΔIWC over seas (7 – 15 mg m^{-3}). West Sumatra Sea and North Australia Sea present low values of ΔIWC (< 2 mg m^{-3}). We can note that the anomalies of Prec and IWC during the growing phase over ~~West Sumatra Sea~~ North Australia Sea at 13:30 LT are positive (~~< 0.15 mg m~~> 0.2 mg m^{-3}, Fig. **??**a and b and > ~~2.50 mg m~~2.5 mg m^{-3}, Fig. **??**c and d, respectively). In the TL, the maxima (up to ~~3 mg m~~3.0 mg

m^{-3}) and minima (down to ~~2~~ 0.2 – ~~3 mg m~~0.3 mg m^{-3}) of ΔIWC are located within the same pixels as in the UT, although 3 ~~– 4~~ to 6 times lower than in the UT. The decrease of ΔIWC with altitude is larger over land (by a factor 6) than over sea (by a factor 3). We can note that the similar pattern between the two layers come from the diurnal cycle of Prec in the calculation of ΔIWC at 146 and 100 hPa. Only the measured value of IWC^{MLS} at 146 and 100 hPa can explain the observed différences in ΔIWC values at these two levels. Thus, similar ΔIWC patterns are expected between the two levels because, according to the model developed in Dion et al. (2019), the deep convection is the main process transporting ice into the UT and the TL during the growing phase of the convection. Convective processes associated to ~~these~~ land and sea are further discussed in Sect. 6.

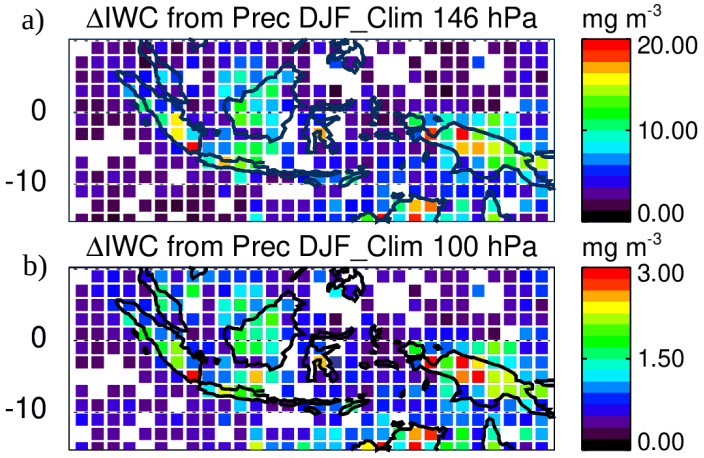

Figure 4. Daily amount of ice injected (ΔIWC) up to the UT (a) and up to the TL (b) estimated from Prec, averaged during DJF 2004-2017.

In order to better understand the impact of deep convection on the strongest ΔIWC injected per pixel ~~into the UT and the TL~~up to the TTL, isolated pixels selected in Fig. ~~4~~ 4a are presented separately in Figure **??**a and f. This Figure shows the diurnal cycles of Prec in four pixels selected for their large ΔIWC in the UT (≥ 15 mg m^{-3}, Fig. **??**b, c, d, e), and the diurnal cycle of Prec in four pixels selected for their low ΔIWC in the UT (but large enough to observe the diurnal cycles of ~~Prec~~ IWC between 2.0 and 5.0 mg m^{-3}, Fig. **??**g, h, i, j). Pixels with low values of ΔIWC over land (Figs. **??**g, h and i) present small amplitude of diurnal cycles of Prec (∼ +0.5 mm h^{-1}), with maxima between 15:00 LT and 20:00 LT and minima around 11:00 LT. The pixel with low value of ΔIWC over sea (Fig. **??**j) presents an almost null amplitude of the diurnal cycle of Prec with low value of Prec all day long (∼ 0.25 mm h^{-1}). Pixels with large values of ΔIWC over land (Fig. **??**b, c, d, e) present longer duration of the increasing phase of the diurnal cycle (from ∼ 09:00 LT to 20:00 – 00:00 LT) than the increasing phase of Prec diurnal cycle over pixels with low values of ΔIWC (from 10:00 LT to 15:00 – 19:00 LT). More precisely, pixels labeled 1 and 2 over New Guinea (Fig. **??**d and e) and the pixel over South of Sumatra (Fig. **??**c) show amplitude of diurnal cycle of Prec reaching 1.0 mm h^{-1}, while the pixel over North Australia (Fig. **??**b) presents lower amplitude of diurnal cycle of Prec (0.5 mm h^{-1}).

IWC measured by MLS during the growing phase of deep convection and the diurnal cycle of IWC estimated from Prec are also shown on Fig. **??**. For pixels with large values of ΔIWC, IWC observed by MLS is between 4.5 and 5.7 mg m^{-3} over North Australia Sea, South Sumatra and New Guinea. For pixels with low values of ΔIWC, IWC observed by MLS is found between 1.9 and 4.7 mg m^{-3}. To summarize, large values of ΔIWC are observed over land in combination to i) longer growing phase of deep convection (> 9 hours) ~~, ii) high value of IWC (> ~4.5 mg m) at 13:30 LT over land and01:30 LT over seas,~~ ~~and~~and/or ~~iii~~ii) large diurnal amplitude of Prec (> 0.5 mm h~~). This shows that ΔIWC is strongly correlated with the shape of the diurnal cycle of Prec.~~$^{-1}$).

In the next section, we estimate ΔIWC using another proxy of deep convection, namely Flash measurements from LIS.

5 Relationship between diurnal cycle of Prec and Flash over MariCont land and sea

Lightning is created into cumulonimbus clouds when the electric potential energy difference is large between the base and the top of the cloud. Lightning can appear at the advanced stage of the growing phase of the convection and during the mature phase of the convection. For these reasons, in this section, we use Flash measured from LIS during DJF 2004-2015 as another proxy of the deep convection in order to estimate ΔIWC (ΔIWC^{Flash}) and check the consistency with ΔIWC obtained with Prec (ΔIWC^{Prec}).

5.1 Flash distribution over the MariCont

Figure **??**a presents the daily mean of Flash in DJF 2004-2015 at 0.25° × 0.25° horizontal resolution. Over land, Flash can reach a maximum of 10~~flashes per day~~$^{-1}$ flashes day^{-1} per pixel while, over seas, Flash are less frequent (∼ 10~~flashes per day~~$^{-3}$ flashes day^{-1} day per pixel). When compared to the distribution of Prec (Fig. **??**c), maxima of Flash are found over the same areas as maxima of Prec (Java, East of Sulawesi coast, Sumatra and North Australia lands). Over Borneo and NewGuinea, coastlines present more Flash (∼10~~flashes per day~~$^{-2}$ flashes day^{-1}) than inland (∼10~~flashes per day~~$^{-3}$ flashes day^{-1}). Differences between Flash and Prec distributions are found over North Australia Sea, with relatively large number of Flash (∼ >10~~flashes per day~~$^{-2}$ flashes day^{-1}) compared to low Prec (4 – 10 mm day^{-1}) (Fig. **??**c), and over NewGuinea where the number of Flash is relatively low (∼10^{-2}- 10~~flashes day~~$^{-3}$ flashes day^{-1}) while Prec is high (∼14 – 20 mm day^{-1}). Figure **??**b shows the hour of the Flash maxima. Over land, the maximum of Flash is between 15:00 LT and 19:00 LT, slightly earlier than the maximum of Prec (Fig. **??**d) observed between 16:00 LT and 24:00 LT. Coastal areas present similar hours of maximum of Prec and Flash, i.e between 00:00 LT and 04:00 LT although, over the West Sumatra Coast, diurnal maxima of both Prec and Flash happen 1–4 hours earlier (from 23:00-24:00 LT) than those of other coasts.

5.2 Prec and Flash diurnal cycles over the MariCont

This section compares the diurnal cycle of Flash with the diurnal cycle of Prec in order to assess the potential for Flash to be used as a proxy of deep convection over land and sea of the MariCont. Diurnal cycles of Prec and Flash over the MariCont land, ~~offshore and coastline~~ coastline and offshore (MariCont_L, MariCont_~~O MariCont-C~~C, MariCont_O, respectively) are

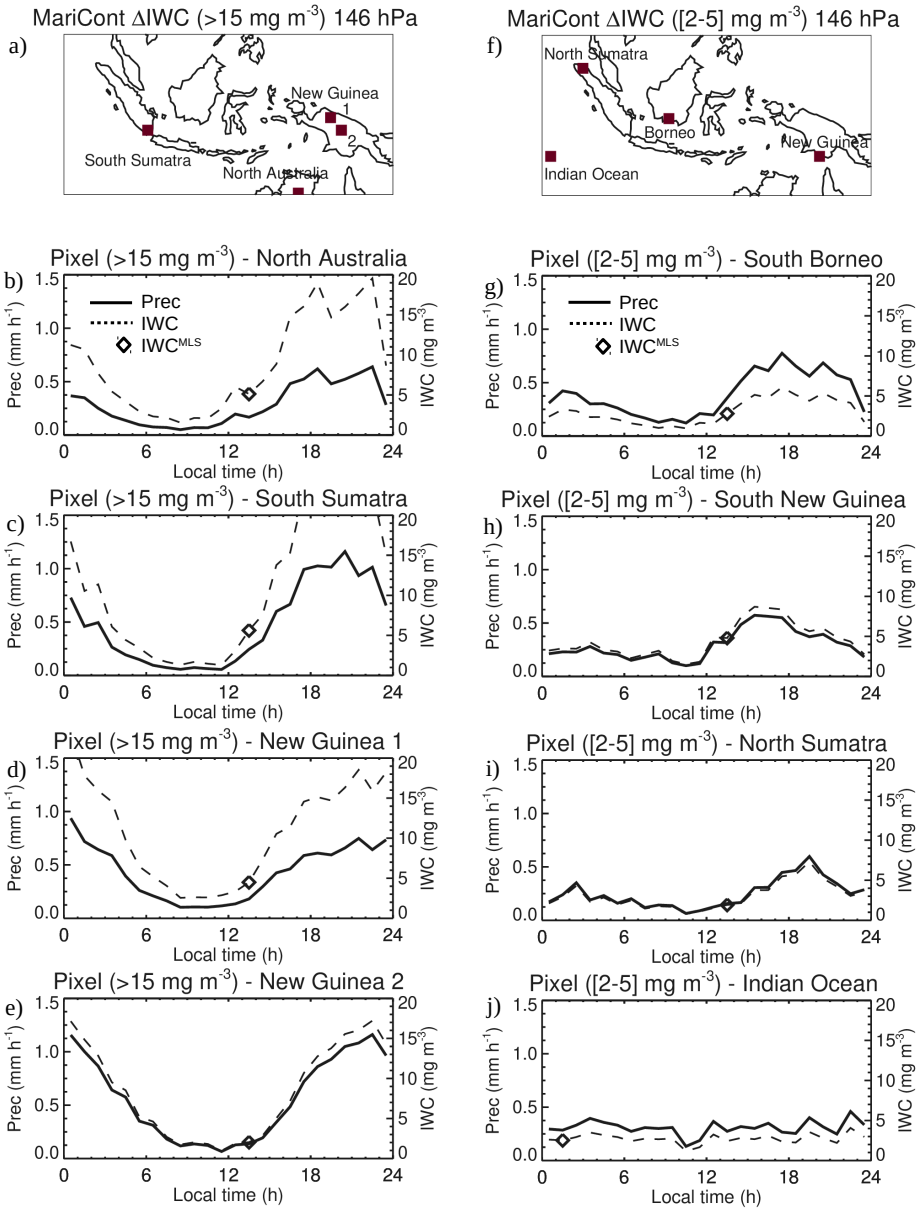

Figure 5. a) and f) location of 2° × 2° pixels where ΔIWC have been found higher than 15 mg m^{-3} (in Fig. 4) and where ΔIWC have been found between 2 and 5 mg m^{-3} (in Fig. 4), respectively. Diurnal cycle of Prec (solid line): (b, c, d, e) over 4 pixels where ΔIWC have been found higher than 15 mg m^{-3} (in Fig. 4), (g, h, i, j) over 4 pixels where ΔIWC have been found between 2 and 5 mg m^{-3} (in Fig. 4), during DJF 2004-2017. The Diamond is IWC^{MLS} measured by MLS during the increasing phase of the convection. The dashed line is the diurnal cycle of IWC estimated from the diurnal cycle of Prec and from IWC^{MLS}.

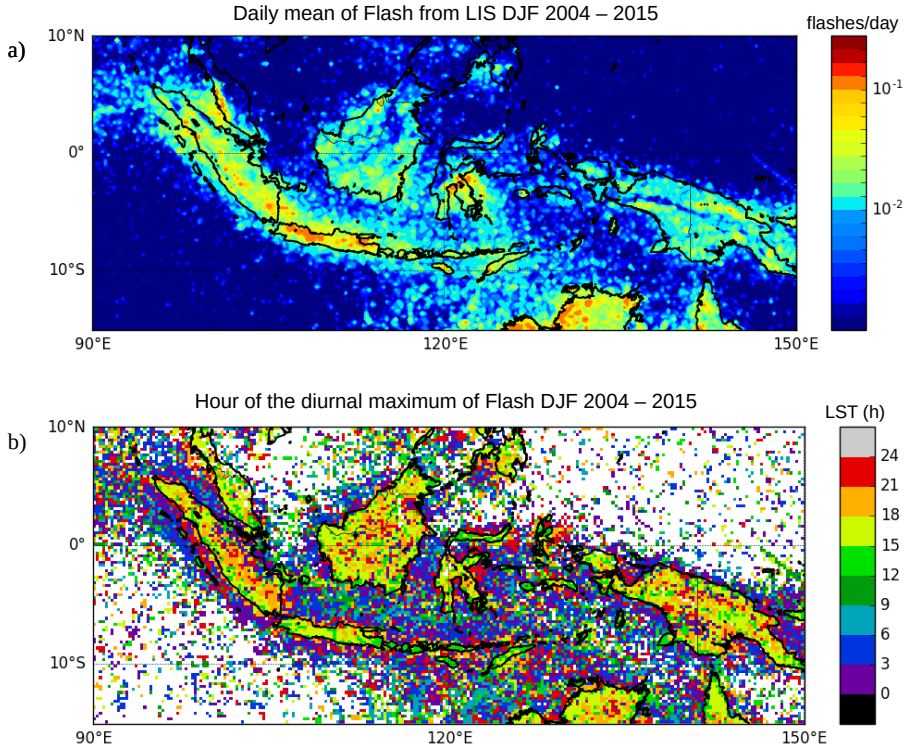

Figure 6. Daily mean of Flash measured by LIS averaged over the period DJF 2004-2015 (a); Hour (local solar time (LST)) of the diurnal maximum of Flash (b).

shown in Figs. **??**a–c, respectively. Within each 0.25° × 0.25° bin, land/coast/ocean ~~/coast~~filters were applied from the Solar Radiation Data (SoDa, http://www.soda-pro.com/web-services/altitude/srtm-in-a-tile). ~~MariCont_C~~ MariCont_C is the average of all coastlines defined as 5 pixels ~~over~~ extending into the sea from the land ~~limits.~~ limit. This choice of 5 pixels has been taken applying some sensitivity tests in order to have the best compromise between a high signal-to-noise ratio and a good representation of the coastal region. The MariCont_O is the average of all offshore pixels defined as sea pixels excluding 10 pixels (2000 km off the land) over the sea from the land coasts, thus coastline pixels are excluded as well as all the coastal influences. MariCont_L is the area of all land pixels. A given 0.25° ×0.25° pixel can contain information from different origins : land/coastlines or sea/coastlines. In that case, we can easily discriminate between land and coastlines or sea and coastlines by applying the land/ocean/coastlines filters. Consequently, this particular pixel will be flagged both as land and coastlines or sea and coastlines

Over land, during the growing phase of the convection, Prec and Flash start to increase at the same time (10:00 LT – 12:00 LT) but Flash reaches a maximum earlier (15:00 LT – 16:00 LT) than Prec (17:00 LT – 18:00 LT). This is consistent with the finding of Liu and Zipser (2008) over the whole tropics. Different maximum times could come from the fact that, while the deep convective activity intensity starts to decrease with the number of flashes, Prec is still high during the dissipating stage of

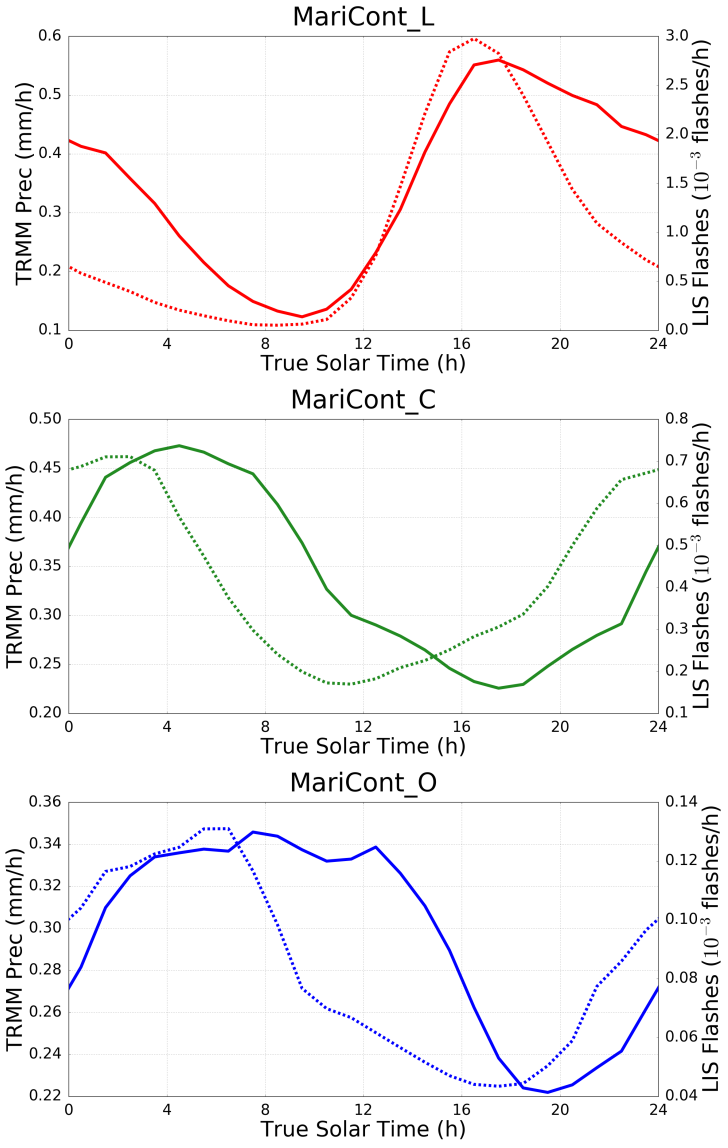

Figure 7. Diurnal cycle of Prec (solid line) and diurnal cycle of Flash (dashed line) over MariCont_L (top), MariCont_~~O~~ C (middle) and MariCont_~~C~~ O (bottom).

the convection and takes longer times to decrease than Flash. Consequently, combining our results with the ones presented in **?**, Flash and Prec can be considered as good proxies of deep convection during the growing phase of the convection over the MariCont_L.

Over ~~offshore areas (Fig. **??**b), minima of diurnal cycle of Prec and diurnal cycle of Flash are in the late afternoon, between 16:00 LT and 17:00 LT (Flash) and 17:00 LT and 18:00 LT (Prec), whilst maxima of diurnal cycle of Prec and Flash are reached in the early morning, between 04:00 LT and 09:00 LT (Flash) and around 08:00 LT – 09:00 LT (Prec). Results over offshore~~

areas are consistent with diurnal cycle of Flash and Prec calculated by ? over the whole tropical ocean, showing the increasing phase of the diurnal cycle of Flash starting 1–2 hours before the increasing phase of the diurnal cycle of Prec. Over coastlines (Fig. ??c), the Prec diurnal cycle is delayed by about + 2 to 7 h with respect to the Flash diurnal cycle. Prec minimum is around 18:00 LT while Flash minimum is around 11:30 LT. Maxima of Prec and Flash are found around 04:00 LT and 02:00 LT, respectively. This means that the increasing phase of Flash is 2-3 h longer than that of Prec. These results are consistent with ? showing a diurnal maximum of precipitation in the early morning between 02:00 LT and 03:00 LT and a diurnal minimum of precipitation around 11:00 LT, over coastal zones of Sumatra. According to Petersen and Rutledge (2001) and ? and ?, coastal zones are areas where precipitation results more from convective activity than from stratiform activity and the amplitude of diurnal maximum of Prec decreases with the distance from the coastline.

Over offshore areas (Fig. ??b), minima of diurnal cycle of Prec and diurnal cycle of Flash are in the late afternoon, between 16:00 LT and 17:00 LT (Flash) and 17:00 LT and 18:00 LT (Prec), whilst maxima of diurnal cycle of Prec and Flash are reached in the early morning, between 06:00 LT and 07:00 LT (Flash) and around 08:00 LT – 09:00 LT (Prec). Results over offshore areas are consistent with diurnal cycle of Flash and Prec calculated by ? over the whole tropical ocean, showing the increasing phase of the diurnal cycle of Flash starting 1–2 hours before the increasing phase of the diurnal cycle of Prec.

The time of transition from maximum to minimum of Prec is always longer than that of Flash. The period after the maximum of Prec is likely more representative of stratiform rainfall than deep convective rainfall. Consistently, over the MariCont ocean, model results from ? have shown that deep the suppression of the deep convection over offshore area in West of Sumatra from the early afternoon due to downwelling wavefront highlighted by deep warm anomalies around noonare coming from a downwelling wavefront which suppresses the convection offshoreduring early afternoon. . According to the authors, later in the afternoon, gravity waves are forced by the stratiform heating profile and propagate slowly offshore. They also highlighted that the diurnal cycle of the offshore convection responds strongly to the gravity wave forcing at the horizontal scale of 4 km.

To summarize, diurnal cycles of Prec and Flash show that:

i) over land, Flash increases proportionally with Prec during the growing phase of the convection,

ii) over offshore areascoastlines, Flash increasing phase is advanced by about 1more than 6–2 7 hours compared to Prec increasing phase,

iii) over coastlinesoffshore areas, Flash increasing phase is advanced by more than 6about 1–7 2 hours compared to Prec increasing phase.

In section ??, we investigate whether this time difference impacts the estimation of ΔIWC over land, coasts, and offshore areas.

5.3 Prec and Flash diurnal cycles and small-scale processes

In this subsection, we study the diurnal cycle of Prec and Flash at $0.25^\circ \times 0.25^\circ$ resolution over areas of deep convective activity over the MariCont. In line with the distribution of large value of Prec (Fig. ??), IWC (Fig. ??) and ΔIWC (Fig. ??), we have selected five islands and five seas over the MariCont. Diurnal cycles of Prec and Flash are presented over land for a) Java, b) Borneo, c) New Guinea, d) Sulawesi and e) Sumatra as shown in Figure ?? and over sea for the a) Java Sea, b) North

Australia Sea (NAusSea), c) Bismark Sea, d) West Sumatra Sea (WSumSea) and e) China Sea as shown in Figure **??**. Diurnal cycles of IWC from ERA5 (IWC^{ERA5}) are also presented in Fig. 8 and 9 and will be discussed in Section 6.

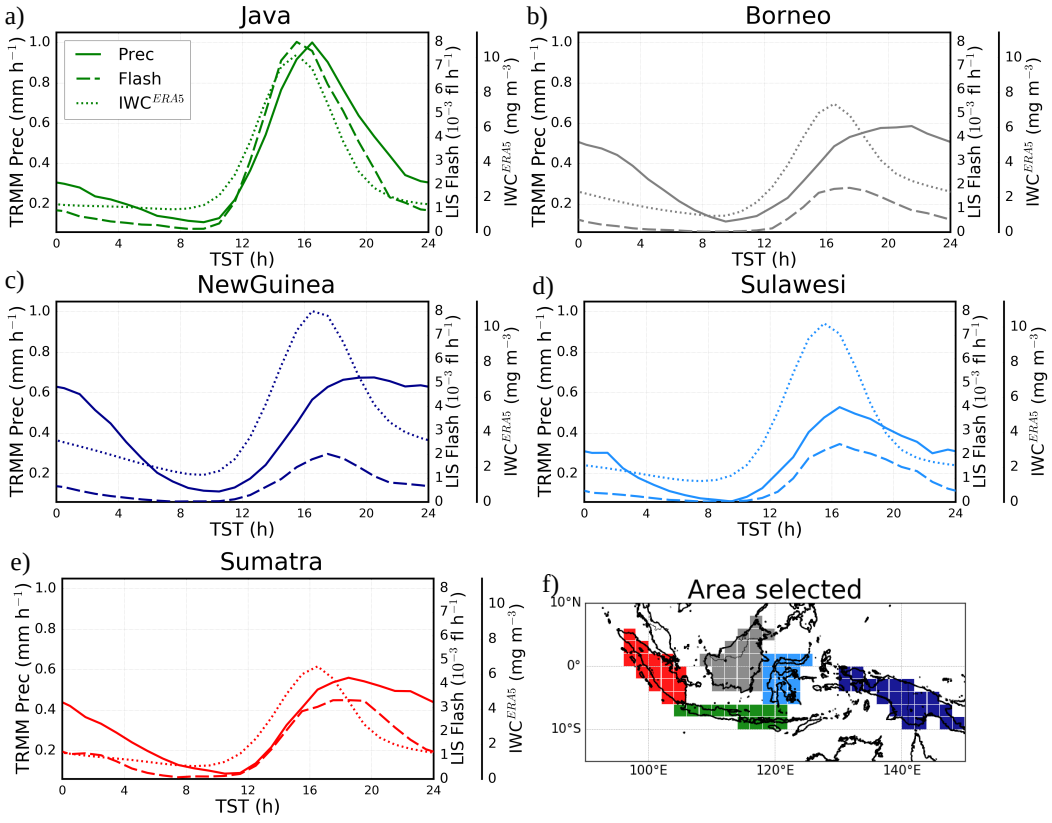

Figure 8. Diurnal cycles of Prec (solid line), Flash (dashed line) and IWC^{ERA5} from ERA5 at 150 hPa (dotted line) over MariCont islands: Java (a), Borneo (b), New Guinea (c), Sulawesi (d) and Sumatra (e) and map of the study zones over land (f).

Over land, the amplitude of the diurnal cycle of Prec is the largest over Java (Fig. **??**a), consistent with **?**, with a maximum reaching 1 mm h^{-1}, while, over the other areas, maxima are between 0.4 and 0.6 mm h^{-1}. Furthermore, over Java, the duration of the increasing phase in the diurnal cycle of Prec is 6-h consistent with that of Flash and elsewhere, the duration of the increasing phase is longer in Prec than in Flash by 1–2 h. The particularity of Java is related to the increasing phase of the diurnal cycle of Prec (6 h), that is faster than over all the other land areas considered in our study (~~8~~ 7 – ~~10 h)and is very consistent with the diurnal cycle of Prec over South America and South Africa (?)~~8 h). The strong and rapid convective growing phase measured over Java might be explained by the fact that the island is narrow with high mountains (up to $\sim$ 2000 m of altitude, as shown in Fig. 2b) reaching the coast. The topography promotes the growth of intense and rapid convective activity. The convection starts around 09:00 LT, rapidly elevating warm air up to the top of the mountains. Around 15:00 LT, air masses cooled in altitude are transported to the sea favoring the dissipating stage of the convection. Sulawesi is also

a small island ~~and presents the same onset of growing phase for the convection as Java, consistent with results presented in Nesbitt and Zipser (2003) and ?~~with high topography as Java. However, the amplitude of the diurnal cycle of Prec and Flash is not as strong as over Java. Other islands, such as Borneo, New Guinea and Sumatra, have high mountains but also large lowland areas. Mountains promote deep convection at the beginning of the afternoon while lowlands help maintain the convective activity through shallow convection and stratiform rainfall (**??**). Deep and shallow convection are then mixed during the slow dissipating phase of the convection (from $\sim$ 16:00 LT to 08:00 LT). However, because Flash are observed only in deep convective clouds, the decreasing phase of Flash diurnal cycles decreases more rapidly than the decreasing phase of Prec. The diurnal maxima of Prec found separately over the 5 islands of the MariCont are much higher than the diurnal maxima of Prec found over tropical land (South America, South Africa and MariCont_L) from **?**: $\sim$ 0.6 – 1.0 mm h^{-1} and $\sim$ 0.4 mm h^{-1}, respectively. However, the duration of the increasing phase of the diurnal cycle of Prec is consistent with the one calculated over tropical land by **?**.

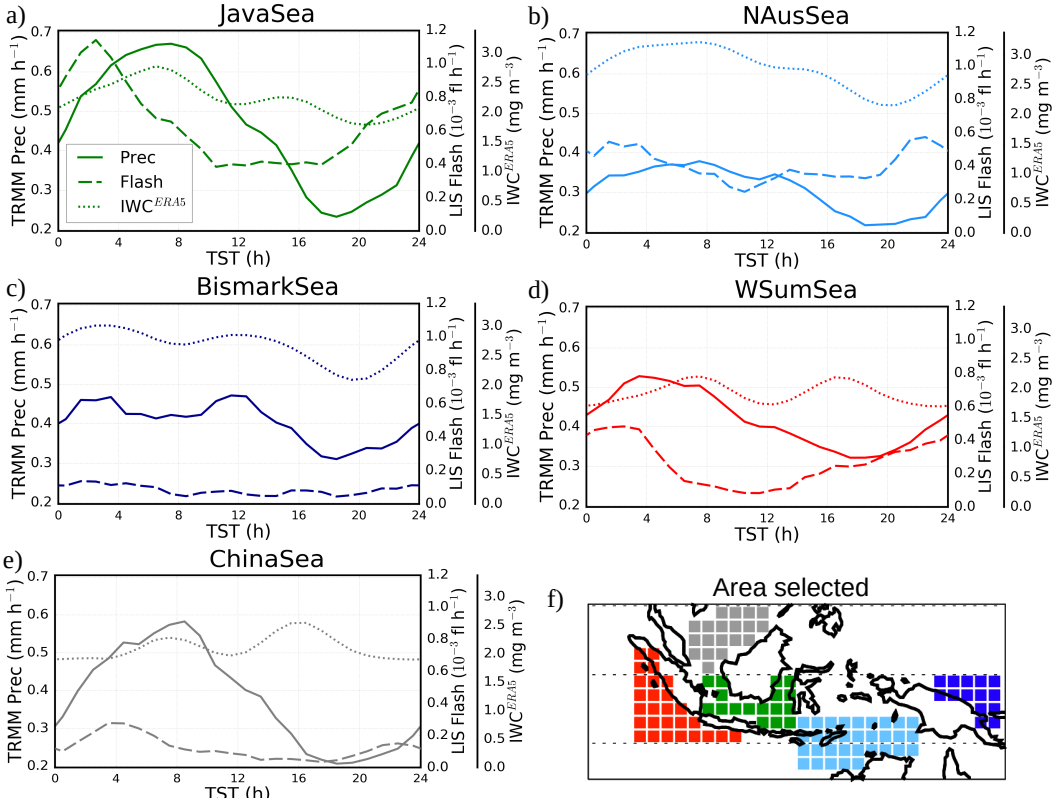

Figure 9. Diurnal cycles of Prec (solid line), Flash (dashed line) and IWC^{ERA5} from ERA5 at 150 hPa (dotted line) over MariCont seas: Java Sea (a), North Australia Sea (NAusSea) (b), Bismark Sea (c), West Sumatra Sea (WSumSea) (d), China Sea (e) and map of the study zones over sea (f).

Over sea, the five selected areas (Fig. **??**a–e) show a diurnal cycle of Prec and Flash either coastline or offshore areas depending onthe area. The diurnal cycle of Prec and Flash over Java Sea is similar to the one over coastlines (Fig. **??**c). Java Sea (Fig. **??**a), an area mainly surrounded by coasts, shows the largest diurnal maximum of Prec ($\sim$ 0.7 mm h^{-1}) and Flash ($\sim$ 1.1 10~~flashes h~~$^{-3}$ flashes h^{-1}) with the longest growing phase. In this area, land and sea breezes observed in coastal areas impact the diurnal cycle of the convection (**?**). During the night, land breeze develops from a temperature gradient between warm sea surface temperature and cold land surface temperature and conversely during the day. Over Java Sea, Prec is strongly impacted by land breezes from Borneo and Java islands (**?**), explaining why Prec and Flash reach largest values during the early morning. By contrast, NAusSea, Bismark Sea and WSumSea (Figs. **??**b, c and d, respectively) present small amplitude of diurnal cycle. In our analysis, these three study zones are the areas including the most offshore pixels. Java Sea and WSumSea present a similar diurnal cycle of Prec and Flash, with Flash growing phase starting about 4 h earlier than that of Prec. China Sea also shows a diurnal maximum of Flash shifted by about 4 hours before the diurnal maximum of Prec, but the time of the diurnal minimum of Prec and Flash is similar. Over ~~NAusSea~~ China Sea and Bismark Sea, the diurnal cycle of Flash shows a ~~very~~ weak amplitude with maxima reaching only 0.1~~flashes h. However, the diurnal minima of Prec and Flash over Bismark Sea are found to be at the same time (~17~~ $\times$ 0.2 10^{-3} flashes h^{-1}. Furthermore, over the Bismark Sea, while the diurnal minimum in Prec is around 18:00 LT, there are several local minima in Flash (08:00, 14:00 and 18:00 LT). Over NAusSea, the diurnal minimum of Prec is delayed by more than 7 hours compared to the diurnal minimum of Flash.

To summarize, over island, Flash and Prec convective increasing phases start at the same time and increase similarly but the diurnal maximum of Flash is reached 1–2 hours before the diurnal maximum of Prec. Over seas, the duration of the convective increasing phase and the amplitude of the diurnal cycles are not always similar depending on the area considered. The diurnal cycle of Flash is advanced by 4 hours over Java Sea and West Sumatra Sea and by more than 7 hours over North Australia Sea compared to the diurnal cycle of Prec. China Sea and Bismark Sea present the same time of the onset of the Flash and Prec increasing phase. In Section 7, we estimate ΔIWC over the 5 selected island and sea areas from Prec and Flash as a proxy of deep convection.

6 Horizontal distribution of IWC from ERA5 reanalyses

The ERA5 reanalyses provide hourly IWC at 150 and 100 hPa (IWC^{ERA5}). The diurnal cycle of IWC over the MariCont from ERA5 will be used to calculate ΔIWC from ERA5 in order to assess the horizontal distribution and the amount of ice injected in the UT and the TL deduced from our model combining MLS ice and TRMM Prec or MLS ice and LIS flash. Figures **??**a, b, c and d present the daily mean and the hour of the diurnal maxima of IWC^{ERA5} at 150 and 100 hPa. In the UT, the daily mean of IWC^{ERA5} shows a horizontal distribution over the MariCont consistently with that of IWC^{MLS} (Fig. **??**e), except over NewGuinea where IWC^{ERA5} (reaching 6.4 mg m^{-3}) is much stronger than IWC^{MLS} ($\sim$ 4.0 mg m^{-3}). The highest amount of IWC^{ERA5} is located over NewGuinea mountain chain and in the West coast of North Australia (reaching 6.4 mg m^{-3} in the UT and 1.0 mg m^{-3} in the TL). Over islands in the UT and the TL, the hour of the IWC^{ERA5} diurnal maximum is found between 12:00 LT and 15:00 LT over Sulawesi and New Guinea and between 15:00 LT and 21:00 LT over Sumatra, Borneo

and Java, that is close to the hour of the diurnal maximum of Flash over islands (Fig. **??**). Over sea, in the UT and the TL, the hour of the IWC^{ERA5} diurnal maximum is found between 06:00 LT and 09:00 LT over West Sumatra Sea, Java Sea, North Australia Sea, between 06:00 LT and 12:00 LT over China Sea and between 00:00 LT and 03:00 LT over Bismark Sea. There are no significant differences between the hour of the maximum of IWC^{ERA5} in the UT and in the TL.

The diurnal cycles of IWC^{ERA5} at 150 hPa are presented in Figs. **??** and **??** over the selection of islands and seas of the MariCont together with the diurnal cycles of Prec and Flash. Over islands (Fig. **??**), the maximum of the diurnal cycle of IWC^{ERA5} is found between 16:00 LT and 17:00 LT, consistent with the diurnal cycle of Prec and Flash. The duration of the increasing phase of the diurnal cycles of Prec, Flash and IWC^{ERA5} are all consistent to each other ~~, ~ 4~~ (6 – ~~5 h~~8 h). Over sea (Fig. **??**), the maximum of the diurnal cycle of IWC^{ERA5} is mainly found between 07:00 LT and 10:00 LT ~~, consistently with the diurnal cycle of Prec (which is 2 – 3 hours after the diurnal maxima for Flash). Over~~ over Java Sea and North Australia Sea, ~~the diurnal maxima and minima are found at the same hours as the diurnal maxima and minima of Prec~~ consistently with the diurnal cycle of Prec and a second peak is found around 16:00 LT. Thus, the duration of the increasing phase of the diurnal ~~cycle~~ cycles of IWC^{ERA5} is consistent with the one of Prec over these two sea study zones ~~, ~~ (~10 hours), but not with the one of ~~Prec~~Flash. Over Bismark Sea, ~~West Sumatra Sea and China Sea, the diurnal cycles~~ the diurnal maxima of IWC^{ERA5} ~~show two maxima:one at the end of the local morning and the other one during the local afternoon. Over Bismark Sea, these two maxima are consistent with those observed in the diurnal cycle of Prec, consequently the increasing phases of the diurnal cycles of IWC^{ERA5} and Prec are consistent to each other. Over West Sumatra Sea and~~ are found at 04:00 LT with a second peak later at noon. Over West Sumatra Sea, two diurnal maxima are found at 08:00 LT and 17:00 LT. Over China Sea, the ~~two maxima in the diurnal cycle~~ diurnal maximum of IWC^{ERA5} are ~~not observed in the~~ found at 16:00 LT with a second peak at 08:00 LT. These differences in the timing of the maximum of the diurnal cycle of Prec~~and Flash, consequently the increasing phase of IWC^{ERA5} is not consistent with the one of Prec nor the one of Flash.~~ , Flash and IWCERA5 observed at small-scale over sea of the MariCont are not well understood. However, these differences do not impact on the calculation of the ΔIWCPrec, ΔIWCFlash or ΔIWCERA5. Results are presented Section 7.

7 Ice injected over a selection of island and sea areas

7.1 ΔIWC deduced from observations

Figure **??** synthesizes ΔIWC in the UT and the TL over the 5 islands and 5 seas of the MariCont studied in the previous section. Eqs. (1-3) are used to calculate ΔIWC from Prec (ΔIWC^{Prec}) and from Flash (ΔIWC^{Flash}). ~~The~~ As presented in the previous section, Prec and Flash can be used as two proxies of deep convection, with differences more or less accentuated in their diurnal cycles as a function of the region considered. Thus, the observational ΔIWC range calculated between ΔIWC^{Prec} and ΔIWC^{Flash} provides an upper and lower bound of ΔIWC calculated from observational datasets.

In the UT (Fig. **??**a), over islands, ΔIWC calculated over Sumatra, Borneo, Sulawesi and New Guinea varies from ~~4.87 to 6.86 mg m~~4.9 to 6.9 mg m^{-3} whilst, over Java, ΔIWC reaches ~~7.89~~7.9 ~~–8.72 mg m~~8.7 mg m^{-3}. ΔIWC^{Flash} is generally greater than ΔIWC^{Prec} by less than 1.0 mg m~~(41~~$^{-3}$ (((ΔIWC^{Flash}-ΔIWC^{Prec})/ΔIWC^{Flash})×100 ranges from 4 to 22%)

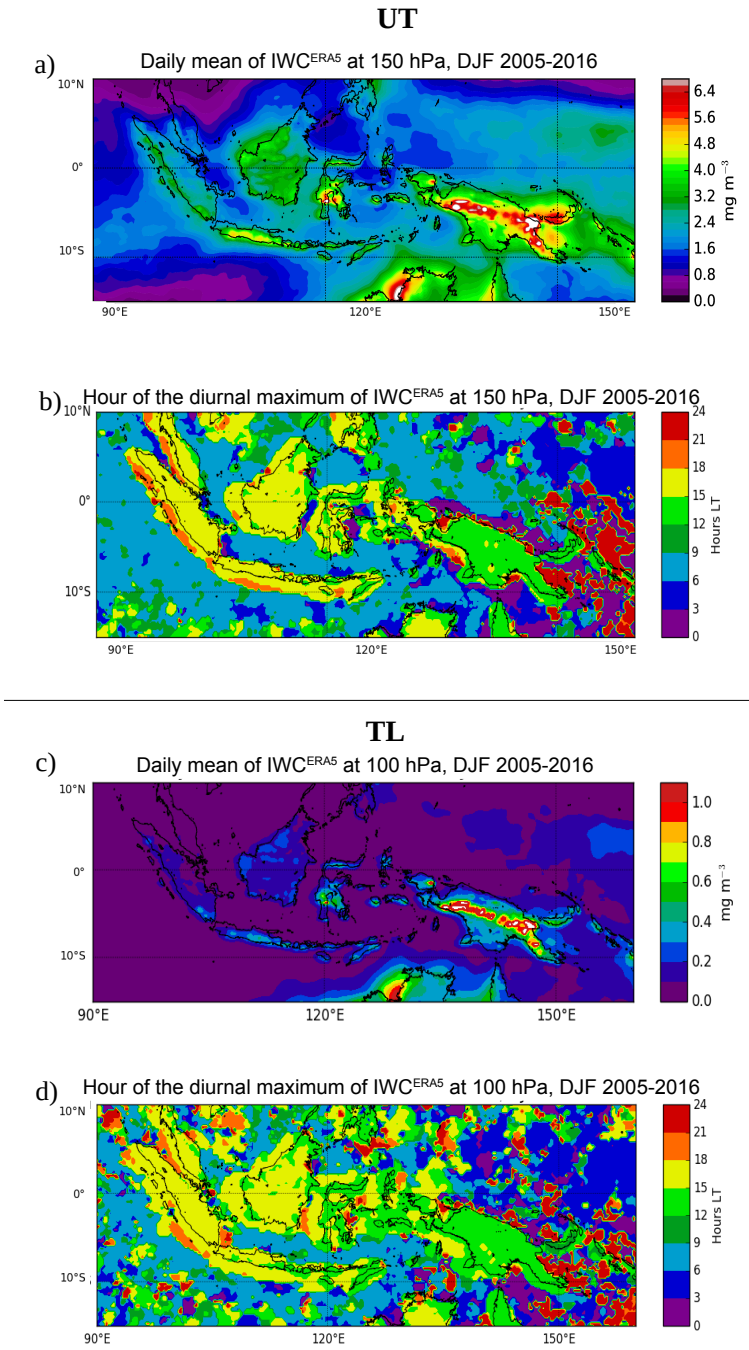

Figure 10. Daily mean of IWC^{ERA5} averaged over the period DJF 2005-2016 at 150 hPa (a) and at 100 hPa (c); Time (hour, local time (LT)) of the diurnal maximum of IWC^{ERA5} at 150 hPa (b) and at 100 hPa (d).

for all the islands, except for ~~New Guinea where the difference reaches 1.40 mg m(20%). Conversely, over Java , ΔIWC^{Prec}~~ Java where is larger than ΔIWC^{Flash} by ~~0.71 mg m(8~~0.7 mg m^{-3} (~~-8~~%). Over sea, ΔIWC varies from ~~1.17 to 4.37 mg m~~1.2 to 4.4 mg m^{-3}. ΔIWC^{Flash} is greater than ΔIWC^{Prec} by 0.6 to ~~2.09 mg m~~2.1 mg m^{-3} (31-50%), except for Java Sea, where ΔIWC^{Prec} is greater than ΔIWC^{Flash} by ~~0.21 mg m(6~~ 0.2 mg m^{-3} (~~-7~~%). Over North Australia Sea, ~~probably because of the 7-hours lagged diurnal cycle of Flash compared to Prec (Fig. **??**),~~ ΔIWC^{Flash} is almost twice as large as than ΔIWC^{Prec} (53%).

In the TL (Fig. **??**b), the observational ΔIWC range is found between ~~0.72 and 1.28 mg m~~0.7 and 1.3 mg m^{-3} over islands and between ~~0.22 and 0.74 mg m~~0.2 and 0.7 mg m^{-3} over seas. The same conclusions apply to the observational ΔIWC range calculated between ΔIWC^{Prec} and ΔIWC^{Flash} in the TL as in the UT with differences less than ~~0.39 mg m~~0.4 mg m^{-3}.

~~At~~ To summarize, independently of the proxies used for the calculation of ΔIWC, and at both altitudes, Java shows the largest injection of ice over the MariCont. Furthermore, it has been shown that both proxies can be used in our model, with more confidence over land: ΔIWC^{Prec} and ΔIWC^{Flash} are consistent to ~~within 4-20 % over islands and 6-50 % over seas~~ each other to within 4-22% over island and 7-53% over sea in the UT and the TL. The largest difference over sea is probably due to the larger contamination of stratiform precipitation included in Prec over sea. ~~Although Flash, is not contaminated by stratiform clouds, it could be a better proxy than Prec over sea but it is unfortunately negligible: less than 10flashes per day (Fig. **??**).~~

7.2 ΔIWC deduced from reanalyses

ΔIWC from ERA5 (ΔIWC^{ERA5}) is calculated in the UT and the TL (z_0 = ~~100 and~~ 150 and 100 hPa, respectively) as the max–min difference in the amplitude of the diurnal cycle. ~~To be consistent~~ Consistently with the MLS observations, we ~~should degrade~~ have degraded the ERA5 vertical resolution to assess the impact of the vertical resolution on ΔIWC^{ERA5}. ~~In the optimal estimation theory (**?**), the vertical distribution of~~ According to Wu et al. (2008), IWC^{ERA5} (IWC^{MLS} estimation derived from MLS represent spatially-averaged quantities within a volume that can be approximated by a box of 300×7×4 km^3 near the pointing tangent height. In order to compare IWC^{MLS} and IWC^{ERA5}~~(z)) should be convolved with the IWC^{MLS} averaging kernels, but this information is not provided by MLS. Instead, we have created a unitary triangular function $\phi(z, z_0, \delta z)$ centered at z_0 with a width at half-maximum of δz.The convolved IWC~~, we degraded: 1) the horizontal resolution of ERA5 from 0.25°×0.25° to 2°×2° (200 km×200 km) and 2) ERA5 data by connecting the vertical profiles of IWC^{ERA5} ~~(z) at z_0 ($\langle IWC^{ERA5}_{z_0} \rangle$) is calculated as:~~with a unitary box function whose width is 5 and 4 km at 100 and 146 hPa, respectively.

$$\langle IWC^{ERA5}_{z_0} \rangle = \int \phi(z, z_0, \delta z) IWC^{ERA5}(z) dz$$

Consistently with **?**, we have fixed δz = 4 and 5 km at z_0 = 146 and 100 hPa, respectively. The ice injected from ERA5 at z_0 = 146 and 100 hPa with degraded vertical resolution ($\langle \Delta IWC^{ERA5}_{z_0} \rangle$) is thus calculated from $\langle IWC^{ERA5}_{z_0} \rangle$.

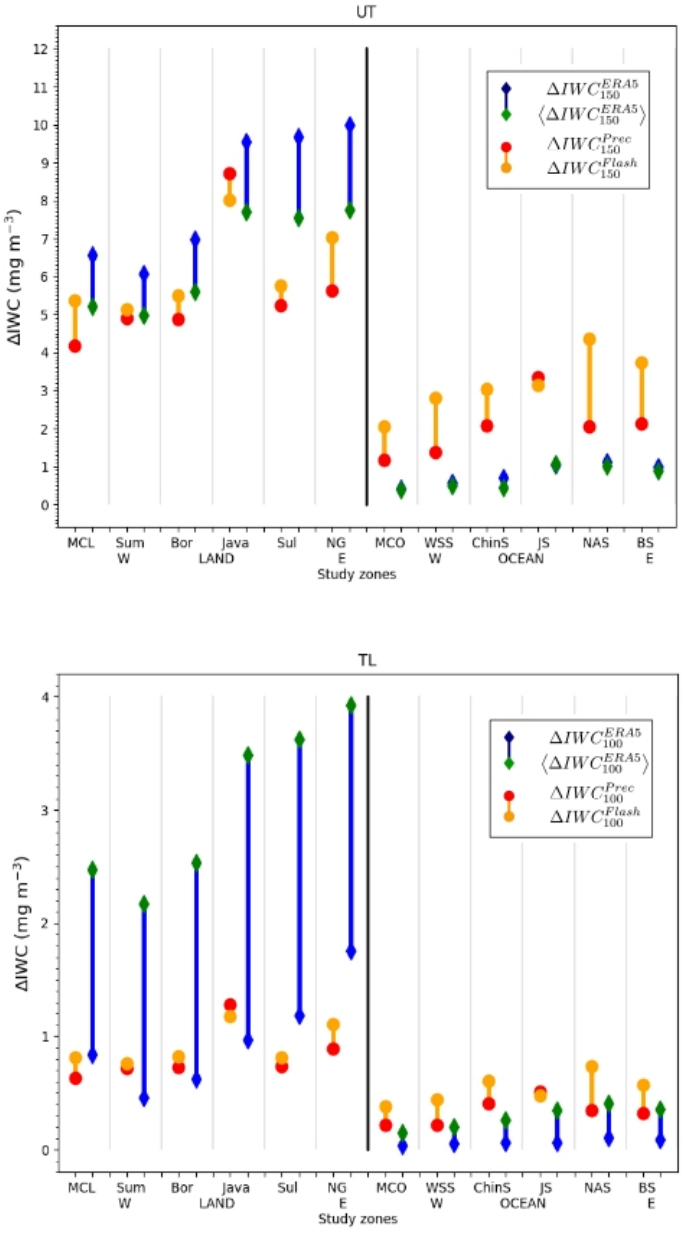

Figure 11. a) ΔIWC (mg m^{-3}) estimated from Prec (red) and Flash (orange) at 146 hPa and ΔIWC estimated from ERA5 at the level 150 hPa and at the level 150 hPa degraded in the vertical, over islands and seas of the MariCont: MariCont_L (MCL) and MariCont_O (MCO); from West (W) to East (E) over land, Sumatra (Sum), Borneo (Bor), Java, Sulawesi (Sul) and New Guinea (NG); and over seas, West Sumatra Sea (WSS), China Sea (ChinS), Java Sea (JS), North Australia Sea (NAS) and Bismark Sea (BS). b), Same as a) but for 100 hPa.

Figure ?? shows ΔIWC^{ERA5} and $\langle \Delta IWC^{ERA5}_{z_0} \rangle$ at z_0 = 150 and 100 hPa, over the island and the sea study zones. In the UT (Fig. ??a), over islands, ΔIWC^{ERA5}_{150} and $\langle \Delta IWC^{ERA5}_{150} \rangle$ calculated over Sumatra and Borneo vary from ~~4.75 to 6.97 mg m(~22 %of variability per study zones~~4.9 to 7.0 mg m^{-3} (the relative variation calculated as ((ΔIWC^{ERA5}-$\langle \Delta IWC^{ERA5} \rangle$)/$\Delta IWC^{ERA5}$)×100 is 18-19 %) whilst ΔIWC^{ERA5}_{150} and $\langle \Delta IWC^{ERA5}_{150} \rangle$ over Java, Sulawesi and New Guinea reach ~~7.41~~7.5–~~9.97 mg m~~10.0 mg m^{-3} (~~23 ~~19-22 % of variability per study ~~zones~~zone). Over sea, ΔIWC^{ERA5}_{150} and $\langle \Delta IWC^{ERA5}_{150} \rangle$ vary from 0.35 to ~~1.11 mg m~~1.1 mg m^{-3} (9 – 32 % of variability per study ~~zones~~zone). Over island and sea, ΔIWC^{ERA5}_{150} is greater than $\langle \Delta IWC^{ERA5}_{150} \rangle$. The small differences between ΔIWC^{ERA5}_{150} and $\langle \Delta IWC^{ERA5}_{150} \rangle$ over island and sea in the UT support the fact that the vertical resolution at 150 hPa has a low impact on the estimated ΔIWC.

In the TL, over land, ΔIWC^{ERA5}_{100} and $\langle \Delta IWC^{ERA5}_{100} \rangle$ vary from ~~0.46 to 3.65 mg m~~0.5 to 3.7 mg m^{-3} (~68% of variability per study ~~zones~~zone) with $\langle \Delta IWC^{ERA5}_{100} \rangle$ being ~~lower~~ larger than ΔIWC^{ERA5}_{100} by less than ~~2.12 mg m~~2.1 mg m^{-3}. Over sea, ΔIWC^{ERA5}_{100} and $\langle \Delta IWC^{ERA5}_{100} \rangle$ vary from ~~0.04 to 0.36 mg m~~0.05 to 0.4 mg m^{-3} (~71 % of variability per study ~~zones~~zone) with ΔIWC^{ERA5}_{100} lower than $\langle \Delta IWC^{ERA5}_{100} \rangle$ by less than ~~0.25 mg m~~0.2 mg m^{-3}. The large differences between ΔIWC^{ERA5}_{100} and $\langle \Delta IWC^{ERA5}_{100} \rangle$ over island and sea in the TL support the fact that the vertical resolution at 100 hPa has a high impact on the estimation of ΔIWC.

7.3 Synthesis

The comparison between the observational ΔIWC range and the reanalysis ΔIWC range is presented in Fig. ??. In the UT, over land, observation and reanalysis ΔIWC ranges overlap (agree to within ~~0 – 0.64 mg m(8 %),~~ 0.1 to 1.0 mg m^{-3}), which highlights the robustness of our model over land, except over Sulawesi ~~with differences of 1.63 mg m(23%~~and New Guinea, where the observational ΔIWC range and the reanalysis ΔIWC range differ by 1.7 and 0.7 mg m^{-3}, respectively). Over sea, the observational ΔIWC range is systematically greater than the reanalysis ΔIWC range by ~ ~~1.00~~ 1.0 – ~~2.19 mg m~~2.2 mg m^{-3} (75 %), showing a systematic positive bias and a too large variability range in our model over sea compared to ERA5. Combining observational and reanalysis ranges, the total ΔIWC variation range is estimated in the UT between ~~4.17 and 9.97 mg m~~4.2 and 10.0 mg m^{-3} (~ 20 % of variability per study ~~zones~~zone) over land and between ~~0.35 and 4.37 mg m~~0.3 and 4.4 mg m^{-3} (~ 30 % of variability per study ~~zones~~zone) over sea ~~, and~~and, in the TL, between ~~0.63 and 3.65 mg m~~0.6 and 3.9 mg m^{-3} (~ 70 % of variability per study ~~zones~~zone) over land, and between ~~0.04 and 0.74 mg m~~0.1 and 0.7 mg m^{-3} (~ 80 % of variability per study ~~zones~~zone) over sea.

The ~~amount~~ amounts of ice injected in the UT deduced from observations and reanalysis are consistent to each other over MariCont_L, Sumatra, Borneo and Java, with significant differences ~~between observations and reanalyses~~ over Sulawesi, New Guinea ~~and MariCont_O~~(within 1.7 to 0.7 mg m^{-3}, respectively) and all individual offshore study zones (within 0.7 to 2.1 mg m^{-3}). The impact of the vertical resolution on the estimation of ΔIWC in the TL is certainly non negligible, with larger ΔIWC variability range in the TL (70 – 80 %) than in the UT (20 – 30 %). At both levels, observational and reanalyses ΔIWC estimated over land is more than twice as large as ΔIWC estimated over sea. Finally, whatever the level considered, although Java has shown particularly high values in the observational ΔIWC range compared to other study zones, the reanalysis ΔIWC range shows that Sulawesi and NewGuinea would also be able to reach similar high values of ΔIWC as Java. ~~Whatever the~~

datasets used, the vertical distribution of ΔIWC in the TTL has shown a gradient of ~ 6 mg mbetween the UT and the TL over land compared to a gradient of ~ 2 mg mbetween the UT and the TL over ocean.

8 Discussion on small-scale convective processes impacting ΔIWC over a selection of areas

Our results have shown that, in all the datasets used, Java island and Java Sea are the two areas with the largest amount of ice injected up to the UT and the TL over the MariCont land and sea, respectively. In this section, processes impacting ΔIWC in the different study zones are discussed.

8.1 Java island, Sulawesi and New Guinea

Sulawesi, New Guinea and particularly Java island have been shown as the areas of the largest ΔIWC in the UT and TL. **?** have used high resolution observations and regional climate model simulations to show the three main processes impacting the diurnal cycle of rainfall over the Java island. The main process explaining the rapid and strong peak of Prec during the afternoon over Java (Fig. **??**a) is the sea-breeze convergence around midnight. This convergence caused by sea-breeze phenomenon increases the deep convective activity and impacts on the diurnal cycle of Prec and on the IWC injected up to the TL by amplifying their quantities. The second process is the mountain-valley wind converging toward the mountain peaks, and reinforcing the convergence and the precipitation. The land breeze becomes minor compared to the mountain-valley breeze and this process is amplified with the mountain altitude. As shown in Fig. **??**b, NewGuinea has the highest mountain chain of the MariCont. The third process shown by **?** is precipitation that is amplified by the cumulus merging processes which is more important over small islands such as Java (or Sulawesi) than over large islands such as Borneo or Sumatra. Another process is the interaction between sea-breeze and precipitation-driven cold pools that generates lines of strong horizontal moisture convergence (**?**). Thus, IWC is increasing proportionally with Prec consistent with the results from **?** and rapid convergence combined with deep convection transports elevated amounts of IWC at 13:30 LT (Fig. **??**) producing high ΔIWC during the growing phase of the convection (Fig. **??** and Fig. **??**) over Java.

8.2 West Sumatra Sea

In section **??**, it has been shown that the West Sumatra Sea is an area with positive anomaly of Prec during the growing phase of the convection but negative anomaly of IWC, which differs from other places. These results suggest that Prec is representative not only of convective precipitation but also of stratiform precipitation. The diurnal cycle of ~~Prec~~ stratiform and convective precipitations over West Sumatra Sea has been studied by **?** using 3 years of TRMM precipitation radar (PR) datasets, following the ~~2A23 Algorithm (?) separating stratiform from convective rainfall type. ?~~ 2A23Algorithm (Awaka, 1998). The authors have shown that rainfall over Sumatra is characterized by convective activity with a diurnal maximum between 15:00 and 22:00 LT ~~,~~ while, over the West Sumatra Sea, the rainfall type is convective and stratiform, with a diurnal maximum during the early morning (as observed in Fig. **??**). Furthermore, their analyses have shown a strong diurnal cycle of 200-hPa wind, humidity and stability, consistent with the PR over Sumatra West Sea and Sumatra ~~island~~Island. Stratiform and convective clouds are

both at the origin of heavy rainfall in the tropics (**??**) and in the West Sumatra Sea, but stratiform clouds are mid-altitude clouds in the troposphere and do not transport ice up to the tropopause. ~~Flash measured~~ Thus, over the West Sumatra Sea ~~would thus be a better proxy of deep convection in order to estimate~~ , the calculation of ΔIWC ~~than Prec because Prec is contaminated by stratiform rainfall~~estimated from Prec is possibly overestimated because Prec include a non-negligible amount of stratiform precipitation over this area.

8.3 North Australia Sea and seas with nearby islands

~~Comparisons~~

The comparisons between Figs. ~~??c and ??a~~ 2c and 6a have shown strong daily mean of Flash (10−2 –10~~flashes day~~−1 flashes day−1) but low daily mean of Prec (~~2~~ 2.0 – ~~8 mm day~~8.0 mm day−1) over the North Australia Sea. ~~Consequently, results in Fig. ?? have shown~~ Additionally, Fig. 11 shows that the strongest differences between ΔIWC^{Prec} and ΔIWC^{Flash} are found over the North Australia Sea, with ΔIWC^{Flash} greater than ΔIWC^{Prec} by ~~2.32 mg m~~2.3 mg m−3 in the UT and by ~~0.39 mg m~~0.4 mg m−2 in the TL (53% of variability ~~). Convective systems of the North Australian land and seas have been studied by ?. The North Australia Sea, mainly composed of the Arafura Sea and the Timor Sea, has~~ between ΔIWC^{Flash} and ΔIWC^{Prec}). These results imply that the variability range in our model is too large and highlight the difficulty to estimate ΔIWC over this study zone. Furthermore, as for Java Sea or Bismarck Sea, North Australia Sea has the particularity to be surrounding by several islands. According to the study from **?**, the ~~strongest convective activity during the DJF season (monsoon months) (?). During this season, isolated pulse convection and many mesoscale convective systems (MCSs) are active, such as the famous "Hector" storm over the Tiwi Islands, North of Darwin (??), squall lines (?) and cloud line (?). ?, identifying clouds from IR imagery, have shown that the number of clouds over the North Australia Sea~~ cloud size is the largest during the afternoon ~~but the size of the cloud is larger in the early morning. Although the number of clouds is low near 01:30 LT, the deepest daily convective activity during the early morning is at the origin of the strong relative value of IWC amount at 01:30 LT (see Fig. ??). Their studies have also shown that the diurnal maximum of number of clouds and cloud sizes over coastal part near NewGuinea is observed during the night , marked by land breeze convergence and gravity waves. Thus, nighttime convective systems over coasts propagate through the North Australia Sea and reinforce the IWC amount in the UT in the~~ over the North Australia land, during the night over North Australia coastline and during the early morning over ~~sea. Figure ?? presents the daily average of horizontal wind in the UT at 150 hPa and in the TL at 100 hPa over the period DJF 2004-2017. The wind direction at both altitudes is Westward, from North Australia land to the North Australia Sea. Thus, we suggest that because 1) the diurnal maximum of deep convection over North Australia land is found during the afternoon (?), and 2) the wind prevalence is from the North Australia land to sea, air masses charged with ice are advected from the North Australia land to~~ the North Australia ~~coastlines and seas at both altitudes. Thus, ΔIWC is injected during the day over the North Australia land in the UT and the TL and would be transported over the sea from the evening to the night and the early morning.~~ sea. These results suggest that deep convective activity moves from the land to the sea during the night. Over the North Australia Sea, it seems that the deep convective clouds are mainly composed by storms with lightning but precipitationd are weak or do not reach the surface and evaporating before.

~~Daily mean of wind speed and direction at 150 hPa (UT) a), and at 100 hPa (TL) b), from NOAA averaged during DJF 2004-2017 over the MariCont. The arrows with arbitrary length unit represent the wind direction.~~

9 Conclusions

The present study has combined observations of ice water content (IWC) measured by the Microwave Limb Sounder (MLS), precipitation (Prec) from the algorithm 3B42 of the Tropical Rainfall Measurement Mission (TRMM), the number of flashes (Flash) from the Lightning Imaging Sensor (LIS) of TRMM with IWC provided by the ERA5 reanalyses in order to estimate the amount of ice injected (ΔIWC) in the upper troposphere (UT) and the tropopause level (TL) over the MariCont, from the method proposed in a companion paper (**?**). ΔIWC is firstly calculated using the IWC measured by MLS (IWC^{MLS}) in DJF from 2004 to 2017 at the temporal resolution of 2 observations per day and Prec from TRMM-3B42 during the same period, to obtain a 1-hour resolution diurnal cycle. In the model used (**?**), Prec is considered as a proxy of deep convection impacting ice (ΔIWC^{Prec}) in the UT and the TL. While **?** have calculated ΔIWC^{Prec} over large convective study zones in the tropics, we show the spatial distribution of ΔIWC^{Prec} into the UT and the TL at 2° × 2° horizontal resolution over the MariCont, highlighting local areas of strong injection of ice up to 20 mg m^{-3} in the UT and up to 3 mg m^{-3} in the TL. ΔIWC injected in the UT and the TL has also been evaluated by using another proxy of deep convection: Flash measured by TRMM-LIS. Diurnal cycle of Flash has been compared to diurnal cycle of Prec, showing consistencies in 1) the spatial distribution of Flash and Prec over the MariCont (maxima of Prec and Flash located over land and coastline), and 2) their diurnal cycles over land (similar onset and duration of the diurnal cycle increasing phase). Differences have been mainly observed over sea and coastline areas, with the onset of the diurnal cycle increasing phase of Prec delayed by several hours depending on the considered area (from 2 to 7 h) compared to Flash. ΔIWC calculated by using Flash as a proxy of deep convection (ΔIWC^{Flash}) is compared to ΔIWC^{Prec} over five islands and five seas of the MariCont to establish an observational ΔIWC range over each study zone. ΔIWC is also estimated from IWC provided by the ERA5 reanalyses (ΔIWC^{ERA5} and IWC^{ERA5}, respectively) at 150 and 100 hPa over the study zones. We have also degraded the vertical resolution of IWC^{ERA5} to be consistent with that of IWC^{MLS} observations: 4 km at 146 hPa and 5 km at 100 hPa. The ΔIWC ranges calculated from observations and reanalyses were evaluated over the selected study zones (island and sea).

With the study of ΔIWC^{Prec}, results show that the largest amounts of ice injected in the UT and TL per 2° × 2° pixels are related to i) an amplitude of Prec diurnal cycle larger than 0.5 mm h^{-1}, ii) values of IWC measured during the growing phase of the convection larger than 4.5 mg m^{-3} and iii) duration of the growing phase of the convection longer than 9 hours. The largest ΔIWC^{Prec} has been found over areas where the convective activity is the deepest. The observational ΔIWC range calculated between ΔIWC^{Prec} and ΔIWC^{Flash} has been found to be within 4 – ~~20~~ 22 % over land and to within ~~6~~ 7 – ~~50~~ 53 % over sea. The largest differences between ΔIWC^{Prec} and ΔIWC^{Flash} over sea might be due to the combination of the presence of stratiform precipitation included into Prec and the very low values of Flash over seas (<10~~flashes day~~$^{-2}$ flashes day^{-1}). The diurnal cycle of IWC^{ERA5} at 150 hPa is more consistent with that of Prec and Flash over land than over ocean. Finally, the observational ΔIWC range has been shown to be consistent with the reanalysis ΔIWC range to within 23 % over

land and to within ~~75~~ 30-50 % over sea in the UT and to within 49 % over land and to within 39 % over sea in the TL. Thus, thanks to the combination between the observational and reanalysis ΔIWC ranges, the total ΔIWC variation range has been found in the UT to be between ~~4.17 and 9.97 mg m~~4.2 and 10.0 mg m^{-3} (to within 20 % per study zones) over land and between ~~0.35 and 4.37 mg m~~0.3 and 4.4 mg m^{-3} (to within 30 % per study zones) over sea and, in the TL, between ~~0.63 and 3.65 mg m~~0.6 and 3.9 mg m^{-3} (to within 70 % per study zones) over land and between ~~0.04 and 0.74 mg m~~0.1 and 0.7 mg m^{-3} (to within 80% per study zones) over sea. The ΔIWC variation range in the TL is larger than that in the UT highlighting the stronger impact of the vertical resolution in the observations in the TL compared to the UT.

The study at small scale over islands and seas of the MariCont has shown that ΔIWC from ERA5, Prec and Flash in the UT agree to within 0 – ~~0.64 mg m~~0.6 mg m^{-3} (8%) over MariCont_L, Sumatra, Borneo and Java with the largest values obtained over Java. However, while Java presents the largest amount of ΔIWC^{Prec} and ΔIWC^{Flash} in the UT and the TL (larger by about 1.0 mg m^{-3} in the UT and about ~~0.25 mg m~~0.3 mg m^{-3} in the TL than other land study zones), New Guinea and Sulawesi reach similar ranges of values of ice injected with ERA5 than

Java in the UT and even larger ranges of values as Java in the TL. Processes related to the strongest amount of ΔIWC injected into the UT and the TL have been identified as the combination of sea-breeze, mountain-valley breeze and merged cumulus, such as over NewGuinea and accentuated over small islands with high topography such as Java or Sulawesi. ~~Over sea areas, ΔIWC is a combination between the vertical transport of air masses by deep convection during night and early morning over offshore sea and by the westward horizontal transport of air masses near the tropopause, coming from land through coastline areas, during the end of the afternoon and at night (such as in North of Australia seas).~~

Author contributions. IAD analysed the data, formulated the model and the method combining MLS, TRMM and LIS data and took primary responsibility for writing the paper. CD has treated the LIS data, provided the Figures with Flash datasets, gave advices on data processing and contributed to the Prec and Flash comparative analysis. PR strongly contributed to the design of the study, the interpretation of the results and the writing of the paper. PR, FC, PH and TD provided comments on the paper and contributed to its writing.

Acknowledgements. We thank the National Center for Scientific Research (CNRS) and the Excellence Initiative (Idex) of Toulouse, France to fund this study and the project called Turbulence Effects on Active Species in Atmosphere (TEASAO – http://www.legos.obs-mip.fr/projets/axes-transverses-processus/teasao, Peter Haynes Chair of Attractivy). We would like to thank the teams that have provided the MLS data (https://disc.gsfc.nasa.gov/datasets/ML2IWC_V004, last access: June 2019), the TRMM data (https://pmm.nasa.gov/data-access/downloads/trmm), the LIS data (https://ghrc.nsstc.nasa.gov/lightning/data/data_lis_trmm.html, last access: June 2019), the ERA5 Reanalysis data (https://cds.climate.copernicus.eu/cdsapp/dataset/reanalysis\protect\discretionary{\char\hyphenchar\font}{}{}era5, last access: June 2019), and the NCEP Reanalysis data provided by the NOAA/OAR/ESRL PSD, Boulder, Colorado, USA, (https://www.esrl.noaa.gov/psd/, last access: June 2019).

References

J. Awaka. Algorithm 2A23—Rain type classification. In Proc. Symp. on the Precipitation Observation from Non-Sun Synchronous Orbit, pages 215–220, 1998.

R. E. Carbone, J. W. Wilson, T. D. Keenan, and J. M. Hacker. Tropical island convection in the absence of significant topography. part i: Life cycle of diurnally forced convection. Monthly weather review, 128(10):3459–3480, 2000.

L. Chappel. Assessing severe thunderstorm potential days and storm types in the tropics. In Presentation at the International Workshop on the Dynamics and Forecasting of Tropical Weather Systems, Darwin, 22-26 January 2001, 2001.

T. Dauhut, J.-P. Chaboureau, J. Escobar, and P. Mascart. ~~Giga-les~~ Giga-LES of hector the convector and its two tallest updrafts up to the stratosphere. Journal of the Atmospheric Sciences, 73(12):5041–5060, 2016.

T. Dauhut, J.-P. Chaboureau, P. Mascart, and T. Lane. The overshoots that hydrate the stratosphere in the tropics. In EGU General Assembly Conference Abstracts, volume 20, page 9149, 2018.

I.-A. Dion, P. Ricaud, P. Haynes, F. Carminati, and T. Dauhut. Ice injected into the tropopause by deep convection–part 1: In the austral convective tropics. Atmospheric Chemistry and Physics, 19(9):6459–6479, 2019.

S. Fueglistaler, A. E. Dessler, T. J. Dunkerton, I. Folkins, Q. Fu, and P. W. Mote. Tropical tropopause layer. Reviews of Geophysics, 47(1), 2009a. doi: 10.1029/2008RG000267. URL https://agupubs.onlinelibrary. wiley.com/doi/abs/10.1029/2008RG000267.

A. J. Geer, F. Baordo,N. Bormann, P. Chambon, S. J. English, M. Kazumori, ... C. Lupu. The growing impact of satellite observations sensitive to humidity, cloud and precipitation. Quarterly Journal of the Royal Meteorological Society, 143(709), 3189-3206, 2017.

R. Goler, M. J. Reeder, R. K. Smith, H. Richter, S. Arnup, T. Keenan, P. May, and J. Hacker. Low-level convergence lines over ~~northeastern~~ North Eastern australia. part i: The ~~north australian~~ North Australian cloud line. Monthly weather review, 134(11):3092–3108, 2006.

H. Hatsushika and K. Yamazaki. Interannual variations of temperature and vertical motion at the tropical tropopause associated with ~~enso~~ENSO. Geophysical research letters, 28(15):2891–2894, 2001.

H. Hersbach. Operational global reanalysis: progress, future directions and ~~syn- ergies~~ synergies with NWP. European Centre for Medium Range Weather Forecasts, 2018.

R. A. Houze and A. K. Betts. Convection in gate. Reviews of Geophysics, 19(4): 541–576, 1981.

G. J. Huffman, D. T. Bolvin, E. J. Nelkin, D. B. Wolff, R. F. Adler, G. Gu, Y. Hong, K. P. Bowman, and E. F. Stocker. The ~~trmm multisatellite precipitation analy- sis (tmpa): Quasi-global~~TRMM multisatellite precipitation analysis (TMPA): quasi-global, multiyear, combined-sensor precipitation estimates at fine scales. Journal of hydrometeorology, 8(1):38–55, 2007.

E. J. Jensen, A. S. Ackerman, J. A. Smith (2007). Can overshooting convection dehydrate the tropical tropopause layer?. Journal of Geophysical Research: Atmospheres, 112(D11), 2007.

C. Liu and E. J. Zipser. Global distribution of convection penetrating the tropical tropopause. Journal of Geophysical Research: Atmospheres, 110(D23), 2005.

C. Liu and E. J. Zipser. Diurnal cycles of precipitation, clouds, and lightning in the tropics from 9 years of TRMM observations. Geophys. Res. Lett., 35, L04819, doi:10.1029/2007GL032437, 2008.

Livesey, N.J., Read,W.G., Wagner, P.A., Froidevaux, L., Lambert, A., Manney, G.L., Millan, L.F., Pumphrey,H.C., Santee, M.L., Schwartz, M.J., Wang, S., Fuller, R.A., Jarnot, R.F., Knosp, B.W.,Martinez, E., and Lay, R.R., Version 4.2x Level 2 data quality and description doc-ument, Tech. Rep. JPL D-33509 Rev. D, Jet Propulsion Laboratory, available at:http://mls.jpl.nasa.gov (last access: 01 09 2019), 2018.

P. Lopez. Direct 4D-Var assimilation of NCEP stage IV radar and gauge precipitation data at ECMWF. Monthly Weather Review, 139(7), 2098-2116, 2011.

B. S. Love, A. J. Matthews, and G. M. S. Lister. The diurnal cycle of precipitation over the maritime continent in a high-resolution atmospheric model. Quarterly Journal of the Royal Meteorological Society, 137(657):934–947, 2011.

L. Millán, W. Read, Y. Kasai, A. Lambert, N. Livesey, J. Mendrok, H. Sagawa, T. Sano, M. Shiotani, and D. L. Wu. Smiles ice cloud products. Journal of Geophysical Research: Atmospheres, 118(12):6468–6477, 2013.

S. Mori, H. Jun-Ichi, Y. I. Tauhid, M. D. Yamanaka, N. Okamoto, F. Murata, N. Sakurai, H. Hashiguchi, and T. Sribimawati. Diurnal land–sea rainfall peak migration over ~~sumatera island, indonesian maritime continent~~Sumatera island, Indonesian Maritime Continent, observed by ~~trmm~~ TRMM satellite and intensive rawinsonde soundings. Monthly Weather Review, 132(8):2021–2039, 2004.

S. W. Nesbitt and E. J. Zipser. The diurnal cycle of rainfall and convective inten- sity according to three years of trmm measurements. Journal of Climate, 16 (10):1456–1475, 2003.

W. A. Petersen, and S. A. Rutledge. Regional variability in tropical convection: Observations from TRMM. Journal of Climate, 14(17), 3566-3586, 2001.

M. Pope, C. Jakob, and M. J. Reeder. Convective systems of the north australian monsoon. Journal of Climate, 21(19):5091–5112, 2008.

J.-H. Qian. Why precipitation is mostly concentrated over islands in the maritime continent. Journal of the Atmospheric Sciences, 65(4):1428–1441, 2008.

C. S. Ramage. Role of a tropical "maritime continent" in the atmospheric ~~circu- lation~~circulation. Mon. Wea. Rev, 96(6):365–370, 1968.

W. J. Randel, F. Wu, H. Voemel, G. E. Nedoluha, and P. Forster. Decreases in stratospheric water vapor after 2001: Links to changes in the tropical tropopause and the brewer-dobson circulation. Journal of Geophysical Re- search: Atmospheres, 111(D12), 2006a.

W.J. Randel and E.J. Jensen. Physical processes in the tropical tropopause layer and their roles in a changing climate. Nature Geoscience, 6:169, 2013. doi: 10.1038/ngeo1733. URL https://doi.org/10.1038/ngeo1733.

S. C. Sherwood. A stratospheric "drain" over the maritime continent. Geophysical research letters, 27(5):677–680, 2000.

A. Stenke and V. Grewe. Simulation of stratospheric water vapor trends: impact on stratospheric ozone chemistry. Atmospheric Chemistry and Physics, 5(5): 1257–1272, 2005.

G. L. Stephens and T. J. Greenwald. The earth's radiation budget and its rela- tion to atmospheric hydrology: 2. observations of cloud effects. Journal of Geophysical Research: Atmospheres, 96(D8):15325–15340, 1991.

G.-Y. Yang and J. Slingo. The diurnal cycle in the tropics. Monthly Weather Review, 129(4):784–801, 2001. 129<0784:TDCITT>2.0.CO;2. doi: 10.1175/1520-0493(2001) URL https://doi.org/10.1175/1520-0493(2001)129<0784:TDCITT>2.0.CO;2.

J. W. Waters, L. Froidevaux, R. S. Harwood, R. F. Jarnot, H. M. Pickett, W. G. Read, ... and J. R. Holden (2006). The earth observing system microwave limb sounder (EOS MLS) on the Aura satellite. IEEE Transactions on Geoscience and Remote Sensing, 44(5), 1075-1092.